Aus dem
Zentrum für Molekulare Medizin
Institut für Kardiovasculäre Pharmakologie
Frankfurt am Main

betreut in der
Abteilung Pharmakologie am
Max-Planck-Institut für Herz- und Lungenforschung, Bad Nauheim
Direktor: Prof. Dr. Stefan Offermanns

The role of endothelial cell death in different pathologies

Dissertation
zur Erlangung des Doktorgrades der theoretischen Medizin
des Fachbereichs Medizin
der Johann Wolfgang Goethe-Universität
Frankfurt am Main

vorgelegt von
Sayali Joseph
M.Tech (Integrierte) Biotechnologie
aus Pune, India

Frankfurt am Main, 2020

Dekan:	Prof. Dr. Josef Pfeilschifter
Referent:	Prof. Dr. Stefan Offermanns
Korreferent:	Prof. Dr. Reinier Boon

Tag der mündlichen Prüfung: 15.01.2020

CONTENTS

1. INTRODUCTION

The vasculature serves as an omnipresent mediator that caters to physiological requirements within vital organs for homeostasis. It functions as a conduit that channels both the fluidic and cellular entities required for the passage of nutrients, gases, metabolites as well as wastes generated in and out of vital organ systems. The vasculature not only regulates the passive function of maintaining a fluidic system but also has a dynamic role in regulating essential functions like vasotone regulation (1), hemostasis (2), vascular barrier maintenance (3) and also forms an integral part of the innate immune system (4). This dynamic nature of the vasculature is regulated largely by the endothelium that lines the lumen of every vessel. The endothelium is equipped to respond to the surrounding environment and modulating responses upon contact with the external physiological stimuli such as fluidic shear stress (5), pathogens (6), change in the partial pressure of gases in the blood (7) etc. Some key functions of the endothelium are highlighted below.

1.1 Physiological functions of the endothelium

Vasotone regulation by the endothelium: The endothelium regulates blood pressure via the release of vasoactive peptides like nitric oxide (NO), prostacyclin (PGI_2), endothelium-derived hyperpolarizing factor (EDHF), thromboxane (TXA_2) and Endothelin-1 (ET-1). These peptides bind to specific receptors on smooth muscle cells (SMCs) and modulate SMCs to either allow vessel constriction or relaxation. NO, PGI_2 and EDHF are known vasodilators, whereas endothelium-derived TXA_2 and ET-1 are potent vasoconstrictors (1). The release of such factors from the endothelium can be altered by extracellular cues such as fluid shear stress or inflammatory mediators (8). Under normal physiological conditions, a balance is maintained between vasoconstrictors and vasodilators for maintaining blood pressure required for optimal blood circulation.

Hemostasis regulation by the endothelium: For hemostasis, the endothelium maintains a balance between coagulation and fibrinolysis, by secretion or expression of factors that can act as pro-coagulant factors whereas some have anti-coagulant functions. For example, during vessel wall injury, platelets are recruited to the site of injury. Activated platelets bind to the site of vessel injury and recruit more platelets to form a platelet-platelet cluster that plugs the site of injury (9). The activated platelets and the endothelium make concerted efforts for activation of the coagulation cascade and formation of fibrin clots (10). The endothelium mediates this pro-coagulant effect through the expression of tissue factor (TF) that triggers the extrinsic coagulation cascade, ultimately leading to fibrin generation and fibrin clot formation. The endothelium sustains this pro-coagulant effect by deactivating fibrinolytic factors via expression of plasminogen activation inhibitors (PAI-1/2) (11). However, it also regulates inactivation of the coagulation cascade by expression of several anti-coagulant factors like tissue factor pathway inhibitor (TFPI), heparan sulfate proteoglycans, thrombomodulin, and endothelial Protein C Receptor (EPCR) (12); and mediates fibrinolysis via tissue plasminogen activator (tPA) and urokinase mediated plasmin activation. Furthermore, NO and PGI_2 secreted by endothelial cells inhibit platelet adhesion and aggregation (2). A fine-tuned balance between coagulation and anti-coagulation factors is maintained by the endothelium to allow adequate blood flow without vessel-blocking thrombi formation.

Vascular barrier-integrity maintenance by the endothelium: The endothelium maintains a vascular barrier by keeping a check on the intercellular trafficking of ions, molecules as well as proteins. Endothelial cells regulate such a check by selective transport of entities across cell-cell junctions. Several protein complexes maintain tight or loose intercellular connections. Broadly the junctional complexes that hold the endothelial cells attached to each are classified into adherens junctions and tight junctions (13). The adherens junctional transmembrane proteins like vascular endothelial cadherin (VE-Cadherin/ CD144), epithelial cadherin (E-cadherin) and platelet endothelial cell adhesion molecules (PECAM1/ CD31) are widely expressed on endothelial cells of several vascular beds and reasonably allow passage of small

molecules; whereas tight junctional membrane proteins like occludins, claudins and junctional adhesion molecules (JAM) serve a more selective barrier-permeability (14). The integral membrane proteins of both adherens and tight junctional complexes allow cell-cell contact via their extracellular domain, and their intracellular domains can interact with linker proteins bound to signaling complexes as well as cytoskeletal proteins and hence serve as messengers to relay extracellular changes to develop an intracellular response (13). Thus the endothelium maintains a selective and responsive barrier protecting and adapting to the external environment.

Endothelial cells in quiescence: Under physiological conditions, endothelial cells maintain a state of quiescence by suppressing chemokine expression, sequestering leukocyte adhesion molecules like P-selectin within Weibel-Palade bodies (WPBs) and thus prevent an activated state or active recruitment of immune cells (15). Resting endothelial cells suppress the surface expression of inflammatory cell adhesion molecules like vascular cell adhesion molecule 1 (VCAM-1), intracellular cell adhesion molecule (ICAM-1) and endothelial-selectin (E-selectin). NO produced by endothelial cells help suppress the expression of pro-inflammatory genes, inhibit platelet activation and aggregation, inhibit fusion of WPBs to the luminal surface of the endothelial cells and hence prevent several inflammatory processes (16). Thus resting endothelium keeps overt inflammation in check.

Role of endothelium in innate immunity: The endothelium, like the cells of the innate immune system, can recognize foreign or pathological entities via pattern recognition receptors (PRR) like the Toll-like receptors (TLRs) via recognizing invading pathogens via pathogen-associated molecular patterns (PAMPs) as well. Endothelial cells are conditional innate immune cells since they need to be activated by PAMP, or cytokines or other factors to facilitate a pro-inflammatory response. Endothelial cell activation that occurs without changes in gene expression over a shorter period of time (response time is within minutes) is classified as Type I endothelial cell activation whereas endothelial cell activation that involves changes in gene expression that take place over a longer duration (response time is over several hours) is called Type II activation. Type II activation of endothelial cells is often initiated by inflammatory cytokines like

Tumor necrosis factor alpha (TNF-alpha) and PAMPs like Lipopolysaccharide (LPS) that stimulate TNFR1 and TLR4 respectively, on endothelial cells to activate the inflammatory pathways like NF-kB, MAPK, PI3K/Akt and their downstream transcription factors that cause upregulation of pro-inflammatory gene expression like monocyte chemoattractant protein (MCP1), ICAM-1, VCAM-1, E-selectin and cyclooxygenase-2 (COX-2).

However, cytokines like TNF-alpha could also have rather deleterious effects on endothelial cells, and cause endothelial cell death (17, 18). Depending on the pathological conditions and the vascular bed affected endothelial cells can undergo different types of cell death.

1.2 Programmed cell death (PCD)

Based on the morphological criteria, cells can undergo either apoptotic or necrotic cell death. Apoptosis involves a decrease in cytoplasmic and nuclear volume, nuclear fragmentation, plasma membrane blebbing and cell fragmentation, whereas necrosis involves cytoplasmic swelling and plasma membrane rupture without nuclear fragmentation (19). Necrosis can either be accidental or is regulated by distinct molecular machinery. Apoptotic, as well as regulated necrotic cell death, is triggered and regulated by the distinct molecular mechanism.

Apoptosis: Apoptosis is a regulated form of cell death that is required for tissue homeostasis but can also occur during pathological conditions. Apoptosis can be initiated by the intrinsic pathway in response to cytotoxic stress such as UV, ionizing radiation etc. The intrinsic pathway is regulated via certain Bcl-2 family proteins, which mediate the release of Cytochrome C from mitochondria (20). Cytochrome C along with apoptotic protease activating factor-1 (APAF-1) and pro-caspase 9 forms the apoptosome, which further activates executioner caspases 3, 6 and 7 that mediate the cleavage of cellular protein and causes cell death (21). Alternatively, the extrinsic pathway is initiated by extracellular ligands like TNF-alpha, FasL, TNF-related apoptosis-inducing ligand (TRAIL) etc. that activate their specific receptors to initiate the assembly of death

signaling complexes (22). Each receptor-ligand complex has a unique set of adaptor proteins that initiate the assembly of death-inducing signaling complexes (DISC) (23). For example, TNF-alpha bound to TNFR1 induces the assembly of Complex I composed of TNF-alpha receptor-associated death domain protein (TRADD), TNF-alpha receptor-associated factor 2 (TRAF2) and 5 (TRAF5), a cellular inhibitor of apoptosis 1 and 2 (cIAP1/2). cIAP1/2 ubiquitinates receptor interacting protein kinase 1 (RIPK1) which then acts as a scaffold. TGF-beta activating kinase 1 (TAK1) is recruited to Complex I and is bound to the RIPK1 polyubiquitin chain. TAK1 undergoes autophosphorylation and activates IKK complex to promote the degradation of IkB, which results in the activation of the NF-kB pathway (24). Thus, Complex I activation upon TNF-alpha stimulation can lead to transcription of inflammatory and pro-survival genes via NF-kB transcription factor.

However, RIPK1 can move to the cytoplasm either due to failure of cIAP1/2 mediated ubiquitination (25) or upon deubiquitination by deubiquitinase cylindromatosis Lysine 63 deubiquitinase (CYLD) (26). RIPK1 assembles with Fas-associated protein with death domain (FADD) and Caspase 8 to form Complex IIa. Caspase 8 activation can then lead to apoptosis via further downstream activation of executioner caspase 3 and 7 (25).

Necroptosis: Necroptosis is one of the regulated forms of necrotic cell death that can occur by TNFR activation as well as activation of receptors like TLR4, Fas etc. In the case of TNF-alpha mediated stimulation, Complex IIa assembly and caspase 8 activation can lead to apoptotic cell death. However, in cases where caspase 8 activity is inhibited by pharmacological agents or when caspase 8 is degraded by TNFR-associated factor 2 (TRAF2) mediated ubiquitination, apoptosis is inhibited (27). Caspase 8 inactivation can then promote necroptotic cell death. RIPK1 autophosphorylation promotes receptor interacting protein kinase 3 (RIPK3) recruitment and phosphorylation. Phosphorylated RIPK3 further recruits mixed lineage kinase domain-like (MLKL) protein and phosphorylates it to form Complex IIb or the necrosome (28). Phosphorylation of MLKL and its oligomerization can lead to pore formation and causes necroptotic cell death via plasma membrane disruption (29).

Proteins regulating the switch between apoptosis and necroptosis: The molecular mechanism of apoptosis and necroptosis is distinct; however, some proteins common to both pathways regulate a switch that can shift cell death from apoptosis to necroptosis.

TAK1 is one component of Complex I that regulates such a switch. Upon TNF-alpha stimulation, pharmacological inhibition of TAK1 or its genetic deletion can increase apoptosis (30). However, in certain cases, TAK1 hyperactivation can lead to a switch from apoptosis to necrosis (31). The role of TAK1 in regulating cell death is different in different cell types (32). In endothelial cells, deletion of TAK1 correlates with an increase in RIPK3 expression and upon TNF-alpha stimulation and caspase 8 inactivation can promote necroptosis (33).

Caspase 8 also plays an important role in regulating apoptosis or switch towards necroptosis. Caspase 8 activation can suppress necroptosis by cleaving important necroptotic proteins such as RIPK1 and RIPK3 (34). However, caspase 8 inactivation by the mechanisms above can tilt the balance towards necroptotic cell death.

RIPK1 activation status dictates its role in apoptosis or necroptosis—ubiquitinated RIPK1 functions as a scaffolding protein for apoptotic Complex IIa. However, in cases deubiquitination of RIPK1 and phosphorylation leads to the necrosome formation, tilting towards necroptotic cell death.

Thus, depending on the cellular context and extracellular cues, a distinct regulatory mechanism controls the type of PCD.

PCD and inflammation: The type of PCD triggered could be critical in the pathological context due to a difference in its immunogenicity (35). Apoptosis generally does not illicit an inflammatory response as dying cells are recognized by tissue-resident macrophages by the surface expression of phosphatidylserine and are phagocytosed (36) (37). Furthermore, after engulfment of dying cells, phagocytes release factors such as Interleukin-10 (IL-10) and prostaglandin E2 that dampens immune response (38). However, after apoptotic cell death, the inflammatory response can be triggered in case dying cells are not rapidly phagocytosed (35). As opposed to apoptotic cell death, necrotic cell death leads to the release of damage-associated molecular patterns (DAMPs) that can trigger inflammation. DAMPs are intracellular

molecules that are released only after plasma membrane rupture, for example, high-mobility group protein 1 (HMGB1), uric acid, ATP, DNA and RNA (39). Thus, induction of apoptotic or necrotic cell death can influence immune cell activation and can contribute to the development or amelioration of pathological condition.

1.3 Role of endothelial cell death in diseases

The physiological functions of the endothelium play an important role in maintaining vital organ function. Injury to the endothelium can have a detrimental effect on organ function and can lead to the development of pathological conditions. For example, retinal microvascular apoptosis due to hyperglycemia promotes the development of diabetic retinopathy (40) (41). Furthermore, the type of endothelial cell death can influence the development of diseases. For example, nicotine-induced endothelial pyroptosis (another regulated form of necrotic cell death) promotes atherosclerosis development by increasing IL-18 and IL-1β production (42). Endothelial cell death can also promote disease progression, for example, tumor cell-induced endothelial necroptosis increases tumor metastasis (33). Therefore, a study of the extent and the type of PCD endothelial cells undergo is relevant for the understanding of disease development and progression.

1.4 Role of endothelium in pathological models with endothelial dysfunction

1.4.1 *Sepsis*

Sepsis is now a highly prevalent condition in ICU patients and is recognized by the World Health Organization (WHO) as of 2017, as a major threat to patient safety and global health (43). Sepsis is defined as a systemic inflammatory response syndrome (SIRS) caused by infection. This hyper-inflammation may lead to organ failure, and such a condition is termed as severe sepsis.

Severe sepsis: Incidences of severe sepsis are often due to cardiovascular, renal and respiratory failure. Dysfunction of the central nervous system may also occur (44). Cardiovascular failure during severe sepsis may be due to hypotension and myocardial dysfunction (45). Renal failure by acute kidney injury (AKI) in sepsis occurs due to increased inflammation, coagulation, oxidative stress and tubular epithelial injury (46). Sepsis-associated acute respiratory distress syndrome (ARDS), which is characterized by pulmonary inflammation and impaired gas exchange, leads to hypoxemia and respiratory failure (47, 48). Mortality due to severe sepsis can occur in an acute phase within few days due to inadequate resuscitation, leading to cardiac and pulmonary failure or can occur in a prolonged phase over weeks due to immune dysfunction or sustained inflammation and multiple organ injury (49).

Septic shock: When sepsis is accompanied with refractory hypotension, it is termed as septic shock (50). Septic shock is a subset of sepsis and which may or may not be always accompanied by multiple organ failure.

Pathophysiology of sepsis:

Immune dysfunction: Sepsis is characterized by immune dysfunction as well as endothelial dysfunction. During infection, infectious agents are recognized by PAMPs like LPS, bacterial flagellin, lipoteichoic acid, peptidoglycan and nucleic acid from viruses (51). LPS is a potent endotoxin that can be recognized by PRR like Toll-like receptor (TLR) family (52). Recognition of pathogens or endotoxins via PRR by innate immune cells induces a pro-inflammatory response (53). Activation of both innate and adaptive immune cells further leads to release of pro-inflammatory cytokines primarily TNF-alpha, IL-6, IL-1, IL-8, and IFN-gamma in the acute phase and anti-inflammatory cytokines like IL-1RA, IL-4, IL-10 and TGF-beta during later stages. Pro-inflammatory cytokines are required for bacterial clearance, whereas anti-inflammatory cytokines inhibit the production of pro-inflammatory cytokines and help in healing. However, the imbalance between the pro-inflammatory and anti-inflammatory responses can lead to a hyper-inflammatory response (54, 55). Such immune dysfunction is reported to correlate with increased mortality in septic patients. For example, higher IL-6 levels correlate with increased mortality in patients with septic shock

(56). However, certain cytokines are reported to be beneficial in some immunosuppressed patients but not others. For example, IFN-gamma exacerbates sepsis via an increase in coagulation protein C5a (57) and is reported to be higher in non-survivors (58). However, in some cases where patients are immunosuppressed, administration of IFN-gamma can prove to be beneficial (59). Therefore, cytokines or chemokines that vary due to immune dysfunction can have beneficial or lethal effects depending on the physiological state of the patient.

Endothelial dysfunction in sepsis: Inflammatory cytokines produced during sepsis have a detrimental effect on endothelial function. Vascular-barrier integrity is compromised due to inflammatory cytokines like TNF-alpha, which disrupts junctional complexes (60). Vascular permeability is also increased due to endothelial glycocalyx degradation (61). Increased vascular permeability allows increased immune cell infiltration. Although immune cell infiltration is required for bacterial clearance, however, they further can cause tissue damage. For example, in cases of acute lung injury increased neutrophil influx correlates with severity of ARDS (62). Activated neutrophils release in alveolar spaces proteinases, cationic polypeptides, cytokines, and reactive oxygen species (ROS) that can cause significant lung injury as well as endothelial damage (63). Chemokines released during sepsis play a key role in the recruitment of neutrophils. For example, chemokines like keratinocyte-derived chemokine (KC or CXCL1) and macrophage inflammatory protein-2 (MIP-2 or CXCL2) have been implicated in neutrophil recruitment in peritonitis-induced sepsis (64).

Furthermore, cytokine or PAMP-induced endothelial activation can increase surface expression of P and E-selectins and ICAM-1 and VCAM-1 to facilitate leukocyte recruitment and adhesion (65) further. The pro-inflammatory environment can also alter endothelial cells to a pro-coagulant state.

Endothelial cell activation can also lead to an increase in tissue factor expression (TF) via the NF-kB pathway and encourage a pro-thrombotic environment. Cytokines can decrease expression of anti-coagulant protein such as thrombomodulin in endothelial cells (65), which further sets the stage for

coagulation. Thus, complement activation during sepsis coupled with a pro-coagulant endothelium can increase the incidence of thrombosis, and lead to an increase in disseminated intravascular coagulation (DIC) (66). DIC can cause significant organ damage due to blockade of blood vessel; therefore, causing hypoxic injury (67). Deregulation of endothelium-mediated vasotone modulation during sepsis is the primary cause of septic shock. Inflammatory cytokines that drive the expression of inducible nitric oxide synthase (iNOS) elevates NO levels, thus causing systemic hypotension. Tissue hypoperfusion during septic shock can further cause tissue injury due to hypoxia (68).

Thus, progression of sepsis from SIRS to severe sepsis is regulated by both immune dysfunction as well as endothelial dysfunction. The immune, as well as endothelial dysfunction, can be induced due to cell death as well. The study of immune cell death during sepsis is well studied. For example, neutrophils undergoing NETosis during sepsis (69-71) and pyroptosis in macrophages (72, 73) and lymphocytes (74) has been widely studied. However, endothelial cell death, even though has been reported in some studies (75-77), the molecular mechanism underlying it is not clear.

1.4.2 Pathophysiology and endothelial dysfunction in ischemia and ischemia-reperfusion injury in different organs

Pathological conditions like DIC, sepsis or severe hypotension, can lead to ischemic injury in organs due to tissue hypoperfusion, whereas during surgeries such as organ transplant ischemia-reperfusion injury is inevitable. Ischemia-reperfusion injury (IRI) occurs when blood flow to a particular organ is restricted which can lead to tissue hypoxia and a consequent change in metabolic activity within the hypoxic tissue leading to injury and is further exacerbated upon reinstating blood flow. The reperfusion initiates a strong inflammatory response that further contributes to organ injury (78). Ischemia, as well as ischemia-reperfusion, induces microvascular dysfunction, which strongly contributes to the development of pathology. IRI can lead to a significant increase in vascular permeability (79), endothelial cell activation (80, 81), vasotone dysregulation (82), and loss of endothelial thromboresistance (81, 83). However, the

endothelium shows significant heterogeneity in different vascular beds. Thus endothelial dysfunction can have a distinct effect in different organs post-injury.

Hindlimb ischemia and ischemia-reperfusion injury

Hindlimb ischemia or IRI can lead to muscle as well as vascular damage due to ROS formation (84). Following ischemia, there are several processes that allow tissue reperfusion through neovascularization, i.e. either by arteriogenesis or by angiogenesis. Arteriogenesis is the remodelling of pre-existing arterio-arteriolar anastomoses into functional arteries, whereas angiogenesis involves proliferation of existing endothelial cells in hypoxic areas for vascularization. Circulating immune cells play a critical part in arteriogenesis. Recruited monocytes or macrophages to the ischemic tissue secrete growth factors that stimulate endothelial as well as smooth muscle cell proliferation that is required for collateral artery growth. CCL2 is an important chemokine noted to play a crucial role in arteriogenesis (85, 86). Throughout literature, several studies have described the role of the endothelium in neovascularization as well. For example, endothelium mediates arteriogenesis by regulation of eNOS levels (87).

Furthermore, endothelial cells are also known to regulate macrophage polarization that can help arteriogenesis after hindlimb ischemia (88). Another example highlights the role of activated endothelial cells in angiogenesis (89). Mice with deletion of Endothelial Angiotensin Type II receptor, type AT1a have suppressed immune cell recruitment and thus reduced angiogenesis and impaired blood flow. Another study highlights the role of endothelial H_2O_2 in regulating inflammatory processes. They used endothelial-specific catalase-overexpressing mice wherein H_2O_2 in endothelial cells is suppressed. These mice had impaired activation of ECs after ischemia as well as impaired recruitment of immune cells leading to impaired angiogenesis following hindlimb ischemia (90). Thus, the endothelium plays a critical role in controlling immune cell infiltration as well as regulating arteriogenesis and angiogenesis post-ischemia injury in the hindlimb.

Kidney ischemia-reperfusion injury

Acute kidney injury (AKI) following a kidney transplant is common in transplant patients (91). The development of chronic kidney disease (CKD) following AKI is also found to be prevalent and microvascular dysfunction plays an important role in the development of CKD (92). The primary cause of AKI following IR is hypoxia, causing reactive oxygen species (ROS) formation leading to tubular necrosis, increased infiltration of immune cells within the kidney, activation of the coagulation cascade which can lead to thrombi formation within vessels and further adds to hypoxia due to tissue hypoperfusion (93). Endothelial cell activation contributes significantly to such damaging processes. For example, activated endothelial cells reduce expression of thrombomodulin (94) and increase expression of TF (95) that can cause increased coagulation and thrombi formation in renal IRI. Also, the increase in endothelial surface expression of ICAM-1, VCAM-1, E and P-selectins increase leukocyte binding, and infiltration further exacerbates AKI (96). Endothelial vasotone regulation is highly affected during renal IRI. A decrease in nitric oxide synthase (NOS3) levels has been reported, which causes a decline in NO further decreasing vasodilation post reperfusion but enhances vasoconstriction. Vasoconstriction further enhances the damaging effect of hypoxia (97). However, endothelial dysfunction observed occurs transiently and is reversed upon healing over time. However, the loss of peritubular capillary density is not easily recovered and can lead to CKD (92) (98). It is hypothesized that peritubular cell loss is either due to endothelial cell death (99) or due to loss of endothelial cells to EndoMT in response to increasing in TGF-beta after renal IRI injury (100). Several therapies are thus targeted to replenish peritubular capillary density to ameliorate CKD (100). Thus, endothelial cells play an important role not only in the pathology of renal IRI but also the development of CKD after AKI.

Cardiac ischemia or ischemia-reperfusion injury

Cardiac ischemia or cardiac ischemia-reperfusion can occur during cardiopulmonary bypass surgery and transplant surgery (101). However, cardiac injury can also occur due to endothelial dysfunction, such as atherosclerotic coronary artery occlusion mediated injury (102). The role of endothelial dysfunction in cardiac injury is widely discussed ranging from sustained vasoconstriction due to suppressed NO and EDHF production (103),

increased endothelial cell activation leading to increased neutrophil influx which mediates a damaging effect via an increase in ROS production (78), to the increased microthrombi formation (104). However, under physiological conditions, endothelial cells can also modulate cardiomyocyte functions such as cardiomyocyte metabolism, growth and their contractility by releasing a variety of signaling molecules. For example, NO diffused from endothelial cells to cardiomyocytes regulates cardiomyocyte contractility, cardiac conduction and oxygen consumption (105). Such regulation of endothelium on cardiomyocytes can be affected in case of endothelial damage. Furthermore, apart from the initial inflammatory phase, endothelial cells can alter immune cell infiltration and thus modulate cardiac remodeling post-myocardial infarction (106, 107) or alter fibrosis in the infarct area via EndoMT (108). Also, after the initial injury phase, endothelial cells can still contribute to neovascularization of the infarct area (109). Thus, the protection of endothelial cells during cardiac injury could influence organ function and recovery as well.

1.5 Role of endothelial cell death in sepsis and ischemia/IRI models

As mentioned previously, endothelial cell death during pathologies such as sepsis has been reported in some studies (75-77), but the molecular mechanism underlying it is not known. Furthermore, the contribution of endothelial cell death to endothelial dysfunction during pathogenesis remains to be studied. Pathogenesis of ischemia or ischemia-reperfusion injury is known to be regulated by microvascular dysfunction. Such injury, however, can induce the activation of cell death pathways, which further can contribute to organ injury (110). However, endothelial cell death and its role in ischemia or ischemia-reperfusion injury are yet unclear (111). Furthermore, studies have equally highlighted the role of the endothelium in the recovery process after injury. Therefore, the study of endothelial cell death in the pathogenesis of severe sepsis, as well as the effect of endothelial cell death inhibition in different organs affected with ischemia or IRI, can give insight on the contribution of endothelial cell death in organ dysfunction post-injury.

2. AIM

The endothelium is involved in regulating essential vascular and organ functions, and endothelial dysfunction can lead to the onset or progression of several pathologies. While endothelial dysfunction like increased vascular barrier permeability and decrease in endothelial thromboresistance have been involved in diseases such as sepsis and ischemia-reperfusion injury, it is not clear whether and to which degree programmed endothelial cell death contributes to these diseases. The aim of this study was to investigate whether programmed cell death of endothelial cells occurs during these pathologies and to investigate the contribution of programed endothelial cell death by using several genetic as well as pharmacological tools.

3. MATERIALS

3.1 Chemicals/Reagents

1. Cell transfection reagents

Name	**Company**
Lipofectamine RNAiMAX	Invitrogen

2. Growth factors/ Recombinant protein/Agonist and antagonist

Name	**Company**
Tumor necrosis factor (TNF)-α	Peprotech
z-VAD(ome)-fmk	APExBIO
Nec-1	Enzo
Lipopolysaccharide (LPS)	Sigma

3. Western blot products

Name	**Company: Catalogue number**
29:1 Acrylamide/Bis Solution	Serva: 10687.03
FUJIFILM super RX	FUJIFILM: 4741008389
Immobilon western chemiluminescence HRP substrate	Millipore: WBKLS0500
Pageruler plus prestained protein ladder	Thermo scientific: SM1812
Pageruler prestained protein ladder	Thermo scientific: SM0672
Pierce ECL western blotting substrate	Thermo scientific: 32106
SuperSignal West FEMTO	Thermo scientific: 34094
TEMED	Applichem: A11480100
Whatman protran nitrocellulose transfer membrane	GE Healthcare: 10401196

4. Other reagents

Name	**Company:** **catalogue number**
Hoechst 33342	Sigma: B2261
Ethidium homodimer III (EthD-III)	Biotium: 40050
DAPI	Invitrogen: D1306

3.2 Buffers

Distilled water used to prepare all the solutions and was filtered.

Phosphate- buffered saline (PBS)	**For 1L**
NaCl (137 mM)	8 g
KCl (2.7 mM)	0.20 g
Na_2HPO_4 (10 mM)	1.44 g
KH_2PO_4 (2 nM)	0.24 g
Distilled water was added to the final volume of 1000 ml. pH was adjusted to 7.4 using HCl.	

Transfer buffer 10X	**For 5L**
Tris	151.4 g
Glycin	720 g
Distilled water was added to the final volume of 5 litres. pH was adjusted to 8.5 using HCl.	

Electrophoresis buffer 10X	**For 5L**
Tris	151.4 g
Glycine	720 g
SDS	50 g
Distilled water was added to the final volume of 5 litres. pH was adjusted to 8.5 using HCl.	

TBST 10X	**For 5L**
Tris	121.1 g
NaCl	1022 g
Tween20	25 ml
Distilled water was added to the final volume of 5 litres. pH was adjusted to 7.5 using HCl.	

Stacking gel buffer	**For 1L**
Tris	30.4 g
20% SDS	10 ml
Distilled water was added to the final volume of 1000 ml. pH was adjusted to 6.8 using HCl.	

Separating gel buffer	**For 1L**
Tris	90.8 g
20% SDS	10 ml
Distilled water was added to the final volume of 1000 ml. pH was adjusted to 8.8 using HCl.	

Laemmli Buffer 4X	**For 200 ml**
1M Tris pH6.8	40 ml
20%SDS	40 ml
0.5M EDTA	3.25 ml
H2O	6 ml
100% Glycerol	40 ml
ß-Mercaptoethanol	8 ml
Bromophenol blue	40 mg

Coomassie staining buffer	**For 250 ml**
Brilliant blue R250	0.5 g
Methanol/distilled water	200 ml (1:1)
Acetic acid	20.0 ml

Blocking buffer for western blot	
Non-fat milk powder	5 % in TBST
Bovine serum albumin	5% in TBST
Dissolved in TBST buffer and stored at 4°C.	

Stripping buffer	
SDS (10%)	20 ml
Tris HCl pH 6.8 0.5 M	12.5 ml
Distilled water	67.5 m
β-mercaptoethanol	800 µl
Mixed in distilled water.	

NP40 buffer	
Tris pH 7.2	10 mM
NP40	1 %
ß-glycerophosphate	1 mM
NaCl	150 mM
NaF	5 mM
Na3VO4	1 mM
Roche Protease Inhibitor	1 tablet /10 ml
Dissolved in distilled water and add protease and phosphatase inhibitors freshly.	

Radioimmunoprecipitation assay buffer (RIPA)	**RIPA 1**	**RIPA 2**	**RIPA 3**
NaCl	150 mM	150 mM	1 M
Tris pH 7.5	50 mM	50 mM	50 mM
DOC	0.25%	0,25 %	0,25 %
NP40	1%	1%	1%
SDS	1**%**	-	0.1%
EDTA	1 mM	1 mM	1 mM
EGTA	1 mM	1 mM	1 mM
PMSF	1 mM	1 mM	1 mM
Na_3VO_4	1 mM	1 mM	1 mM
NEM	2 mM	2 mM	2 mM
Roche Protease Inhibitor	1 tablet /10 ml	1 tablet /10 ml	1 tablet /10 ml
Dissolved in distilled water and add protease and phosphatase inhibitors freshly.			

3.3 Primers

RT-PCR primers

Primer	Sequence (5´-3´)
Human_CASP8	ggaaagcaatctgtccttcct
	cagcaaatccagtctattaattcg
Human_RIPK3	agaggagcaggttccacaag
	tctggagtctggggaggtt
Human_MAP3K7	gtgctgaaccattgccatatt
	ccactccttgggaacactgta
Bovine_GAPDH	tcaccagggctgcttttaat
	gaaggtcaatgaaggggtca
Bovine_CASPASE8	ggaccacaaaaacaaagactgc

	atcggagccatagatgatgc
Bovine_MAP3K7	ttttccactttagaatgggtattca
	gacctagtctagccatctttccat
Bovine_RIPK3	ggtgctcgggatgtgcta
	acattggagggcttgaggt

3.4 Antibodies

Name	**Company/ catalogue number**	**Dilution**	**Application**
ERG	Abcam (ab110639)	1:100 1:1000	IF WB
CD31	BD Biosciences (550274)	1:50	IF
Cleaved caspase-3	Cell Signal (9661S)	1:100	IF
Annexin V	Santa Cruz Biotechnology (sc-4252)	1:100	IF
α-tubulin	Sigma (T 9026)	1:3000	WB
GAPDH	Cell signaling (2118L)	1:3000	WB
VE-cadherin	Santa cruz (sc-6458)	1:1000	WB
Dystrophin	Life Technologies GmbH (PA121011)	1:200	IF
Ki67	Abcam (ab15580)	1:200	IF
CD68	Serotec (MCA1957)	1:200	IF
CD45	Biorad (MCA1031GA)	1:200	IF
Isolectin B4 (IB4)	Thermo Fischer Scientific (I32450)	1:200	IF

3.5 siRNAs (sigma)

Gene name	Target sequence (5'->3')
siTAK1 #1	GUGUUUACAGUGUUCCCAA
	UUGGGAACACUGUAAACAC
siTAK1 #2	CAAUAUCCUUGUCAGUAUU
	AAUACUGACAAGGAUAUUG

3.6 Cell lines

Name	Origin	Source
HUVEC	Human Umbilical Vein Endothelial Cells	LONZA
BAEC	Bovine aortic endothelial cells	LONZA

3.7 Kits

RNA isolation- RNAeasy Mini kit (Qiagen, Cata no. 47106)
cDNA synthesis kit (Roche)
TaqMan Probe Master (Roche)
Lightcycler 480 probes master (Roche)
Universal probe library set (Roche)
Mouse serum creatinine (Crystal Chem; Cat no: 80350)
Lactate dehydrogenase assay kit Colorimetric (Abcam Cat.no: ab102526)

3.8 Genetic mouse models

Control C57BL/6J animals were purchased from Charles River. TAK1$^{loxP/loxP}$ animals (112) crossed to Tamoxifen-inducible Tie2-CreER^{T2} animals to obtain Tie2-CreER^{T2};TAK1$^{loxP/loxP}$ animals (TAK1^{ECKO}). Caspase-8$^{loxP/loxP}$ animals were kindly provided by Stephen Hedrick (Department of Cellular and Molecular Medicine, UCSD, USA) and crossed to Tamoxifen-inducible Tie2-CreER^{T2};TAK1$^{loxP/loxP}$ animals to obtain Tie2-CreER^{T2}; TAK1$^{loxP/loxP}$;Caspase-

$8^{loxP/loxP}$ animals (TAK1;$Casp8^{ECdKO}$). Tie2-$CreER^{T2}$; $RIPK3^{loxP/loxP}$ were generated in the institute by Dr. Lida Yang (113). Mice were maintained under specific pathogen-free conditions. Protocols were performed according to institutional and national guidelines.

4. METHODS

4.1 Cell culture

HUVEC cells were cultured in growth factor-supplemented EGM-2 medium and passages <P7 were used for all experiments. Cells were seeded on cell culture plates coated with Collagen Type II solution. (Collagen Type II diluted 1:100 in sterile autoclaved 0.1% Acetic acid in MQ water). Cells were tested negative for mycoplasma contamination before experiments. All cells were incubated at 37°C and 5% CO_2. Confluent cells were washed with PBS for one time and treated with 0.25% Trypsin-EDTA solution for 1 to 3 min approximately until the cells were dissociated. Next, complete growth medium was added, and re-suspended cells were centrifuged for 4 min at 800 rpm and seeded onto the cell culture dish.

BAEC cells were cultured in growth factor-supplemented EGM-2 MV medium and passages <P10 were used for all experiments. Cells were seeded on cell culture plates coated with 1% Gelatin. Cells were tested negative for mycoplasma contamination before experiments. All cells were incubated at 37°C and 5% CO_2. Confluent cells were washed with PBS for one time and treated with 0.25% Trypsin-EDTA solution for 1 to 3 min approximately until the cells were dissociated. Next, complete growth medium was added, and re-suspended cells were centrifuged for 4 min at 800 rpm and seeded onto the cell culture dish.

4.2 siRNA transfection in cell lines

Cells were transfected using Lipofectamine RNAiMAX (Life Technologies) with different sets of siRNA (Sigma or Qiagen) and cultured on 6 well plates or 96 well plates.

Transfection mix preparation:
First tube:

Plates	**6 well**	**96 well**
Opti-MEM	150.0 µl	10 µl
siRNA	28.5 nM	28.5 nM

Second tube:

Plates	**6 well**	**96 well**
Opti-MEM	150.0 µl	10 µl
RNAiMAX	1.5 µl	0.05 µl

The two tubes were combined by gentle pipetting and incubation for 20 minutes at room temperature and then added to the medium.

The medium was changed 6 hours post-transfection. 16 hours later, a second transfection step was performed with medium change 24 hours post-transfection.

4.3 Protein expression analysis by western blotting

6 well plate of cells were directly lysed in 180 µl ice-cold RIPA lysis buffer (composition as described in *Materials*). Cell plate was scrapped with a scraper to collect entire lysate in cold 1.5 ml Eppendorf tube. The tubes were then placed in a constant vertical rotating wheel for 20 min at 4°C. After that, the lysates were centrifuged at 14000 rpm for 20 min at 4°C. 60 µl 4X Laemmli buffer was added to the supernatant and, boiled at 99°C for 5 min. Once the

tubes are cooled, they were centrifuges shortly and stored in -20°C. Denatured protein lysates were run by electrophoresis in 10% SDS-PAGE through stacking gel at 100V and through separating gel at 120 V. Protein separated by SDS PAGE were transferred onto nitrocellulose membrane by wet transfer method by applying 0.4 A for 2 hours. The membrane was blocked using blocking buffer (composition as described in *Materials*) for one hour at RT and incubated with respective primary antibody (as described in *Materials*) at 4°C overnight. The membrane was washed with TBST three times at RT and incubated with respective secondary antibody tagged with HRP for one hour at RT. The membrane was washed with TBST three times at RT again. Proteins to be detected were visualized using an enhanced chemiluminescence system (ECL) (GE Healthcare and Millipore).

4.4 mRNA expression analyses

Cells from 6 well plate were harvested, and RNA isolation and transcription was performed according to the manufacturer's protocols (Qiagen, Roche). Quality control of samples was carried out using Nanodrop ND-100 Spectrophotometer. RNA was reverse transcribed using the Transcriptor high fidelity cDNA synthesis kit (Roche) according to manufacturer's instructions. For quantitative RT–PCR using the Roche LightCycler480 Probes Master System, 30 ng cDNA per reaction were used. Primers were designed with the online tool provided by Roche, and only primer pairs from the top three results were chosen. Relative expression levels were obtained by normalizing with GAPDH.

4.5 Cell death assays and analysis

Cells were cultured in 96-well plates for 24 hours and treated with agonists upon confluency. In case of assays with gene knockdown cells, cells were transfected with siRNAs as per protocol (mentioned in the siRNA transfection protocol) and treated. 1.6 µM EthD-III was added to the medium overnight

culture before agonist treatment, and 2 µM was added shortly before automated image acquisition. Hoechst 33342 was used for all nuclear staining. Imaging was performed in a Controlled Atmosphere Chamber (37°C, 5% CO_2) using an Olympus IX81 microscope. Morphological criteria for discriminating apoptotic from necrotic cells as compared to living cells were defined as follows: a living cell appears with a normal round to kidney-shaped nucleus (as visualized by Hoechst) and is negative for EthD-III. An apoptotic cell appears with a strong condensed and frequently fragmented nucleus and is negative for EthD-III. A necroptotic cell appears with a normal round to kidney-shaped nucleus or with a minor degree of nuclear shrinkage (no condensation and no fragmentation) and is positive for EthD-III. A late apoptotic cell is positive for EthD-III but can be discriminated from a necrotic/necroptotic cell because of its strong condensation (and frequent fragmentation) of the nucleus. To all images to be analyzed, a Gaussian blur with a radius of 2 pixels was applied to prevent repeatedly counting of fragmented parts of apoptotic nuclei. The total number of cells was determined through a low threshold and application of a watershed on the resulting binary image overall Hoechst positive nuclei. The number of EthD-III-positive cells was determined through an independent second low threshold only. In cases where this automated analysis failed, the mode of cell death was determined manually for each endothelial cell by application of the criteria summarized above. All images were analyzed in ImageJ (NIH). Each experiment was performed at least three times with a minimum of six wells per condition and four independent images acquired per well.

4.6 Immunofluorescence

Organs were harvested from euthanized mice after whole-body perfusion with PBS and 4% PFA. Organs were fixed in 4% PFA overnight at 4°C and put in 10%, 20% and 30% sucrose each for one day in order. Organs were embedded in O.C.T. Tissue Tec solution (Sakura Finetechnical) and frozen on dry ice. 10 µm cryo-sections of the tissue were washed three times in PBS, incubated for 1 hour with 5% BSA in PBS + 0.1% Triton X-100 for blocking and

permeabilization, and sections were then incubated overnight with primary antibodies in suitable dilution. Slides were washed three times in PBS and then incubated for 1 h at room temperature with secondary antibodies and DAPI. After washing three times in PBS, slices were mounted in Mowiol and analyzed using the Leica TCS SP5 confocal microscope.

4.7 Genetic mouse models

For studies with WT mice, age and gender-matched c57bl6J mice were used. Endothelial-specific knockouts for TAK1, CASPASE8 and RIPK3 were generated by crossing Tie2-CreER^{T2} to mice with the respective homozygous floxed allele. To induce recombination, animals were treated with 5 x 1 mg/day tamoxifen (Sigma) intraperitoneally, and 7-9 days later experiments were started. For all experiments using knockouts, their Cre-negative littermates served as littermates.

4.8 Sepsis model

Sepsis was induced in mice by intraperitoneal (i.p.) injection of Lipopolysaccharide (LPS) from E.Coli (Sigma) solubilized in sterile PBS. Control mice were injected with PBS i.p. The severity of LPS-induced sepsis was altered by an increase in the dose of LPS injected. Mild sepsis (sublethal) was induced with a single injection of 10 mg/kg bd wt i.p. whereas severe sepsis was induced by injecting 15 mg/kg bd wt i.p. Progression of sepsis was monitored either via the record of sepsis score (a summation of the pre-assignment score for each symptom of endotoxemia) or via the record of core body temperature using DSI Temperature measurement telemeters.
For visualization and quantification of cell death, intravital staining of necrotic cell death by EthD-III injection via retroorbital plexus (ROP). After induction of severe sepsis, mice were sacrificed within 12 hours after LPS injection or earlier in case a humane end point is reached.

4.9 Hindlimb ischemia and hindlimb ischemia-reperfusion model

C57BL/6J mice, age-matched and sex-matched groups, were subjected to right limb femoral artery ligation (FAL) distally to the origin of the femoris branch using a 7-0 silk braided suture (Peasalls Sutures, Somerset, Great Britain).
For the hindlimb ischemia ischemia-reperfusion model, FAL was performed for 45 min, and ligation was released to allow perfusion. During the procedure, mice were anaesthetized using isoflurane and were maintained on a heating pad set at 37°C. The left limb underwent a sham operation and was used as control. EthD-III was injected i.v. 15 minutes before mice were euthanized. Adductor and gastrocnemius muscle was harvested to study cell death in these muscles after 2 hours of perfusion.
For hindlimb ischemia injury model perfusion of the paws was measured after permanent FAL using Laser Speckle Imaging system under temperature-controlled conditions. The paw perfusion measurements were performed before FAL (basal), immediately after FAL and then at 3d, 7d, 14d and 21 days after FAL. Colour-coded images of the paws representing the flux value were used to calculate the ratio of the tissue perfusion of the ligated to the sham-operated paw, i.e. R/L ratio.
Analysis of collateral artery growth was performed by harvesting adductor muscles at day 3 post-FAL and analyzed for vessel diameter.
Angiogenesis after FAL was measured at day 7 in gastrocnemius muscle by immunofluorescence staining of capillaries.

4.10 Bilateral kidney ischemia-reperfusion model

Adult age-matched and gender-matched mice were used in all experimental groups. Mice were treated with metamizole (200 mg/kg i.e. 0.8 ml/ 500 ml) via drinking water 2 days before surgery. Before the surgical procedure, all hair from the intended surgical area was removed, for surgery mice were anaesthetized with isoflurane. Buprenorphine 0.1 mg/kg was injected subcutaneously. Small incisions were made in the skin and muscle layer on the left and right retroperitoneal side. The kidneys were exposed by carefully separating them from the surrounding fat, and the adrenal glands were carefully

dislodged from the kidneys. The renal artery for the left and the right kidney was clamped with micro-serrefine (Fine science tools, 18055-05) for 30 min for mild ischemia and 37 min for severe ischemia. During ischemia, a damp gauze is placed on the surgical area. For reperfusion, the clamps are removed, and reperfusion was checked visually. The incisions were closed after reperfusion was performed. During the operative procedure, mice were placed on a heating pad maintained at 37°C. Post-surgery mice were treated with Buprenorphine 0.1m/kg twice daily until no more symptoms of pain were visible. To avoid dehydration, 0.9% NaCl was injected i.p. post-surgery. For the sham group, all the above-mentioned steps were included except clamping of the kidneys.
Histological analysis of cell death was performed via intravital staining of necrotic cells by EthD-III injection via ROP. Tissue injury post-IRI was analyzed via H and E staining of 10 µm sections of the paraffin-embedded organ.
Kidney function was studied by measurement of serum creatinine using Mouse creatinine enzymatic kit (Crystal Chem, Cat no: 80350) at different time points.

4.11 Cardiac ischemia-reperfusion injury and myocardial infarction model

Adult mice, age-matched and sex-matched were used in all experimental groups. Mice were treated with metamizole (200 mg/kg, i.e. 0.8 ml/ 500 ml) via drinking water, 2 days before surgery. Before the surgical procedure, all hair from the intended surgical area was removed. Buprenorphine 0.1 mg/kg was administered subcutaneously (s.c.) For surgery, mice were anaesthetized with isoflurane. A small incision was made in the neck to visualize the trachea intubation made using a 20-gauge intravenous catheter with a blunt end. Artificial ventilation was provided at a rate of 150 strokes per minute. Incision between the intercostal space was made such that the heart is visible. A piece of PE-10 tube is placed on the heart above the left coronary artery and is ligated using a Prolene suture (7-0), such that the pressure of the PE-tube blocks the Left anterior descending artery (LAD). Ischemia is confirmed by discoloration of the left ventricle. Ischemia is maintained for 45 min. For reperfusion, the PE-tube is carefully dislocated, which relieves the pressure from the LAD and reinstates blood flow. The chest cavity was closed with a silk suture (5-0). Mice

were extubated and allowed to recover. Thirty minutes after initiation of reperfusion, mice were injected EthD-III via retro-orbital plexus. Fifteen minutes post-injection, the mice were sacrificed, and hearts were harvested for histological analysis.

For myocardial infarction (MI) model, mice were prepared for surgery in a similar manner as for the ischemia-reperfusion model. However, for myocardial infarction, a permanent ligation was made to the LAD with a Prolene suture (7-0).

For heart, functional analysis post-MI, Magnetic resonance imaging (MRI) was used. MRI imaging was performed pre-surgery, 2 weeks post-surgery as well as 4 weeks post-surgery. Using Q.Mass v8.1 software, images from MRI were analyzed to obtain left ventricular function.

5.15 Statistical analysis

If not stated otherwise, one representative of at least 2-3 independently performed experiments is shown. Depicted are mean values ± SD or ± SEM as indicated in the figure legends. Statistical significance was defined as *$p < 0.05$; **$p < 0.01$; ***$p < 0.001$; n.s., not significant. Statistical analysis was performed using GraphPad Prism6 or using Excel.

5. ABBREVIATIONS

AKI	Acute kidney injury
APAF-1	Apoptosis protein activatiung factor-1
ARDS	Acute respiratory distress syndrome
COX-2	Cyclooxygenase-2
CYLD	Cylindromatosis Lysine 63 deubiquitinase
DAMP	Damage assciated molecular pattern
DAPI	4′,6-diamidino-2-phenylindole
DIC	Disseminated intravascular coagulation
EC	Endothelial cell
EDHF	Endothelial-derived hyperpolarizing factor
EPCR	Endothelial protein C receptor
ET-1	Endothelin 1
EthD-III	Ethidium homodimer - III
FADD	Fas-associated death domain protein
FAL	Femoral artery ligation
HMGB1	High mobility group protein 1
ICAM-1	Intracellular cell adhesion molecule 1
IF	Immunofluorescence
IFN-gamma	Interferon gamma
IRI	Ischemia-reperfusion injury
JAM	Junctional adhesion molecule
LAD	Left anterior descending artery
LDH	Lactate dehydrogenase
LPS	Lipopolysaccharide
MAPK	Mitogen-activated pathway kinase
MCP1	Monocyte chemoattractant protein 1
MI	Myocardial infarction
MIP-2	Macrophage inflammatory protein 2
MLKL	Mixed lineage kinase like pseudokinase
Nec-1	Necrostatin-1
NF-kB	Nuclear factor kappa-light-chain-enhancer of activated B cells

NO	Nitric oxide
NOS	Nitric oxide synthase
PAI-1/2	Plasminogen activator inhibitor-1/2
PAMP	Pathogen associated molecular pattern
PCD	Programmed cell death
PECAM1	Platelet endothelial cell adhesion molecule 1
PGI2	Prostacyclin
PI3K	Phosphoinositide 3 kinase
PRR	Pathogen recognition receptor
RIPK1/2	Receptor interacting protein kinase 1 and 2
ROS	Reactive oxygen species
SIRS	Systemic inflammatory response syndrome
SMC	Smooth muscle cells
TAK1	Transforming growth factor beta-activated kinase 1
TFPI	Tissue factor pathway inhibitor
TLR	Toll-like receptor
TNF-alpha	Tumor necrosis factor alpha
TNFR1	TNF receptor 1
tPA	tissue plasminogen activator
TRADD	TNF-receptor associated death domain protein
TRAF2	TNF-receptor associated factor 2
TRAF5	TNF-receptor associated factor 5
TRAIL	TNF-related apoptosis-inducing ligand
TXA2	Thromboxane 2
VCAM-1	Vascular cell adhesion molecule 1
WPB	Weibel palade bodies
zVAD	z-VAD-FMK

6. RESULTS

6.1 LPS-induced sepsis causes programmed necrosis in lung endothelial cells which further complements inflammation

6.1.1 Lung cells undergo apoptotic and necrotic cell death in LPS-induced sepsis

Severe sepsis with organ dysfunction is caused due to a dysregulated inflammatory response with the release of cytokines like TNF-alpha, in response to several factors including PAMP, DAMPs leading to tissue injury due to cell death. Several publications to date have reported cell death in different organs in septic mice (114-116). However, some studies have provided evidence of cell death by detecting cell death via TUNEL staining, which does not accurately describe the type of programmed cell death. IF/IHC staining of proteins marking cell death, which are performed after fixation and organ harvest, may underestimate cell death occurring by necrotic rupture. In order to better detect and quantify cell death, we performed intravital staining with cell-membrane impermeable dye Ethidium homodimer-III (EthD-III) which can stain necrotic cells as well as secondary necrosis in apoptotic cells (117). EthD-III was injected i.v. 15 minutes before euthanizing mice. We then performed immunostaining for cell death markers post-fixation of the organs. In order to distinguish between apoptotic and necrotic cells, we performed immunostaining with cleaved caspase 3 antibody. Cleaved caspase 3 is an executioner caspase causing apoptotic cell death. Hence, cells positive for cleaved caspase 3 are deemed apoptotic. Cells positive for both cleaved caspase 3 and EthD-III, are characterized as late apoptotic cells since they are apoptotic cells undergoing secondary necrosis and hence positive for both markers. Cells which are only positive for EthD-III alone are necrotic cells.

A lethal dose of LPS can lead to the development of systemic inflammatory response, which can further develop into severe sepsis with organ failure. This progression of sepsis in mice was monitored by recording scores, based on a predetermined scoring scheme for each symptom of sepsis, as described

previously (118) and we used the same scoring scheme for our LPS-induced sepsis model (Figure 1A).

A

VARIABLE	SCORE AND DESCRIPTION
Appearance	0- Coat is smooth 1- Patches of hair piloerected 2- Majority of back is piloerected 3- Piloerection may or may not be present 4- Mouse appears emaciated
Level of consciousness	0- Mouse is active 1- Mouse is active but avoids standing upright 2- Mouse activity is noticeably slowed. The mouse is ambulent 3- Activity is impaired. Mouse only moves when provoked. 4- Activity is severely impaired
Activity	0- Normal amount of activity 1- Slightly suppressed activity 2- Suppressed activity with occasional movements 3- No activity. Mouse is stationary 4- No activity with tremors in hindlimb
Response to stimulus	0- Strong response to touch 1- Moderate response to touch 2- Mild response to touch 3- Little or no response to touch 4- No response to touch. Cannot right itself if pushed over
Eyes	0- Open 1- Eyes not fully open, possibly with secretions 2- Eyes half-closed, possibly with secretions 3- Eyes half-closed or more, possibly with secretions 4- Eyes closed or milky
Respiration rate	0- Normal, rapid mouse respiration 1- Slightly reduced respiration (rate not quantifiable by eye) 2- Moderately reduced respiration 3- Severely reduced respiration (rate is easily countable by eye) 4- Extremely reduced respiration (>1 s between breaths)
Respiration quality	0- Normal 1- Brief periods of laboured breathing 2- Laboured, no gasping 3- Laboured with intermittent gasps 4- Gasping

B

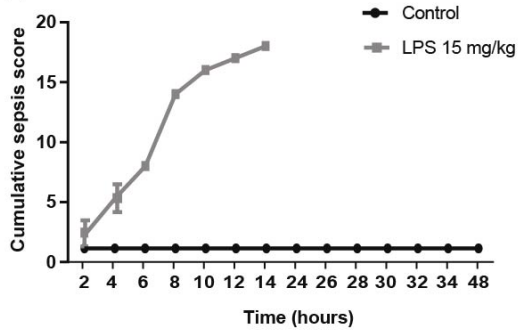

Figure 1: Sepsis scoring scheme

(A) Shown is the scoring scheme for determination of sepsis progression. (B) Sepsis score after LPS (15 mg/kg) i.p. injection.

The severity of sepsis was determined based on the cumulative score. According to the scoring scheme previously established, cumulative sepsis score of 3 indicated development of SIRS (characterized by the development of systemic inflammatory response) whereas higher scores indicate development of sepsis. In our sepsis model, C57BL/6J mice were injected with a lethal dose of LPS (15 mg/kg) i.p. With this dose of LPS, a sepsis score ≥ 6 was attained around 6 hours after injection (Figure 1B). Hence, at 6 hours when the mice have developed sepsis, they were injected with EthD-III i.v. and euthanized for organ harvest. Organs like lung, kidney, liver and aorta were checked for positivity of cell death markers EthD-III and cleaved caspase 3. Confocal imaging of the lung section showed an increase in EthD-III positive cells as well as cleaved caspase 3 positive cells as early as 6 hours after LPS injection (Figure 2). We did not observe an increase in either of the cell death markers in sections from the liver, the kidney and the aorta (Figure 2). Therefore, to further study cell death during LPS-induced sepsis we focused on the lungs of septic mice.

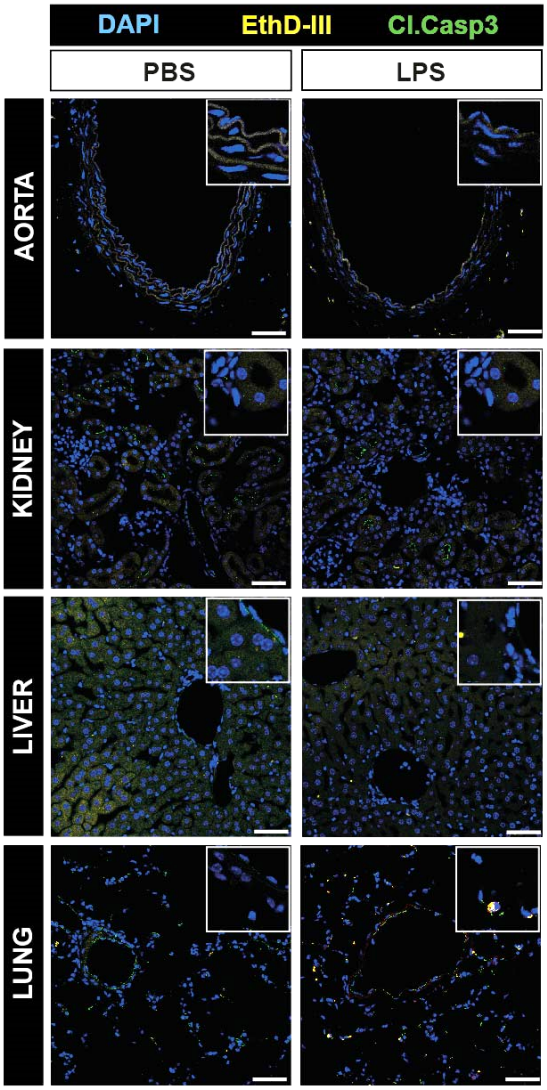

Figure 2: Cell death in different organs during LPS-induced sepsis

Shown are representative confocal images of the aorta, kidney, liver and lung sections stained with indicated markers from C57BL/6J mice injected with LPS (15 mg/kg) i.p. after 6 hours. PBS injected mice served as controls. Bar length: 50 µm. The inset image shows zoomed in image of DAPI positive cells (blue) with or without EthD-III (yellow) and cleaved caspase 3 (green) staining.

In order to determine the extent of cell death in lungs during the progression of sepsis from mild to severe sepsis, we quantified the degree of cell death at different time-points. According to the scoring scheme, sepsis progresses rapidly to a severe condition from 6 to 16 hours after LPS injection. Hence, we analyzed cell death in the lungs at 6, 9 and 12 hours after LPS injection before

humane end point is reached. Confocal imaging of lung sections revealed cleaved caspase 3 positive cells as well as cells positive for EthD-III (Figure 3A) at each time point. However, compared to cleaved caspase 3 positive cells, a higher percentage of cells were EthD-III positive (Figure 3B and C). Notably, the cumulative percentage of cells undergoing cell death (i.e. cells which are both apoptotic and necrotic) was also observed to increase over time.

Further, the extent of necrosis was also determined by measuring lactate dehydrogenase enzyme (LDH) activity in the serum. LDH is a ubiquitously expressed intracellular enzyme that is released from the cells undergoing necrosis. Hence, levels of LDH in the serum can indicate the extent of necrosis. We observed increased LDH at 12 hours after LPS injection in septic mice compared to controls (Figure 3D).

In summary, we observed cell death both by apoptosis and necrosis in the lungs and cell death was found to be highest at the stage the mice have acquired severe sepsis indicated by a high sepsis score (Figure 1B).

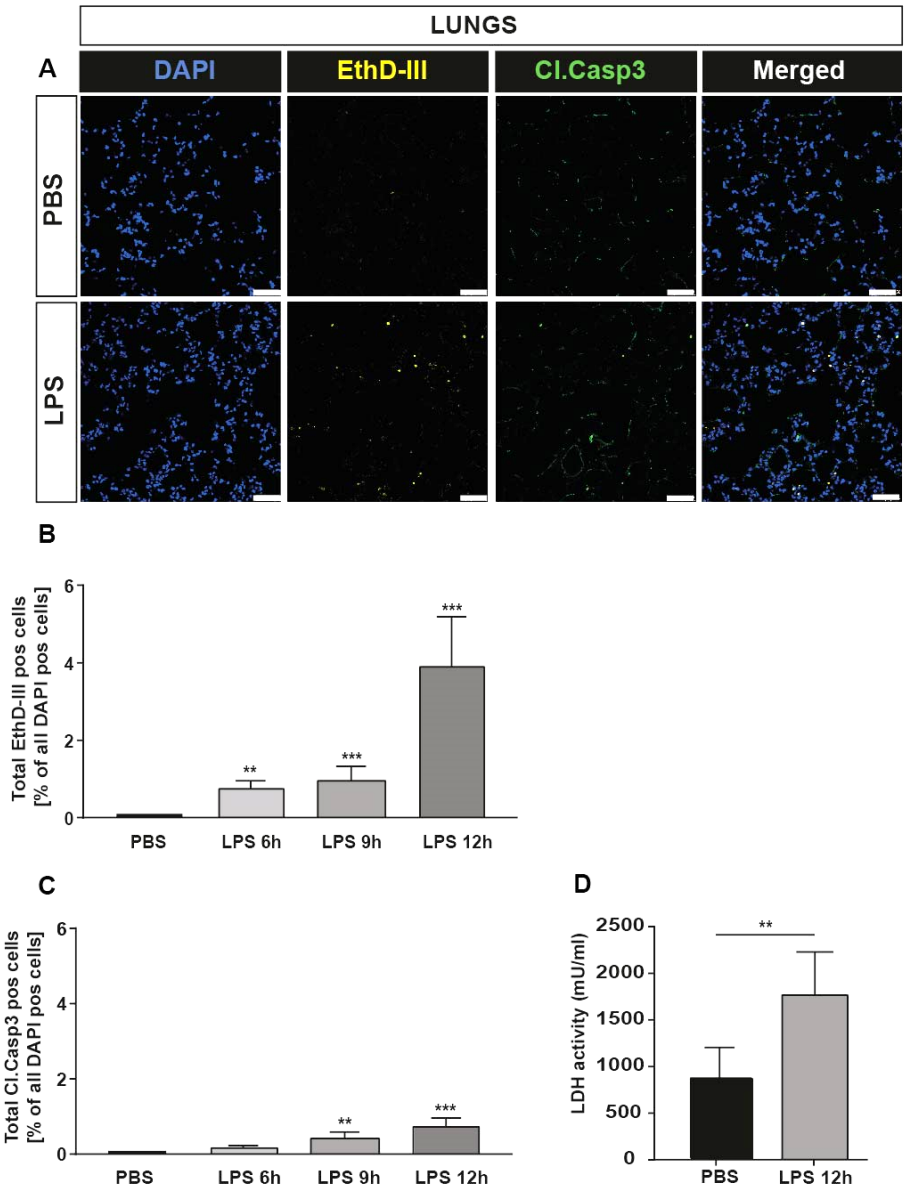

Figure 3: Lung cells undergo cell death during LPS-induced sepsis

(A) Shown are representative confocal images of lungs from PBS and LPS injected mice 12 hours after LPS (15 mg/kg) i.p. injection and stained with indicated markers. Bar length: 50 µm. (B) Quantification of EthD-III positive cells (yellow) and (C) cleaved caspase 3 positive cells (green) in lungs at indicated time points. (n=4 mice per group). (D) Serum LDH activity measured at 12 hours after LPS injection. (n=4 mice per group). (B-D) Shown are representative data with mean values ± s.d. $^{**}P < 0.01$; $^{***}P < 0.001$. Statistical analysis was performed using One-way ANOVA and Bonferroni's post hoc test (B, C) and unpaired two-tailed Student's t-test (D).

6.1.2 Lung endothelial cells undergo necrosis during severe sepsis

We further examined which cell type was mainly affected during severe sepsis. Through literature, we know that during sepsis several cell types in different organs can undergo cell death depending on the infectious agent and route of infection, for example, hepatocytes (119), renal tubular epithelial cells (120), leukocytes (121, 122) and endothelial cells (123) can undergo cell death. In order to determine the predominant type of cells undergoing cell death in the lungs, we first performed IF staining of lung sections with endothelial markers CD31 and ERG as well as leukocyte marker CD45 (Figure 4A and B). Interestingly, a majority of cells undergoing necrosis, stained positive for CD31 and ERG (Figure 4A). Quantifications of the lung endothelial cells (ECs) undergoing cell death was performed by analyzing the number of cleaved caspase 3 or EthD-III cells double positive for CD31. The quantification showed a similar pattern mentioned previously, with a majority of ECs undergoing necrosis as compared to apoptosis (Figure 4C and D). However, it was noted that some cells that were EthD-III and CD31 positive were ERG negative. Very few (less than 0.5 %) CD45 positive cells were EthD-III positive.

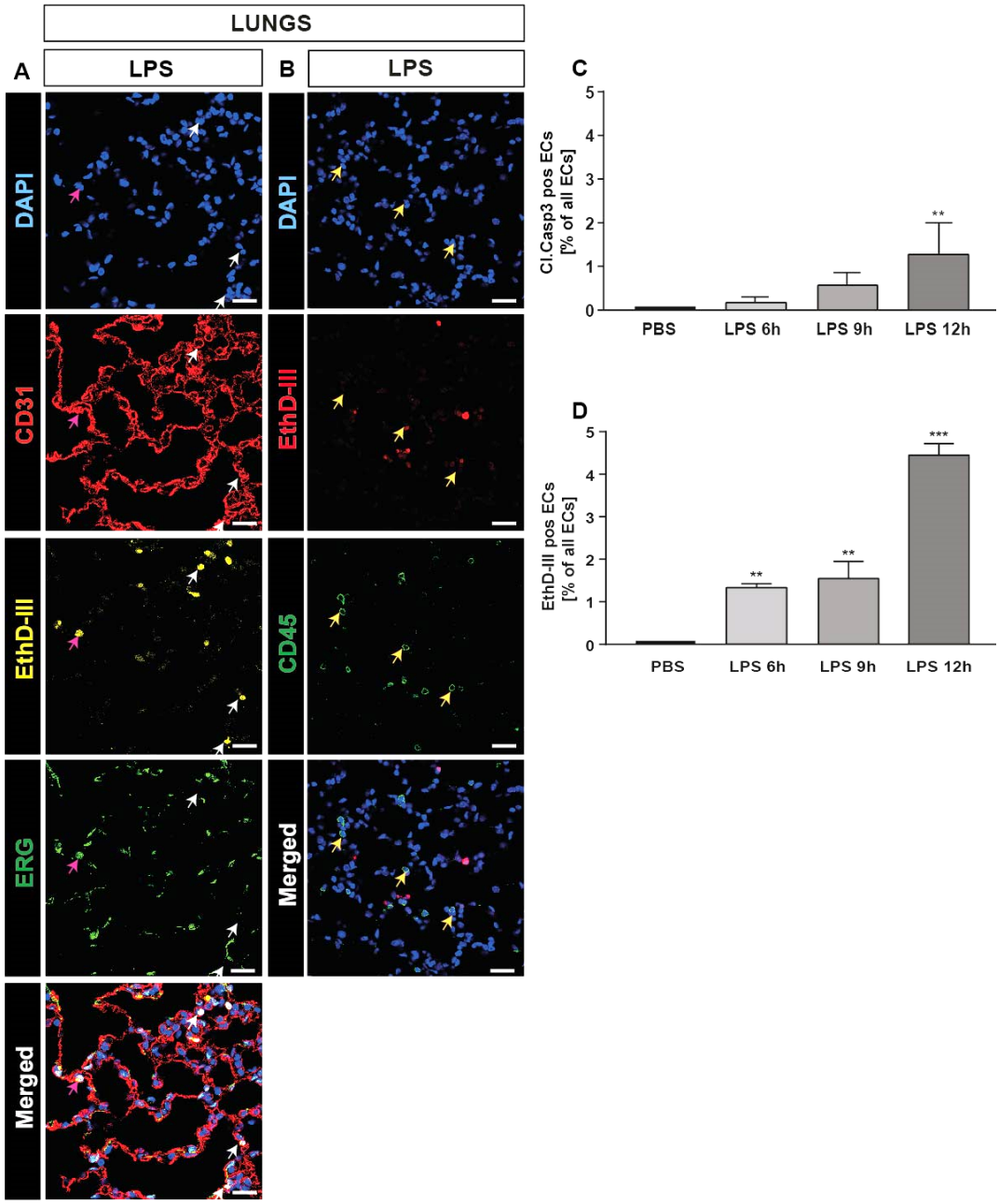

Figure 4: Lung endothelial cells undergo necrosis during LPS-induced sepsis

(A) Shown are representative confocal images of lungs 12 hours after LPS (15 mg/kg) i.p. injection. White arrows indicate cells that are EthD-III (yellow) and CD31 (red) positive but negative for ERG (green). Magenta arrows indicate cells that are positive for ERG, CD31 and EthD-III. (B) Shown are representative confocal images of lungs 12 hours after LPS (15 mg/kg) i.p. injection. Bar length: 30 µm Yellow arrows indicate CD45 positive cells (green) which are negative for EthD-III (red). Quantification of (C) cleaved caspase 3 and CD31 double positive cells and (D) EthD-III and CD31 double positive cells in lungs at indicated time points. (C,D) Shown are representative data with mean values ± s.d. (n=4 mice per group). $^{**}P < 0.01$; $^{***}P < 0.001$. Statistical analysis was performed using One-way ANOVA and Bonferroni's post hoc test (C, D).

6.1.3 LPS-induced sepsis causes RIPK1-mediated necroptosis, and inhibition of RIPK1 can prolong survival in septic mice

In order to determine whether the lung cells were undergoing regulated necrosis we treated C57BL/6J mice with a lethal dose of LPS (15 mg/kg) i.p. additionally with Necrostatin-1 (Nec-1), an inhibitor of RIPK1. RIPK1 is a known positive regulator of necroptosis (regulated necrosis). Nec-1 (6 mg/kg) was injected i.v. 15 minutes before and 6 hours after LPS injection (Figure 5A). IF staining of lung sections revealed that mice treated with Nec-1, had significantly reduced number of EthD-III positive cells, as compared to mice that received no Nec-1 treatment (Figure 5B and C). The percentage of cleaved caspase 3 positive cells was not decreased (Figure 5D). Since Nec-1 treatment could reduce EthD-III positive cells, this indicated that necrosis in lungs of septic mice was caused by RIPK1 and hence could be abolished upon RIPK1 inhibition.

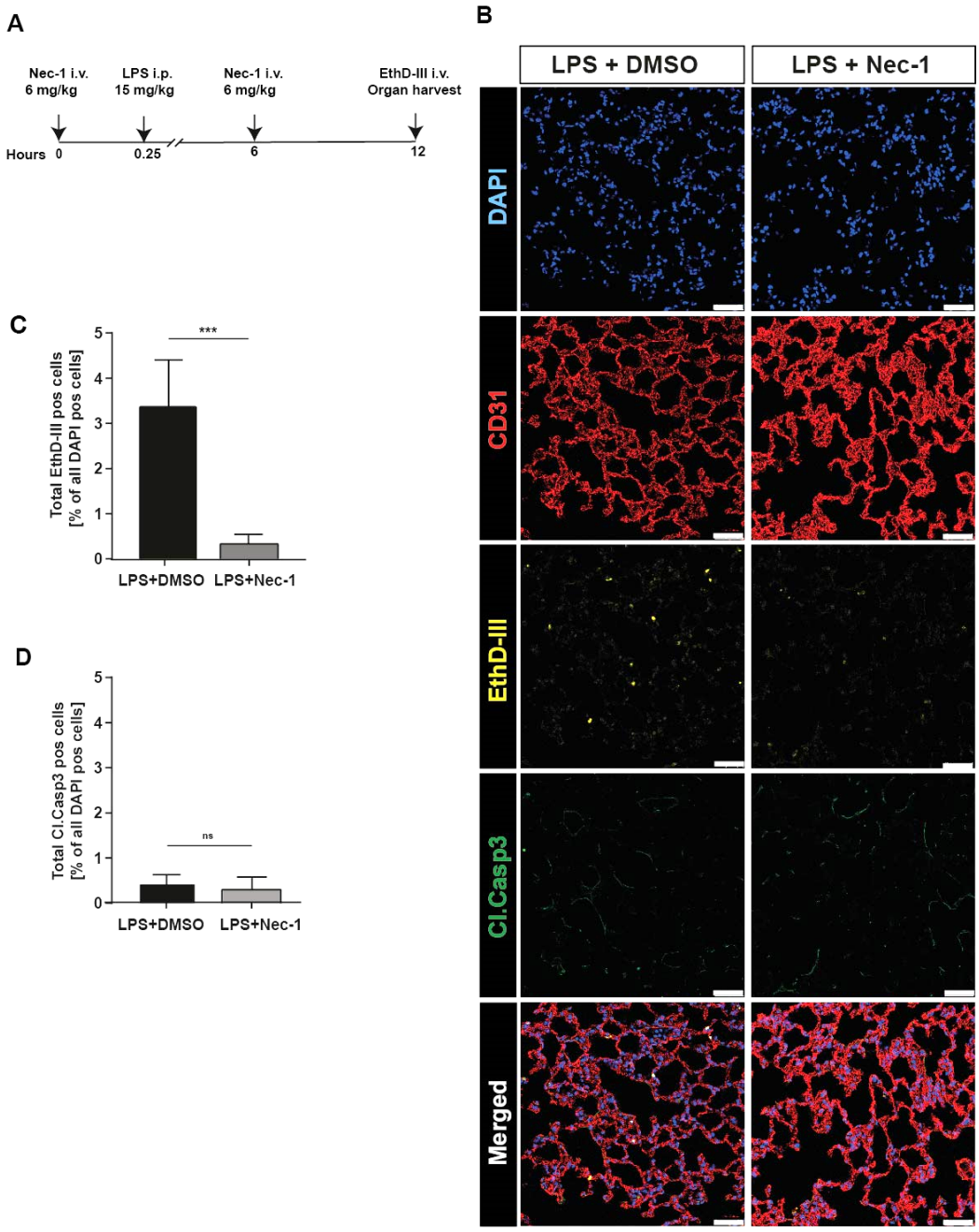

Figure 5: Programmed necrosis induced in LPS-induced sepsis is inhibited upon Nec-1 treatment

(A) Experimental layout. (B) Shown are representative confocal images of lungs from C57BL/6J mice at 12 hours, after LPS (15 mg/kg) + DMSO injection and mice with LPS (15 mg/kg) + Nec-1 (6 mg/kg) i.v. injection, stained with indicated markers. Bar length: 50 µm. Quantification of (C) EthD-III positive cells and (D) cleaved caspase 3 positive cells in the lungs. (C,D) Shown are representative data with mean values ± s.d. (n=4 mice per group) ns= not significant; ***P < 0.001. Statistical analysis was performed using unpaired two-tailed student's t-test (C, D).

To further evaluate whether necroptosis inhibition can affect sepsis severity, we monitored survival in control, and Nec-1 treated mice (both at a low dose and a

high dose) (Figure 6A), we observed that the Nec-1 treated mice had prolonged survival compared to the control mice (Figure 6B and C). This prolonged survival by Nec-1 treatment indicated a strong role of RIPK1-mediated cell death in LPS-induced sepsis progression. Thus, we could conclude that LPS-induced sepsis causes RIPK1-mediated programmed necrosis or necroptosis in lung endothelial cells and prolonged survival after Nec-1 treatment in septic mice indicated that inhibition of RIPK1-mediated necroptosis also influences sepsis progression.

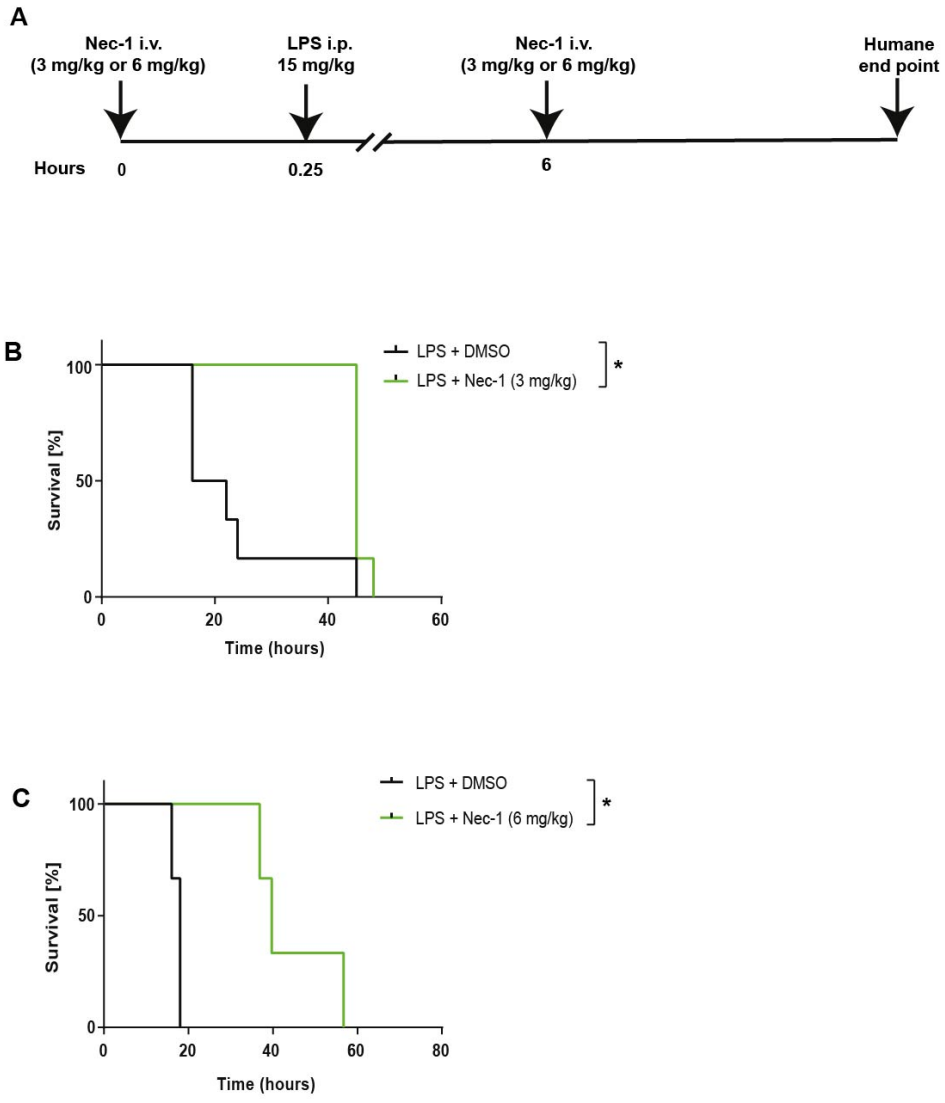

Figure 6: Inhibition of programmed necrosis by Nec-1 prolongs survival in Nec-1 treated septic mice.

(A) Experimental layout. Shown are Kaplan-Meier survival curves of C57BL/6J mice treated with LPS (15 mg/kg) + DMSO and (B) Nec-1 (3 mg/kg) or (C) Nec-1 (6 mg/kg) i.v. (n=4 mice per condition). *$P < 0.05$. Statistical analysis was performed using the Mantel-Cox test (B, C).

6.1.4 LPS induces endothelial necroptosis upon caspase inhibition *in vitro*

Histological examination of lungs showed that LPS-induced sepsis causes endothelial necroptosis. The inflammatory cytokines produced during sepsis, for example, TNF-alpha can also cause this endothelial necroptosis (33). However, whether LPS itself can induce EC necroptosis is unclear.

To test whether LPS can induce endothelial cell death, we treated Bovine Aortic Endothelial cells (BAEC) with LPS. We preferred to use BAECs since they have a relatively higher expression of mCD14 compared to passaged Human umbilical vein endothelial cells (HUVECs) (124). During our studies, we found HUVECs to be more resistant to LPS-induced cell death owing to reduced mCD14 levels upon passaging. Thus, we performed all *in vitro* analysis in BAECs.

To visualize cell death, BAECs were stained with Hoechst 33342 and EthD-III, 12 hours after LPS treatment. EC death was determined by morphological characteristics of cells previously described (113). Cells with Hoechst 33342 positive fragmented nuclei alone or cells with fragmented nuclei along with EthD-III positive staining were categorized as apoptotic cells and late apoptotic cells respectively. Cells with intact nuclei and cell swelling, along with EthD-III positivity were categorized as necrotic. We observed that BAECs upon LPS treatment undergo cell death (i.e. both apoptosis as well as necrosis) in a dose-dependent manner (Figure 7A).

To further determine the type of programmed cell death induced in BAECs by LPS, we treated LPS stimulated cells with inhibitors of key cell death regulators. The pan-caspase inhibitor z-VAD-FMK (zVAD) can inhibit apoptosis regulated by caspases and RIPK1 inhibitor Nec-1, which can inhibit apoptosis to only a certain extent as well as necroptosis (125). To inhibit LPS-induced apoptosis, we treated cells with zVAD. However, zVAD itself could not inhibit cell death, but instead, there was a shift from apoptosis to necrosis. This necrotic cell death induced in cells with LPS + zVAD treatment could be completely inhibited by additional treatment with Nec-1 (Figure 7B). The induction of necrosis in LPS-treated BAECs upon zVAD treatment could be visualized (Figure 7C).

Since the necrosis induced in BAECs after LPS + zVAD treatment could be inhibited by a RIPK1 inhibitor, we conclude that LPS induces in ECs RIPK1-mediated necrosis (or necroptosis) (Figure 7C).

Taken together, the *in vitro* data shows that LPS induces endothelial necroptosis where caspase activity is dispensable, and hence upon caspase inhibition, ECs can still undergo necroptosis which can be inhibited by Nec-1 treatment.

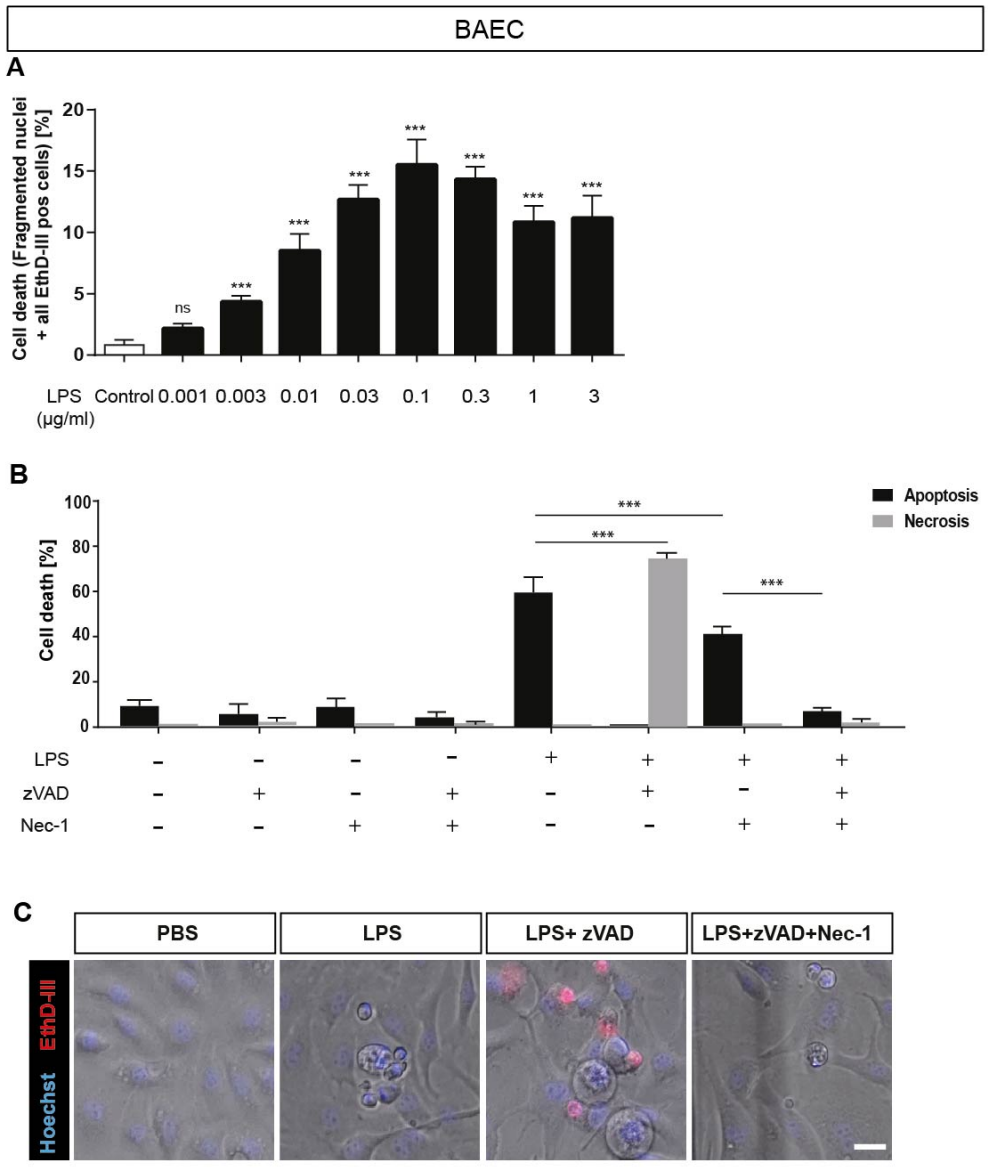

Figure 7: LPS induces endothelial necroptosis *in vitro*

(A) Quantification of cell death (both apoptotic and necrotic) in BAECs upon treatment with LPS (at indicated concentrations) for 12 hours. (B) Quantification of cell death in BAECs, by apoptosis or by necrosis, after 12 hours LPS treatment and in the presence or absence of Nec-

1 (30 μM) or zVAD (100μM). (C) Representative live cell images of BAECs labelled with Hoechst 33342 (2 μM) and EthD-III (1.5 μM), undergoing apoptosis upon LPS (0.1 μg/ml) treatment, necrosis upon LPS (0.1 μg/ml) + zVAD (100μM) treatment and rescue of cell death upon LPS (0.1 μg/ml) + zVAD (100 μM) + Nec-1 (30 μM) treatment for 12 hours. ns= not significant; ***P < 0.001. (A,B) Shown are representative data from two independent experiments with mean ± s.d. (n= 6 wells per condition). (A, B) Statistical analysis was performed using one-way ANOVA and Bonferroni's post hoc test

6.1.5 TAK1 deletion in endothelial cells sensitizes them to LPS-induced necroptosis *in vitro*

In vivo, we observed lung endothelial necroptosis increases with the severity of sepsis (Figure 4A, C and D) and pharmacological inhibition of necroptosis by Nec-1 (not specific to the endothelium) delays sepsis progression (Figure 6B and C). Since inhibition of necroptosis delayed sepsis progression, we questioned whether endothelial necroptosis significantly contributes to sepsis progression, i.e. specifically whether it is a cause or a consequence of severe sepsis. To understand this causal link, we sought to generate a model with increased endothelial necroptosis and to observe its influence on sepsis progression. For this purpose, we chose TAK1 as a candidate gene, which is known to regulate endothelial cell death (30).

TAK1 is one of the molecular mediators of the NF-kB pathway and also a negative regulator of necroptosis (30, 33). However, the function of TAK1 is dependent on cell type and stimuli (32, 126). Endothelial TAK1 has been shown previously to play a critical role in ECs survival. Previous work by our group has shown that deletion of TAK1 sensitizes ECs to necroptotic cell death and can facilitate increased tumor metastasis (33). To first analyze whether TAK1 is involved in LPS-induced endothelial necroptosis, we tested whether TAK1 deletion in ECs also influences LPS-induced cell death *in vitro*.

Therefore, we first transiently knocked-down TAK1 in BAECs using siRNAs. Knockdown efficiency of two different TAK1-targeting siRNAs was checked (Figure 8A). To determine whether TAK1 silencing affects EC survival, we analyzed BAEC cell death via live cell imaging after siRNA-mediated TAK1 knockdown. We observed knockdown of TAK1 in BAECs increases cell death

(i.e. a combined increase in apoptotic as well as necrotic cell death) *in vitro* (Figure 8B).

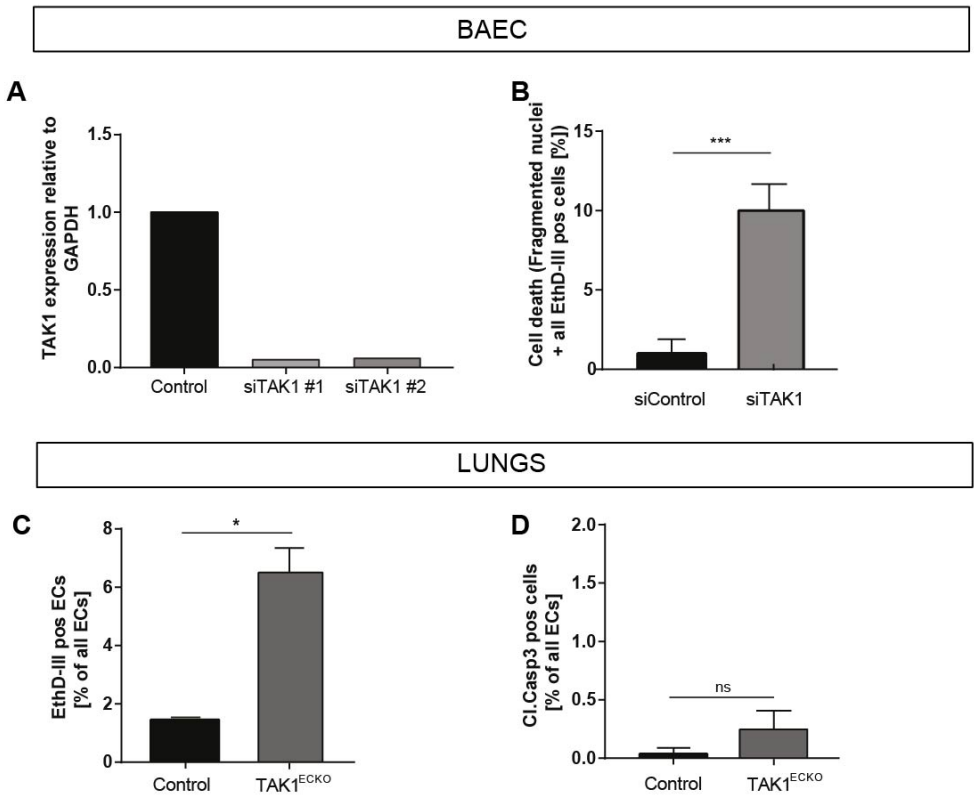

Figure 8: TAK1 regulates endothelial cell death *in vivo* and *in vitro*

(A) TAK1 knockdown efficiency in BAECs. (B) Quantification of cell death in BAECs upon transient TAK1 knockdown (n=6 well per condition). Quantification of endothelial cells undergoing (C) necrosis and (D) apoptosis in lungs of $TAK1^{ECKO}$ mice compared to Cre-negative control mice at day 14 after tamoxifen induction. (C-D) Shown are representative data from two independent experiments with mean ± s.d. (n=4 mice per group). ns= not significant; **P* < 0.05; ****P* < 0.001. Statistical analysis was performed using unpaired two-tailed Student's t-test (B-D).

To test whether TAK1 deletion influences LPS-induced endothelial necroptosis, siTAK1 and siControl BAECs were treated with LPS (0.1 µg/ml) for 12 hours (Figure 9A). We observed an increase in ECs undergoing apoptosis in siTAK1 ECs as compared to siControl ECs upon LPS treatment (Figure 9C). Upon zVAD mediated caspase inhibition, siTAK1 ECs treated with LPS had a significant increase in EthD-III positive necrotic cells compared to siControl, which could be inhibited upon additional Nec-1 treatment (Figure 9B).

From the *in vitro* cell death analysis, we could conclude that ECs with TAK1 deficiency have increased susceptibility to LPS-induced necroptosis.

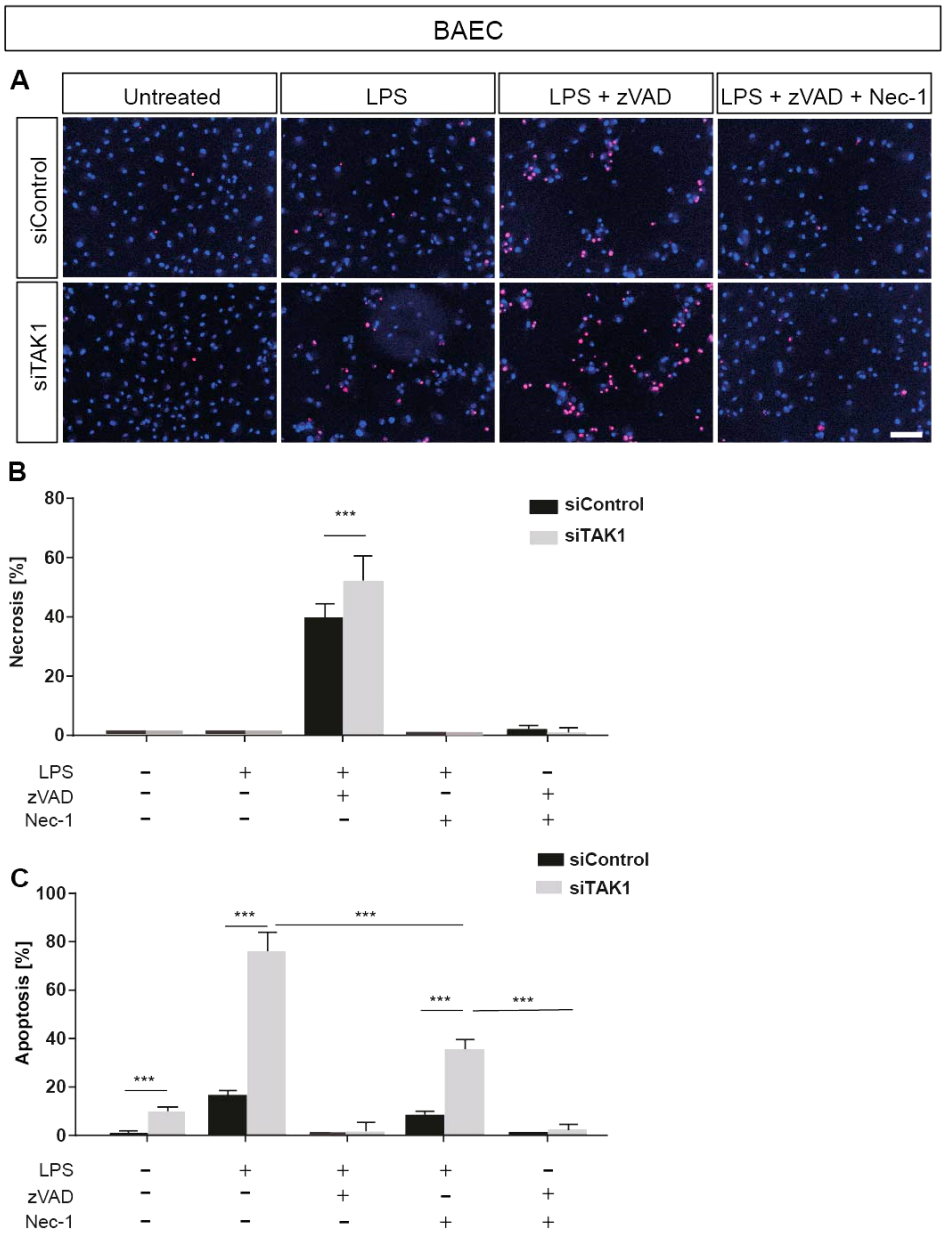

Figure 9: TAK1 deletion sensitizes ECs to LPS-induced necroptosis

(A) Representative images of siControl and siTAK1 BAECs undergoing cell death upon LPS (0.1 µg/ml) treatment in the presence and/or absence of zVAD (100µM) and Nec-1 (30 µM) after 12 hours. Cells are stained with Hoechst 33342 (blue) and EthD-III (red). Quantification of BAECs undergoing (B) necrosis and (C) apoptosis upon LPS treatment in siTAK1 ECs compared to siControl. (B-C) Shown are representative data from two independent experiments with mean values ± s.d. (n=6 wells for each condition). ***P < 0.001. Statistical analysis was performed using two-way ANOVA and Bonferroni's post hoc test (B, C).

6.1.6 TAK1 deletion in endothelial cells sensitizes them to LPS-induced sepsis *in vivo*

For *in vivo* endothelium-specific TAK1 deletion, we used tamoxifen-inducible endothelial-specific TAK1 knockout mice (Tie2-CreER^{T2};TAK1$^{fl/fl}$ (TAK1^{ECKO})). Knockout was induced by tamoxifen injection i.p. at 1 mg/kg per day for 5 days. At day 14 mice were injected i.v. with EthD-III and euthanized for organ harvest. Histological analysis for cell death markers in lung sections of TAK1^{ECKO} mice showed an increase in EthD-III positive ECs (Figure 8C) compared to the Cre-negative (Control) mice. There was no increase in cleaved caspase 3 positive ECs (Figure 8D) of the lungs. Thus, TAK1 deletion in lung ECs is found to increase endothelial necroptosis under basal conditions *in vivo*. Deletion of TAK1 in ECs does not affect lung function and vascular barrier integrity (33).

As mentioned before, we aimed to verify whether increased endothelial necroptosis causes increased sepsis severity. From our, *in vitro* results (Figure 9A-C), we know that ECs with TAK1 deletion have increased susceptibility to necroptosis upon LPS treatment. Therefore, to determine whether increased endothelial necroptosis increases sepsis severity, we studied sepsis progression in TAK1^{ECKO} mice.

We induce sepsis in TAK1^{ECKO} mice and Cre-negative controls with a sublethal dose of LPS at 10 mg/kg i.p. A sublethal dose of LPS does not cause severe sepsis and mice generally recover from it without organ failure. Sepsis progression can be monitored by measuring core body temperature as the severity of sepsis positively correlates with a reduction in body temperature (68, 127, 128). For an uninterrupted and reliable assessment of sepsis progression, we monitored core body temperature using telemeters implanted in the peritoneal cavity of the mice. The temperature was recorded every 5 minutes; 24 hours before LPS treatment and measurements were continued after LPS injection for longer period. The TAK1^{ECKO} mice displayed a rapid decrease in body temperature compared to control mice (Figure 10A) and increased mortality compared to control mice (Figure 10C) at a sublethal dose of LPS.

Thus, TAK1^{ECKO} mice were found to be more sensitized to LPS-induced sepsis and displayed an accelerated progression of sepsis and increased mortality compared to control mice.

In order to determine whether this effect of TAK1 deletion on sepsis progression can be rescued by inhibition of necroptosis or apoptosis specifically in ECs, we genetically deleted pro-apoptotic regulator Caspase 8 or pro-necroptotic regulator RIPK3 in TAK1 deleted mice. Deletion of RIPK3 can abrogate EC necroptosis, whereas Caspase 8 deletion can abrogate EC apoptosis *in vivo* (113). Therefore, we used tamoxifen-inducible endothelial-specific Tie2-CreER^{T2};TAK1$^{fl/fl}$;RIPK3$^{fl/fl}$ (TAK1;RIPK3^{ECdKO}) and tamoxifen-inducible endothelial-specific Tie2-CreER^{T2}; TAK1$^{fl/fl}$;Caspase8$^{fl/fl}$ (TAK1;CASP8^{ECdKO}) mice and studied sepsis progression in these mice.

We injected TAK1^{ECKO}, TAK1;RIPK3^{ECdKO} and TAK1;CASP8^{ECdKO} and Cre-negative control mice with a sublethal dose of LPS (10 mg/kg) i.p. Sepsis progression was monitored via measurement of core body temperature as described before. We observed that upon double deletion of Caspase 8 and TAK1 in ECs of TAK1;CASP8^{ECdKO} mice, they were less sensitive to LPS-induced hypothermia compared to TAK1^{ECKO} mice (Figure 10B and D). However, mice with TAK1 and RIPK3 deletion in ECs were more resistant to developing LPS-induced hypothermia and had reduced mortality compared to the TAK1^{ECKO} group (Figure 10B and D).

Thus, we could interpret that RIPK3 deletion in TAK1^{ECKO} mice partially protects them from LPS-induced hypothermia and mortality upon treatment with sublethal doses of LPS, while Caspase 8 deletion in TAK1^{ECKO} mice has minor rescuing effects.

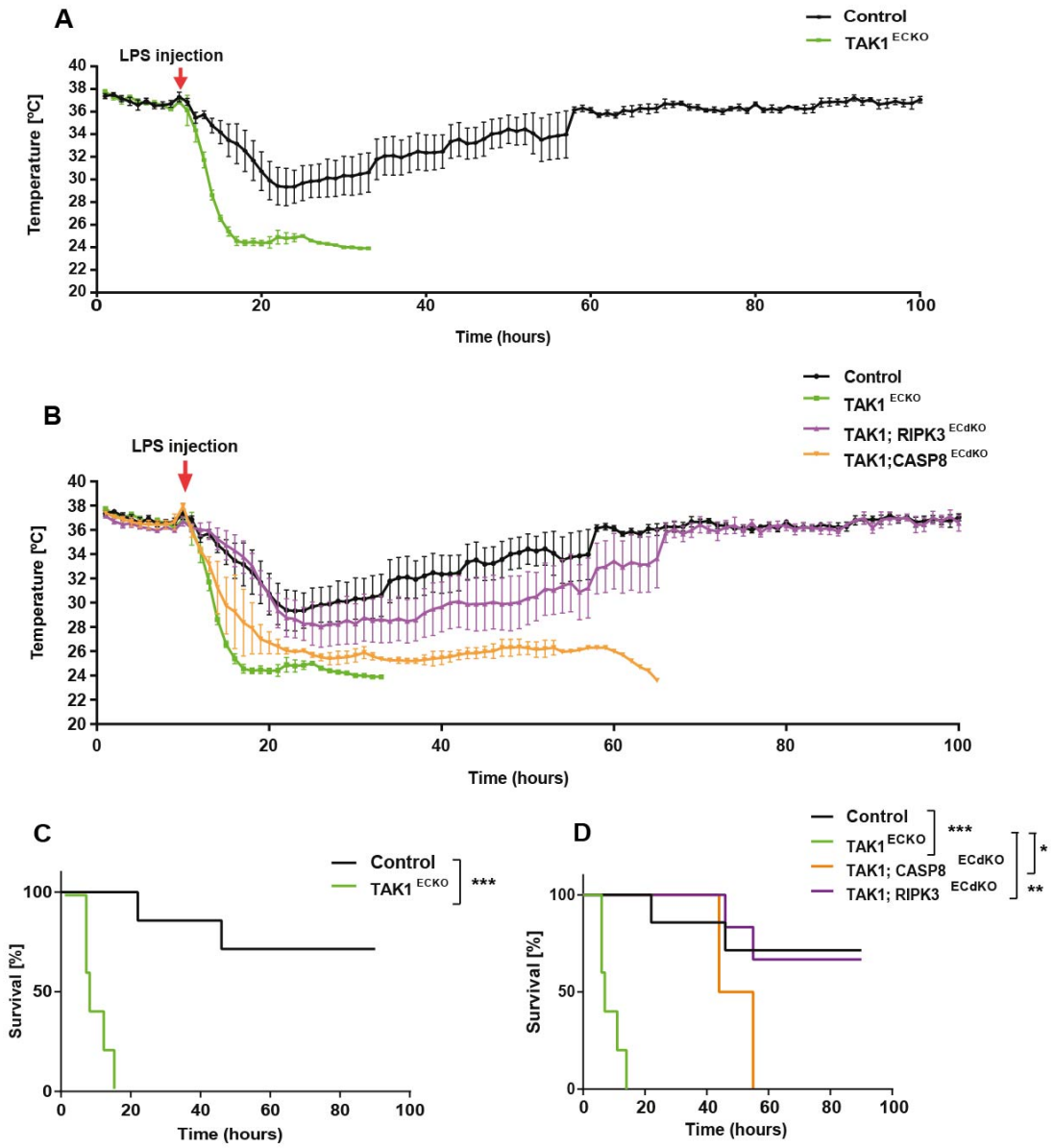

Figure 10: EC-specific TAK1 deletion sensitizes mice to LPS-induced sepsis

Core body temperature in (A) Cre-negative control and TAK1^{ECKO} mice and (B) Control and TAK1^{ECKO} mice in comparison with TAK1;CASP8^{ECdKO} and TAK1;RIPK3^{ECdKO} mice, 10 hours before LPS treatment and body temperature after sublethal dose of LPS (10 mg/kg) injection. Kaplan-Meier survival curves of (C) Control and TAK1^{ECKO} mice treated with a sublethal dose of LPS at 10 mg/kg and (D) survival curves in comparison with TAK1;CASP8^{ECdKO} and TAK1;RIPK3^{ECdKO} mice. Shown are representative data with mean values ± s.e.m from two independent experiments. (n=3-4 mice for each condition). *P < 0.05; **P < 0.01; ***P < 0.001. Statistical analysis was performed using Mantel-Cox test (C-D).

6.1.7 TAK1 deletion in ECs does not directly compromise endothelial function in septic mice

Sepsis is a consequence of sustained pro-inflammatory environment coupled with a dysfunctional endothelium. Therefore, we questioned whether increased EC necroptosis in TAK1^{ECKO} mice causes drastic endothelial dysfunction leading to accelerated sepsis progression. To answer this, we compared endothelial function such as vasotone regulation and hemostasis in septic TAK1^{ECKO} and control mice.

An *ex vivo* as well as *in vivo* analysis of EC-regulated vasotone modulation after LPS treatment in control and TAK1^{ECKO} mice was performed. We first studied contraction and relaxation responses in saphenous arteries isolated from control and TAK1^{ECKO} mice by wire myography. Untreated saphenous arteries from control and TAK1^{ECKO} mice had a comparable response to Acetylcholine-induced relaxation (Figure 11A). Contraction-induced by phenylephrine was also unchanged in TAK1^{ECKO} mice compared to the control (Figure 11B). Saphenous arteries that were ex vivo treated with LPS for 40 min were then subjected to phenylephrine and acetylcholine responses. Both control and TAK1^{ECKO} derived saphenous arteries had comparable relaxation and contraction response even after LPS treatment (Figure 11C and D). Further, we also qualified mean arterial blood pressure by telemetric measurement of blood pressure in control and TAK1^{ECKO} mice (Figure 11E) before and after LPS treatment. As observed, even though the severity of sepsis was increased in TAK1^{ECKO} mice, the gradual decline of blood pressure was comparable between the control and TAK1^{ECKO} mice.

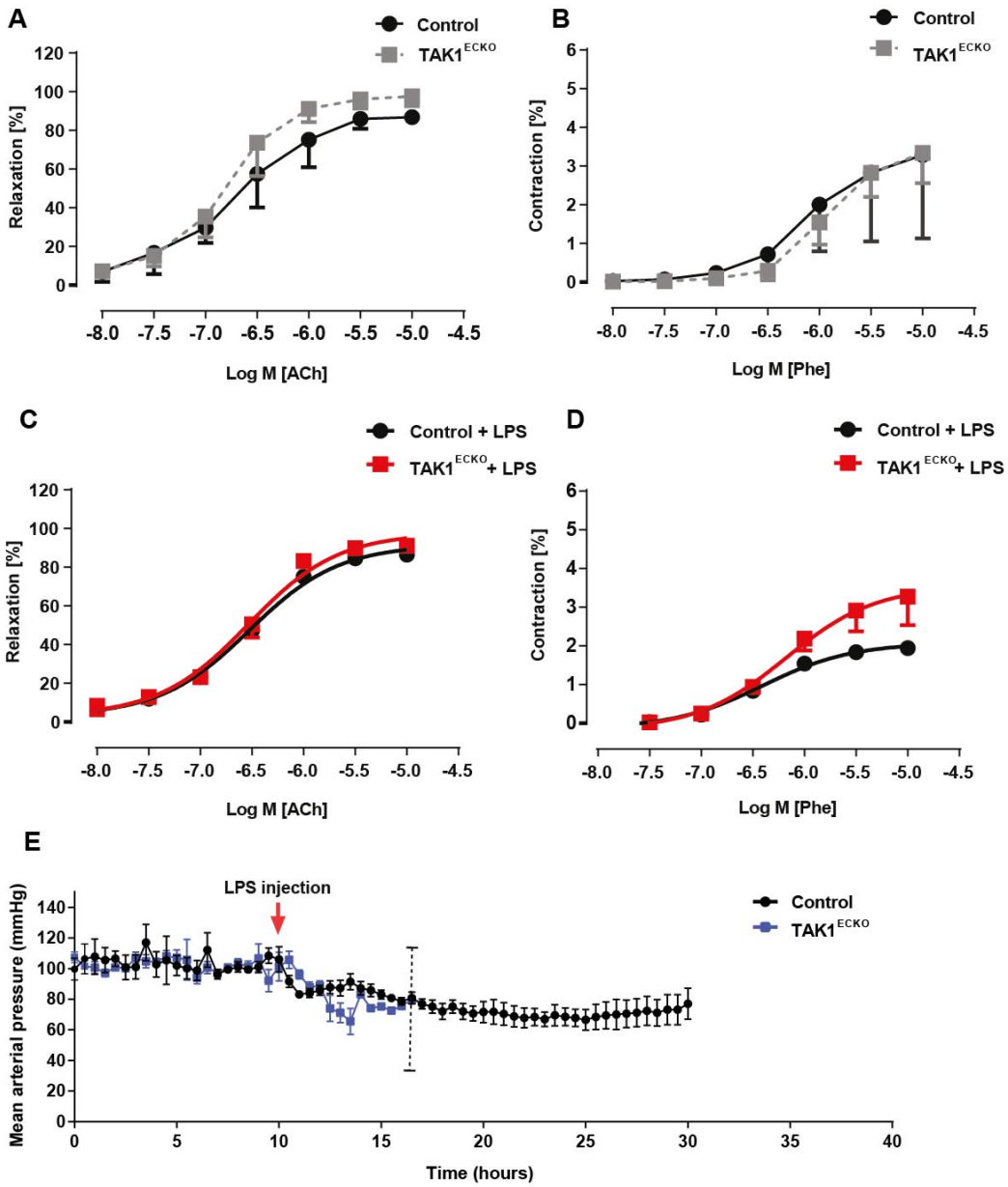

Figure 11: TAK1 deletion in ECs does not directly alter endothelial vasotone control in septic mice

(A) Relaxation responses of Control and TAK1^{ECKO} saphenous arteries to Acetylcholine treatment and (B) contractile responses of both groups to Phenylephrine treatment recorded by wire myography (n=4-6 per condition). Saphenous arteries isolated from Control and TAK1^{ECKO} mice, treated with 50 µg/ml LPS for 40 min ex vivo, and their response to (C) Acetylcholine and (D) Phenylephrine. Shown are representative data with mean values ± s.d. from two independent experiments. (E) Representative data with mean arterial pressure in Control and TAK1^{ECKO} mice before and after LPS (10 mg/kg i.p.) treatment. The dotted line depicts mortality. Shown are mean values ± s.e.m from three independent experiments (n=4-5 mice per group).

Another key function of the endothelium that is compromised during sepsis is hemostasis. A decline in thromboresistance by ECs can increase the incidence of disseminated intravascular coagulation leading to organ failure (129). Therefore we checked whether the TAK1^{ECKO} mice had a decline in endothelial thromboresistance and a consequent increase in disseminated intravascular coagulation. To this end, we analyzed plasma platelets count as readout for increased coagulation. Even though after sepsis induction, there was a dip in the plasma platelet count, there was no significant difference observed between the control and the TAK1^{ECKO} group (Figure 12C). Among other organs in the septic mice, intravascular coagulation was most prominent in the liver. Hence we examined the liver of the septic mice to estimate the extent of disseminated intravascular coagulation (DIC). After hematoxylin and eosin staining, the number of thrombi in the tissue was quantified in untreated mice and liver from mice 6 hours after LPS treatment from both control and TAK1^{ECKO} mice (Figure 12A and B). Apart from the significant increase in the number of clots in the blood vessels after LPS treatment, there was no significant difference in the number of DIC observed in the liver between the control and TAK1^{ECKO} group.

Taken together, plasma platelet count as well as DIC observable in the liver in TAK1^{ECKO} septic mice indicates that TAK1 deletion in ECs did not alter thromboresistance function of the endothelium under septic conditions.

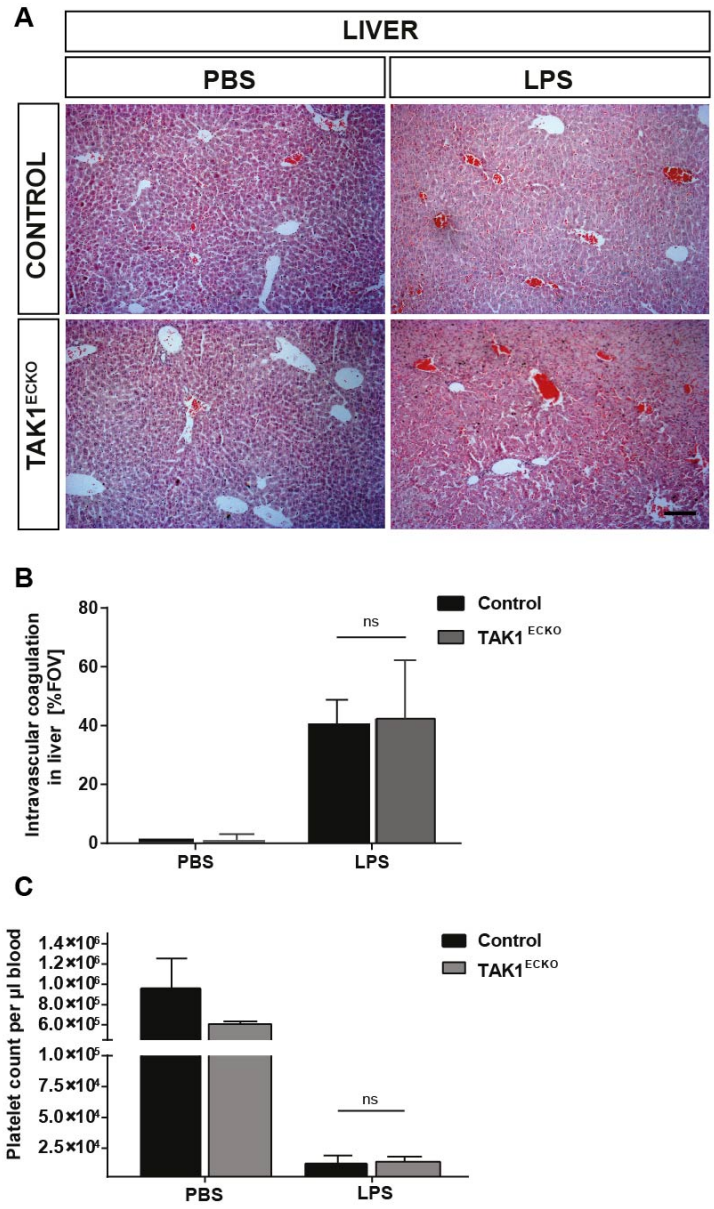

Figure 12: TAK1 deletion in ECs does not affect endothelial thromboresistance

(A) Representative H and E stained images of the liver sections before and 6 hours after LPS (10 mg/kg) treatment in control and TAK1^{ECKO} mice. (B) Quantification of intravascular thrombosis observable in the liver at 6 hours after LPS (10 mg/kg) treatment (n=4 mice per group). (C) Quantification of platelets in the plasma before and after LPS treatment in control and TAK1^{ECKO} mice at 6 hours after LPS (10 mg/kg) treatment. Shown are representative data with mean values ± s.d. ns = not significant. (B-C) Statistical analysis was performed using two-way ANOVA and Bonferroni's post-hoc test.

As observed from the results above (section 6.1.7), TAK1 deletion in ECs does not alter vascular functions compared to the control during sepsis. However, based on the fact that lung endothelial cells undergo necroptosis in septic mice,

we wondered whether the increased mortality to be due to acute respiratory distress syndrome (ARDS). ARDS is characterized by lung inflammation, acute lung injury, pulmonary edema, and hypoxemia (130, 131). Several publications highlight a strong link between endothelial activation and injury to the development of ARDS and severity of sepsis outcome (132-134). Hence, we analyzed paraffin-embedded lung sections from control and $TAK1^{ECKO}$ mice before LPS injection and 6 hours after LPS-induced sepsis and performed H and E staining. We observed thickening of the alveolar walls as well as markers of immune cell infiltration (Figure 13C) in $TAK1^{ECKO}$ mice before septic induction as well. The observed differences in the lung during non-septic conditions could be due to increased necrosis in lungs of $TAK1^{ECKO}$ mice. Increased CD68 positive cells were also observed in the lungs of $TAK1^{ECKO}$ mice under non-septic conditions (Figure 13A and B). Apart from a mild lung inflammation, the $TAK1^{ECKO}$ mice have a normal respiratory function and 100 percent survival after induction of the knockout without sepsis induction.

However, the basal inflammation observed in the $TAK1^{ECKO}$ mice could be further exacerbated upon LPS-induced sepsis hence leading to severe sepsis with ARDS.

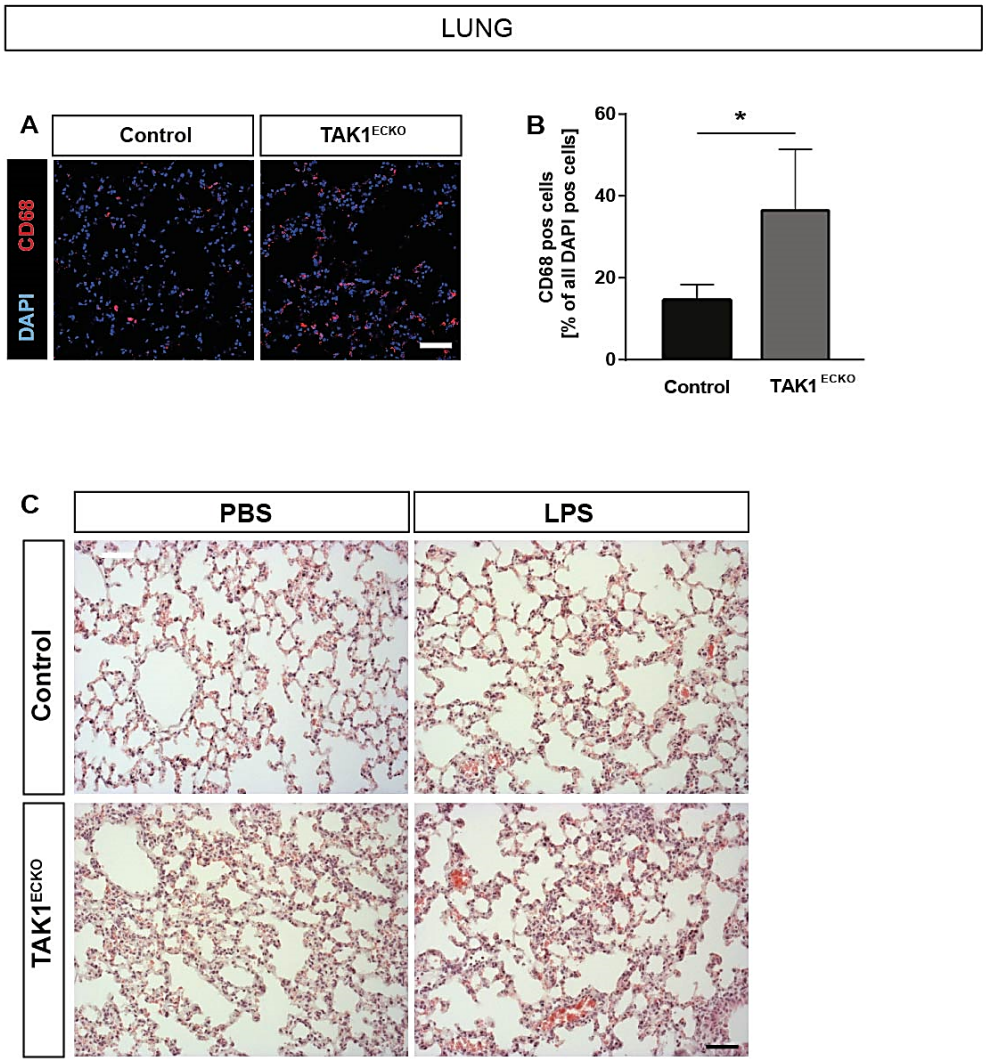

Figure 13: TAK1 deletion in ECs leads to an increase in macrophage infiltration and tissue inflammation under basal condition

(A) Representative confocal images of lungs from Control and TAK1^{ECKO} mice showing increased macrophages in the lung, stained with indicated markers. Bar length: 50 µm. (B) Quantification of CD68 positive macrophages in the lungs of Control and TAK1^{ECKO} mice under physiological conditions. (C) Representative images of H and E stained lung sections from Control and TAK1^{ECKO} mice before and 6 hours after LPS treatment. Bar length: 50 µm. (n=3-4 mice per condition). (B) Shown are representative data with mean values ± s.d. *P < 0.05. (A) Statistical analysis was performed using unpaired two-tailed t-test.

We next questioned whether the basal inflammation of lungs in the TAK1^{ECKO} mice is further exacerbated to a hyper-inflammatory environment that could lead to ARDS. To this end, we checked the expression of protein thrombomodulin whose expression is reduced by inflammatory cytokines like TNF-alpha or even

endotoxins like LPS in ECs. (65). Expression of thrombomodulin thus can serve as a marker for higher or lower inflammatory conditions in the lungs. Membrane-bound thrombomodulin is an endothelial glycoprotein expressed on all endothelial cells. Thrombomodulin plays an important function in conferring thromboresistance via recruitment of thrombin and preventing further thrombus formation (135, 136). IF staining of thrombomodulin in lung sections from control and TAK1^{ECKO} mice was performed before and 6 hours after LPS treatment (Figure 14A and B). Reduction of thrombomodulin in TAK1^{ECKO} mice lungs after LPS treatment compared to the control suggested a stronger pro-inflammatory environment in the lungs of septic mice.

From all the histological analysis of lungs from septic TAK1^{ECKO} mice, showing increased immune cell infiltration and reduced thrombomodulin expression, suggests elevated pro-inflammatory response in the lungs of these mice that can cause ARDS.

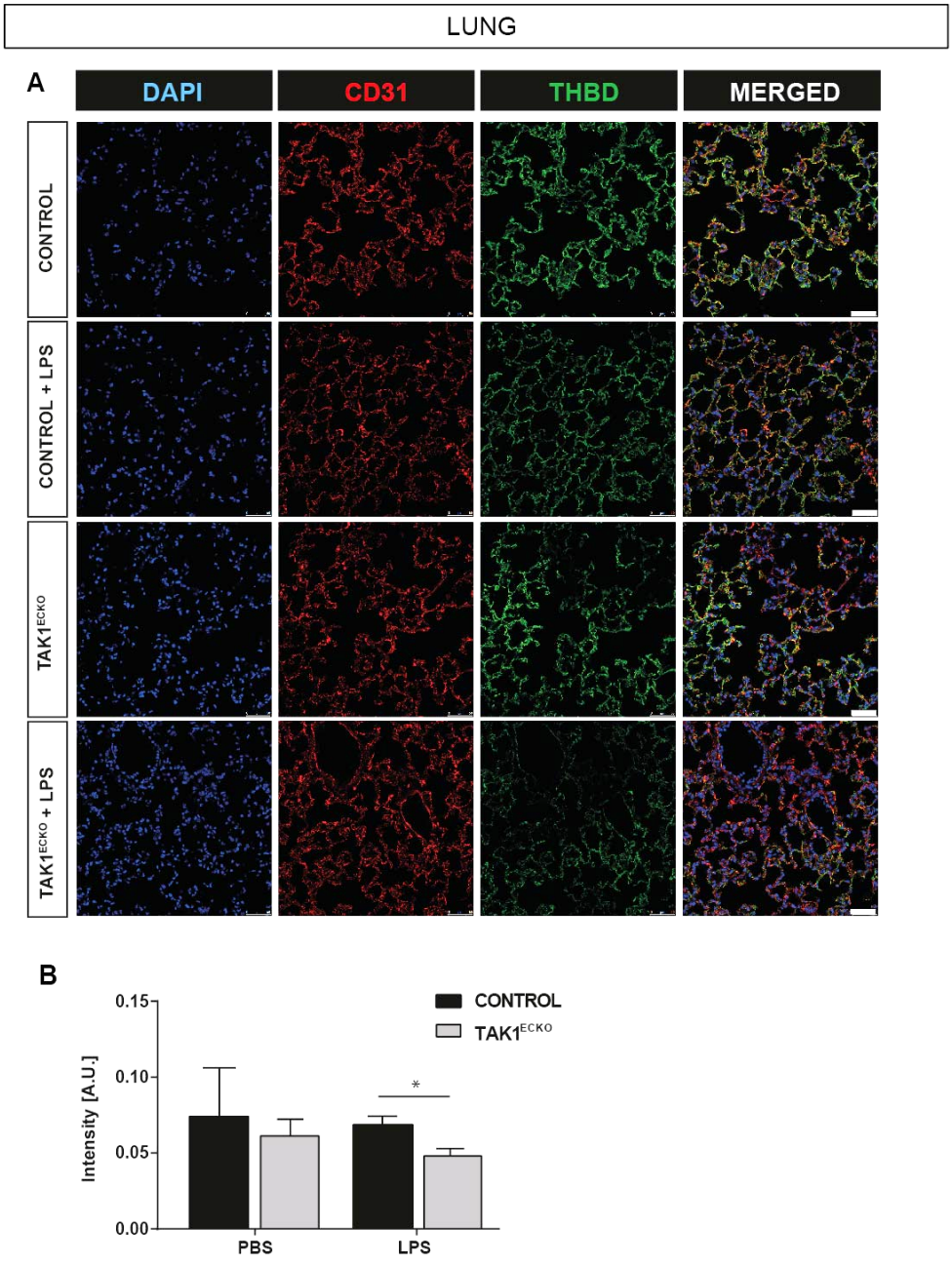

Figure 14: TAK1^{ECKO} mice have reduced thrombomodulin expression in lung endothelial cells after LPS-induced sepsis

(A) Representative confocal images of lungs from Control and TAK1^{ECKO} mice before and 6 hours after LPS (10 mg/kg) injection. Bar length: 50 µm. (B) Quantification of the intensity of thrombomodulin staining in control and TAK1^{ECKO} mice group. Shown are representative data with mean values ± s.d. *P < 0.05. (B) Statistical analysis was performed using two-way ANOVA and Bonferroni's post hoc test (n=3-4 mice per condition).

6.1.8 TAK1 deletion in ECs increases endothelial activation in response to LPS treatment

Increased inflammation observed in the lungs of septic TAK1^{ECKO} mice (Figure 13C) could be due to a higher propensity of TAK1 deficient ECs to switch to an activated state due to increased activity of pro-inflammatory pathways like activated MAPKs or due to decrease in anti-inflammatory proteins.

To test this hypothesis, we stimulated control and TAK1-deficient ECs with LPS and checked for ERK1/2 phosphorylation. We observed that BAECs and HUVECs both show sustained phosphorylation of ERK1/2 with time, after LPS treatment (Figure 15A and B). Sustained phospho-ERK1/2 signaling on LPS treatment in ECs indicates sustained pro-inflammatory signaling (137).

Another transcription factor called ETS related gene (ERG) is expressed in endothelial cells and cells of the hematopoietic lineage (138). ERG expression in ECs is decreased by inflammatory cytokines (139). IF-staining of lungs from septic mice also showed that ECs which were positive for CD31 were negative for ERG (Figure 15E). ERG expressing cells were further reduced in lung ECs of TAK1^{ECKO} mice. We also checked the protein level of ERG expressed in siControl and siTAK1 HUVECs and HMVEC-Lungs upon LPS-treatment. The expression of ERG was further decreased in siTAK1 ECs upon LPS treatment (Figure 15C and D). ERG has a known function for repressing ICAM-1 and IL-8 expression (140) and thus exerts its quiescent or anti-inflammatory effect (141, 142). However, a decrease in ERG expression further highlights the fact that ECs lacking TAK1 have higher propensity to sustain activated pro-inflammatory state upon stimulation.

In summary, increased expression of pro-inflammatory proteins in response to LPS like phospho-ERK and reduced expression of anti-inflammatory proteins like ERG in TAK1-deficient ECs after LPS treatment indicates a pro-inflammatory activated endothelium.

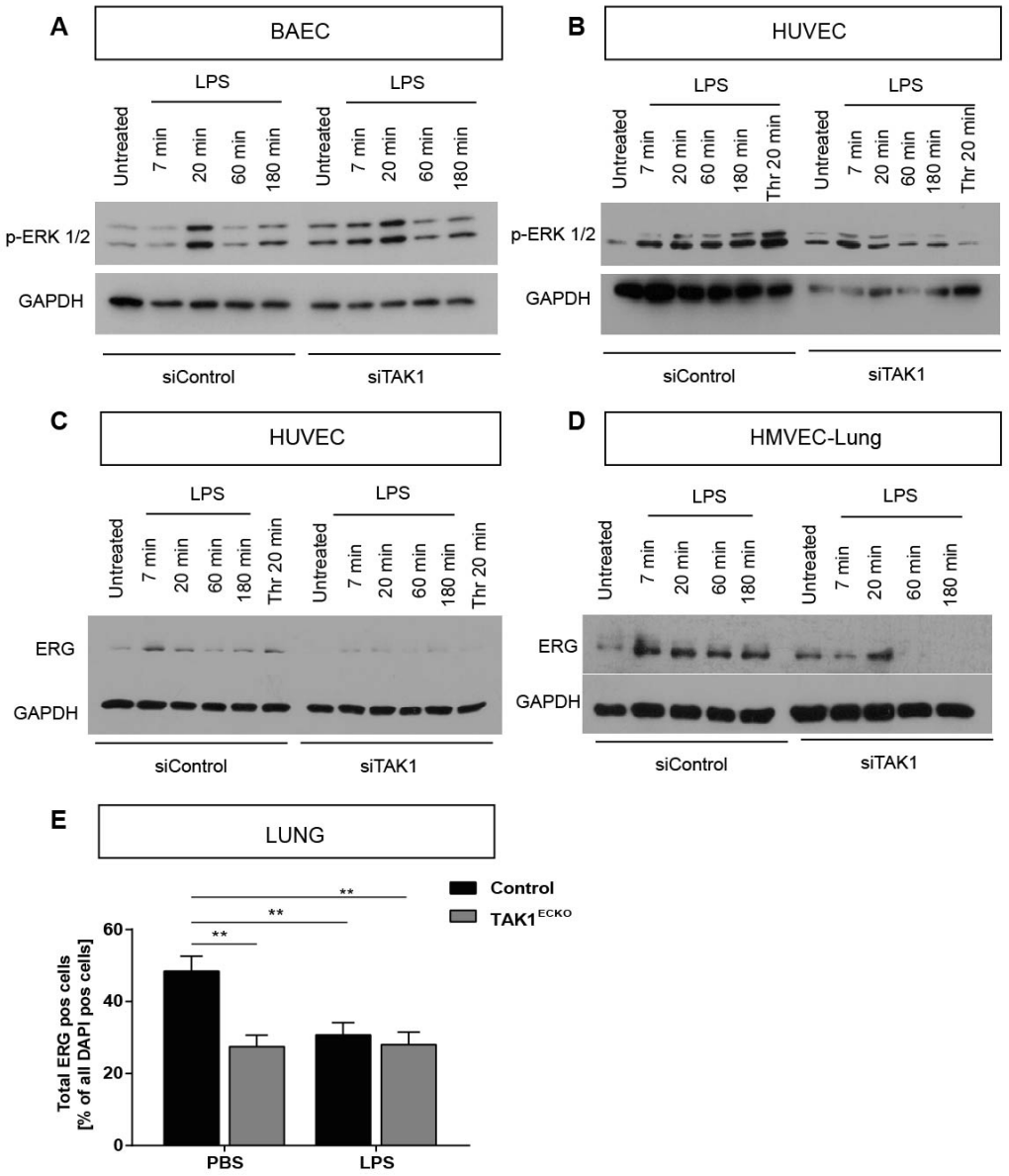

Figure 15: TAK1 deletion in ECs sustains LPS-induced ERK1/2 phosphorylation and downregulates ERG expression

Determination of ERK1/2 phosphorylation in siControl and siTAK1 upon treatment with LPS (1 µg/ml) stimulation at indicated time points in (A) BAEC cells and in (B) HUVECs by western blot. Expression of ERG in (C) HUVECs and (D) HMVEC-Lung cells after LPS (1 µg/ml) and Thrombin (1 U/ml) treatment at indicated time points. (E) Quantification of ERG-positive cells in the lungs of Control and $TAK1^{ECKO}$ mice before and 9 hours after LPS treatment. Shown are representative data with mean values ± s.d. $^{**}P < 0.01$. (E) Statistical analysis was performed using two-way ANOVA and Bonferroni's post hoc test (n=3-4 mice per condition).

6.1.9. Immunomodulatory effects of endothelial necroptosis

As mentioned earlier, sepsis is a consequence of pro-inflammatory cytokines coupled with endothelial dysfunction. The accelerated sepsis progression in TAK1^{ECKO} mice does not seem to be due to a drastic endothelial dysfunction. However, increased necroptosis in TAK1^{ECKO} mice could increase the pro-inflammatory response during sepsis. Therefore, we tested whether TAK1^{ECKO} mice after LPS treatment have differences in the serum cytokines and chemokines compared to control mice, 4 hours after LPS-induced sepsis.

Septic TAK1^{ECKO} mice have a significant increase in serum levels of Macrophage inflammatory protein 2 (MIP-2) and a strong increase in Interferon-gamma (IFN-gamma) levels (Figure 16). MIP-2 (or CXCL2) is secreted by monocytes and neutrophils during infections, and its expression positively correlates with the severity of sepsis(143). IFN-gamma produced primarily by NK cells is known to exert its cytotoxic effect by having a synergistic effect along with TNF alpha (144) but does not always correlate with sepsis severity (145).

Thus, TAK1^{ECKO} mice could have an accelerated sepsis progression due to altered cytokine milieu further encouraged by endothelial necroptosis.

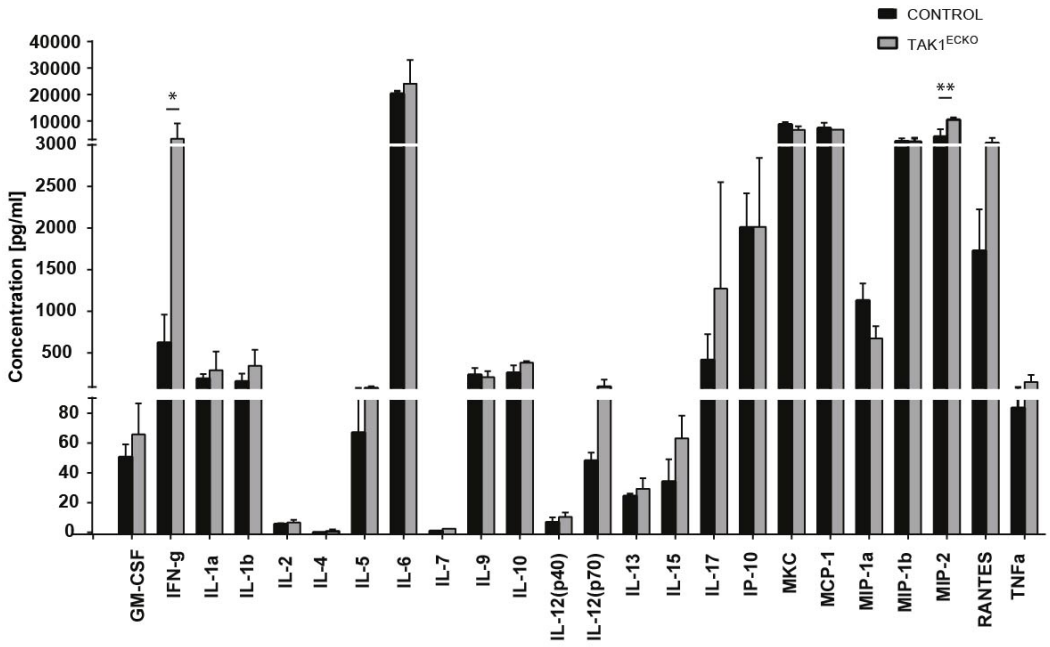

Figure 16: Enhanced pro-inflammatory cytokines and chemokines in the serum of septic TAK1^{ECKO} mice

Quantification of serum levels of cytokines and chemokines in Control and TAK1^{ECKO} mice 4 hours after LPS (10 mg/kg) i.p. injection Shown are representative data with mean values ± s.e.m. *P < 0.05.; **P < 0.01. Statistical analysis was performed using two-way ANOVA and Bonferroni's post hoc test.

In summary, septic TAK1^{ECKO} mice, which have increased lung EC necroptosis, are more susceptible to LPS-induced sepsis probably due to the development of ARDS. This increased lung EC necroptosis and accelerated sepsis mortality correlates with increased pro-inflammatory cytokine IFN-gamma and chemokine MIP-2. Study of sepsis progression in mice with TAK1 deletion along with RIPK3 deletion, allow us to conclude that inhibition of endothelial necroptosis offers resistance to severe sepsis development and prolongs survival.

6.2 Endothelial programmed cell death during ischemia/IRI injury and its influence on organ recovery and function

Ischemia-induced hypoxia can induce microvascular dysfunction, such as increased vascular leakage. Furthermore, complement activation and platelet-leukocyte aggregation can aggravate microvascular dysfunction after ischemia-reperfusion (83), which can further lead to organ dysfunction. RIPK3 mediated necroptosis can also lead to organ dysfunction in different organs like heart,

kidney, liver, brain etc. (146). For example, necroptosis has been observed in the neonatal brain due to ischemia (147), renal allograft due to ischemia (148) or in the kidney due ischemia-reperfusion injury (IRI) (149). However, limited studies have highlighted the effect of specifically endothelial cell death in organ dysfunction even though microvascular endothelium plays a critical role in regulating organ recovery post-ischemia or IRI by regulating post-ischemia angiogenesis or vascular remodeling, immune cell recruitment and healing (90, 150, 151).

Thus, we have investigated the type of PCD and extent of endothelial cell death in hindlimb ischemia, kidney IRI and cardiac ischemia or IRI models, and the effect of abrogation of endothelial necroptosis in the organ or microvascular function recovery using EC-specific RIPK3 knockout mice.

6.2.1 Role of endothelial cell death in hindlimb ischemia-reperfusion injury

In order to estimate the extent of vascular injury and identify the programmed cell death pathways involved in the hindlimb after ischemia-reperfusion injury (IRI), we surgically induced ischemia-reperfusion (IR) by femoral artery ligation in C57BL/6J mice. Ligation was performed for 45 min, followed by 2 hours of reperfusion. Mice were subjected to IR only for the right limb, whereas the left limb served as a sham control. From confocal imaging of the hindlimb adductor muscle after IRI, we observed cells were primarily EthD-III positive whereas no cleaved caspase 3 positive cells were detected (Figure 17A and B). Further, we quantified the percentage of CD31 positive ECs undergoing necrosis post-IRI in the hindlimb (Figure 17A and C). Nearly 10% of ECs in the adductor muscles undergo necrosis. Since ECs undergo necrosis post-IRI in the hindlimb, we questioned whether inhibition of RIPK3-regulated necroptosis could improve hindlimb neovascularization post-injury. Neovascularization post-hindlimb ischemia is mediated by arteriogenesis and angiogenesis. The mechanisms that regulate each of these different aspects are distinct (152). Nevertheless, the role of the endothelial cell death in both or either of the aspect thus could be distinct. Hence, we study whether inhibition of endothelial necroptosis can help or hinder either arteriogenesis or angiogenesis *in vivo*

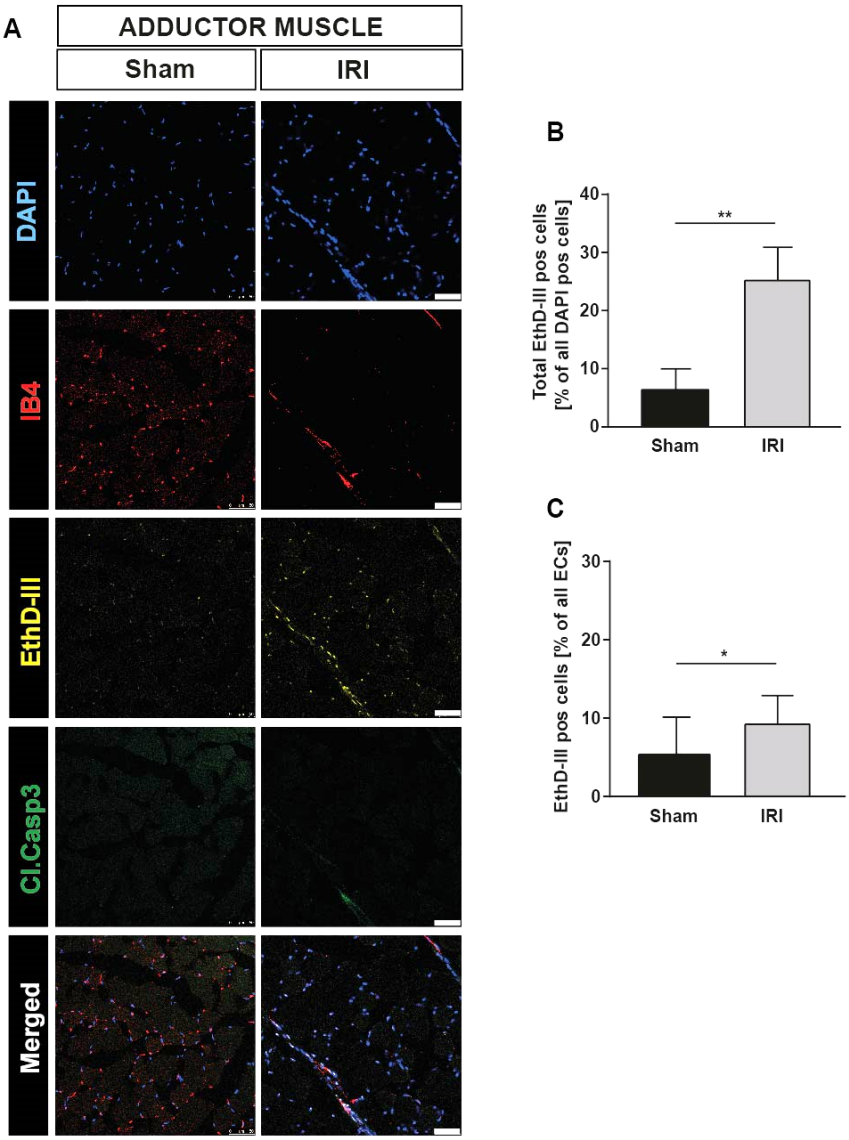

Figure 17: Hindlimb ischemia-reperfusion leads to endothelial as well as myocyte necrosis

(A) Representative confocal images of adductor muscle post-hindlimb ischemia for 45 min and reperfusion of 2 hours. Cryosections are stained with the indicated markers. Bar length: 50 µm. (B) Quantification of total cells undergoing necrosis in the adductor muscle post 2 hours of reperfusion compared to the sham limb. (C) Quantification of endothelial cells undergoing necrosis in the adductor muscle post 2 hours of reperfusion compared to the sham limb. (n=3-4 mice per group). Shown are representative data with mean values ± s.d. *$P < 0.05$; **$P < 0.01$. (B-C) Statistical analysis was performed using unpaired two-tailed t-test.

Hence, we chose to study the role of endothelial RIPK3 in hindlimb ischemia model. The hindlimb ischemia injury is induced by permanent femoral artery ligation and offers the advantage to monitor blood perfusion post-ligation. Using

laser speckle imaging, perfusion was analyzed in paws before and after ligation and again at day 7, 14 and 21 in both groups, post-femoral artery ligation (FAL). No difference could be observed in the gradual gain of perfusion in both groups (Figure 18A). To determine whether RIPK3 deletion in ECs affects collateral arteriogenesis, we performed a histological examination of collateral artery development in the adductor muscle post-FAL (Figure 18B). No difference was observed in collateral arteriogenesis at day 7 post-FAL.

During hindlimb ischemia, there is a reduction of blood flow, especially is the distal parts of the limb. The lower limb muscle, namely the gastrocnemius muscle, is subjected to more ischemia post-FAL. To analyze ischemia-induced angiogenesis, we analyzed capillary density at day 7 in these muscles. However, no significant difference was observed in the capillary density between the two groups (Figure 18C and D).

Hence, inhibiting RIPK3-regulated cell death in endothelial cells in the hindlimb ischemia model did not alter angiogenesis, nor did it alter capacity for collateral arteriogenesis.

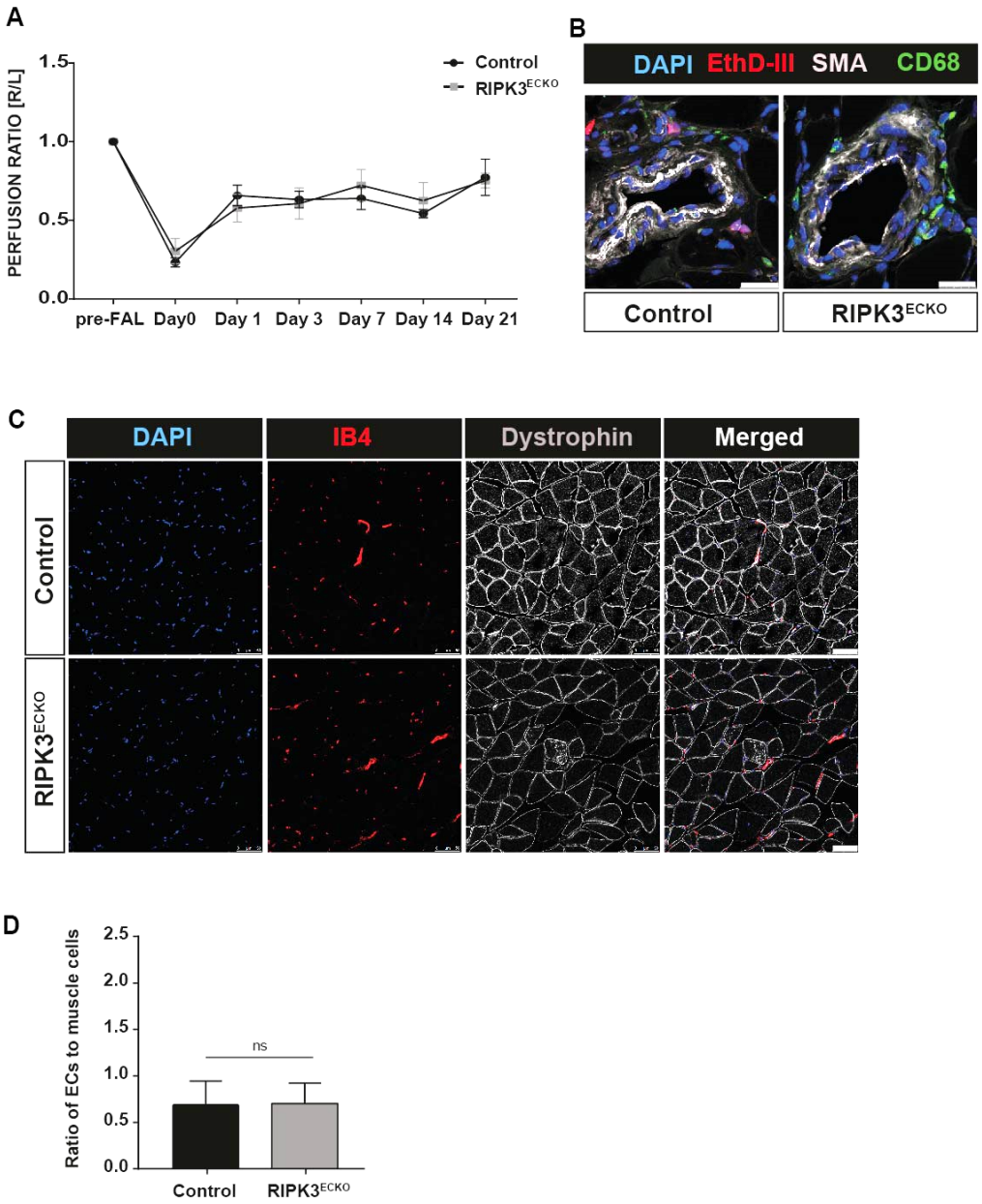

Figure 18: Inhibition of RIPK3-mediated endothelial necrosis does not alter arteriogenesis or angiogenesis post-FAL

(A) Graph showing the perfusion ratio in Control and RIPK3^{ECKO} mice before FAL and, on days as depicted, post-FAL (n=3-5 per condition). (B) Representative confocal images of collateral arteries at day 3 in the adductor muscle post permanent FAL. Bar length = 25 µm. (C) Representative confocal images of capillary density in gastrocnemius muscle 7 days post permanent FAL. Bar length: 50 µm. (D) Quantification of endothelial cell ratio to muscle cells in gastrocnemius muscle at day 7 post permanent FAL in Control and RIPK3^{ECKO} mice (n=3-5 mice per condition). Shown are representative data with mean values ± s.d.. ns= not significant. (D) Statistical analysis was performed using unpaired two-tailed t-test.

6.2.2 Role of endothelial cell death in kidney ischemia-reperfusion injury

Recent studies have reported regulated necrosis after ischemia-reperfusion in the kidney is an underlying cause for acute kidney injury and failure (149, 153). However, fewer studies have discussed cell death in a cell-type specific manner. Hence, to evaluate the type of programmed cell death and the extent of vascular injury after ischemia-reperfusion injury, we performed bilateral renal IRI in C57BL/6J mice. Ischemia was performed by renal artery ligation for 30 min and reperfusion again for 30 min. Histological evaluation of kidney sections revealed that cells largely undergo necrosis in both kidneys undergoing IR (Figure 19A). An interesting observation was that after 30 min ischemia and 30 min reperfusion, majority of the necrotic cells are endothelial cells (Figure 19B) whereas very few non-endothelial cells undergo necrosis (Figure 19C). However, other studies have shown that other cells such as renal tubules also undergo necrosis at least at 48 hours of reperfusion (154). Thus our data shows that ECs are the first site of injury, in terms of cell death, after IRI in kidneys.

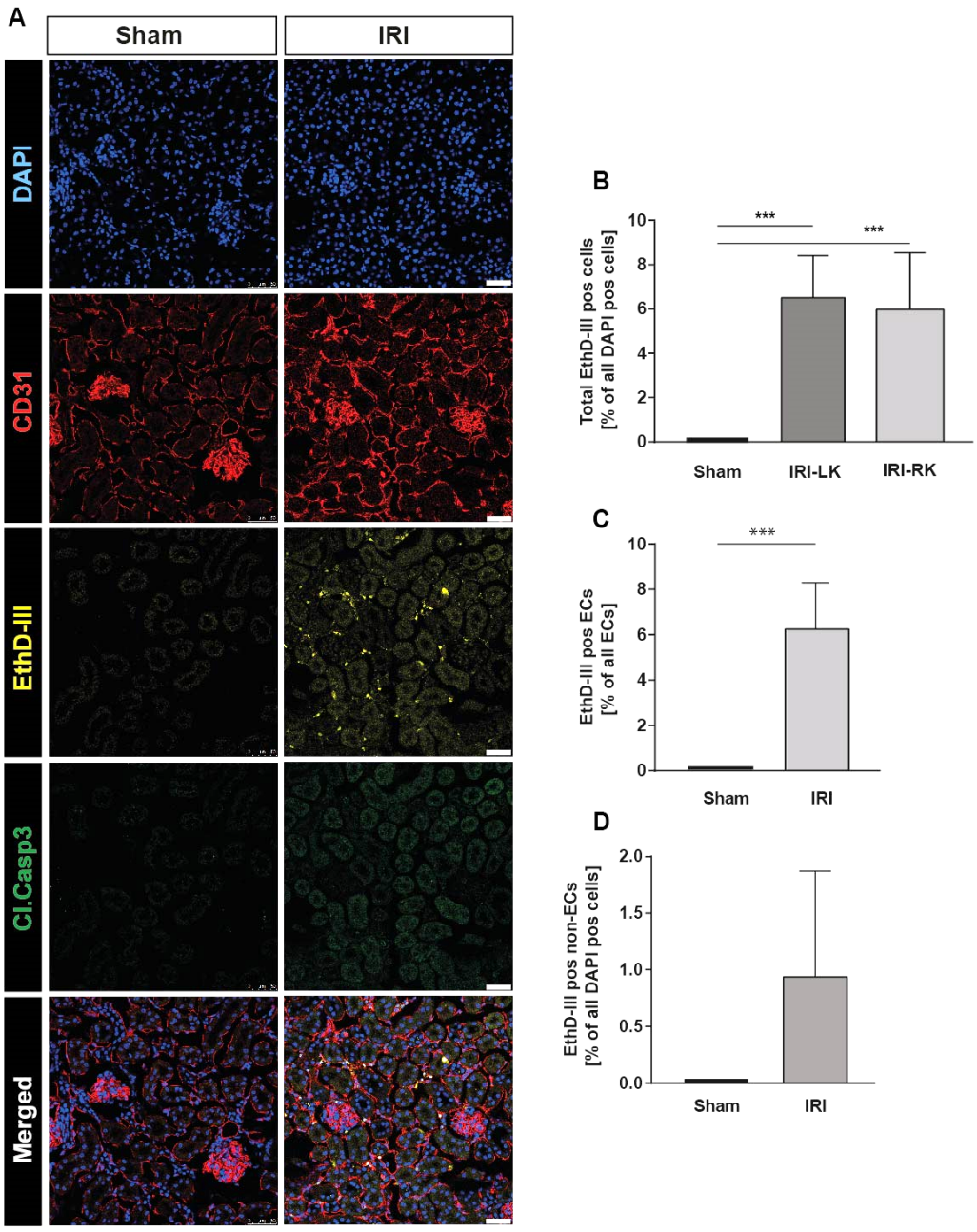

Figure 19: Mild bilateral kidney IR leads to majorly endothelial necrosis

(A) Representative confocal images of kidney from sham mice and mice undergoing bilateral kidney ischemia for 30min and reperfusion for 30min. Bar length: 50 µm. (B) Quantification of EthD-III positive cells in both the left and right kidney after IRI injury. (C) Quantification of EthD-III positive ECs (D) Quantification of non-ECs undergoing necrosis. Shown are representative data with mean values ± s.d. (n=3-4 mice per condition). ***P < 0.001. Statistical analysis was performed using (B) one-way ANOVA and Bonferroni's post hoc test and (C,D) unpaired two-tailed t-test.

To evaluate whether inhibition of RIPK3-regulated endothelial necroptosis can limit vascular injury and improve renal function, we compared kidney function in control and RIPK3^{ECKO} mice undergoing bilateral renal IRI. Mice from RIPK3^{ECKO} group were subjected to bilateral renal ischemia for 30 min and then subjected to reperfusion. We further analyzed tissue necrosis in different regions of the kidney (including the cortex, medulla and the papilla) in both control and RIPK3^{ECKO} group after renal IRI by hematoxylin and eosin staining of paraffin-embedded kidney sections (Figure 20A). Even though the extent of tubular necrosis was of similar degree in the control and RIPK3^{ECKO} group, the RIPK3^{ECKO} mice were protected from glomerular damage with reduced glomerular tuft retraction and reduced vessel wall thickening (Figure 20A). However, even though the glomeruli were more protected, the tubules showed a significant amount of necrosis. Also, RIPK3^{ECKO} group did not show a significant decrease in serum creatinine levels at 48 hrs and 96 hrs post-IRI (Figure 20B).

Hence, deletion of RIPK3 in ECs could protect kidneys from glomerular damage; however, this had no significant impact on recovering organ function.

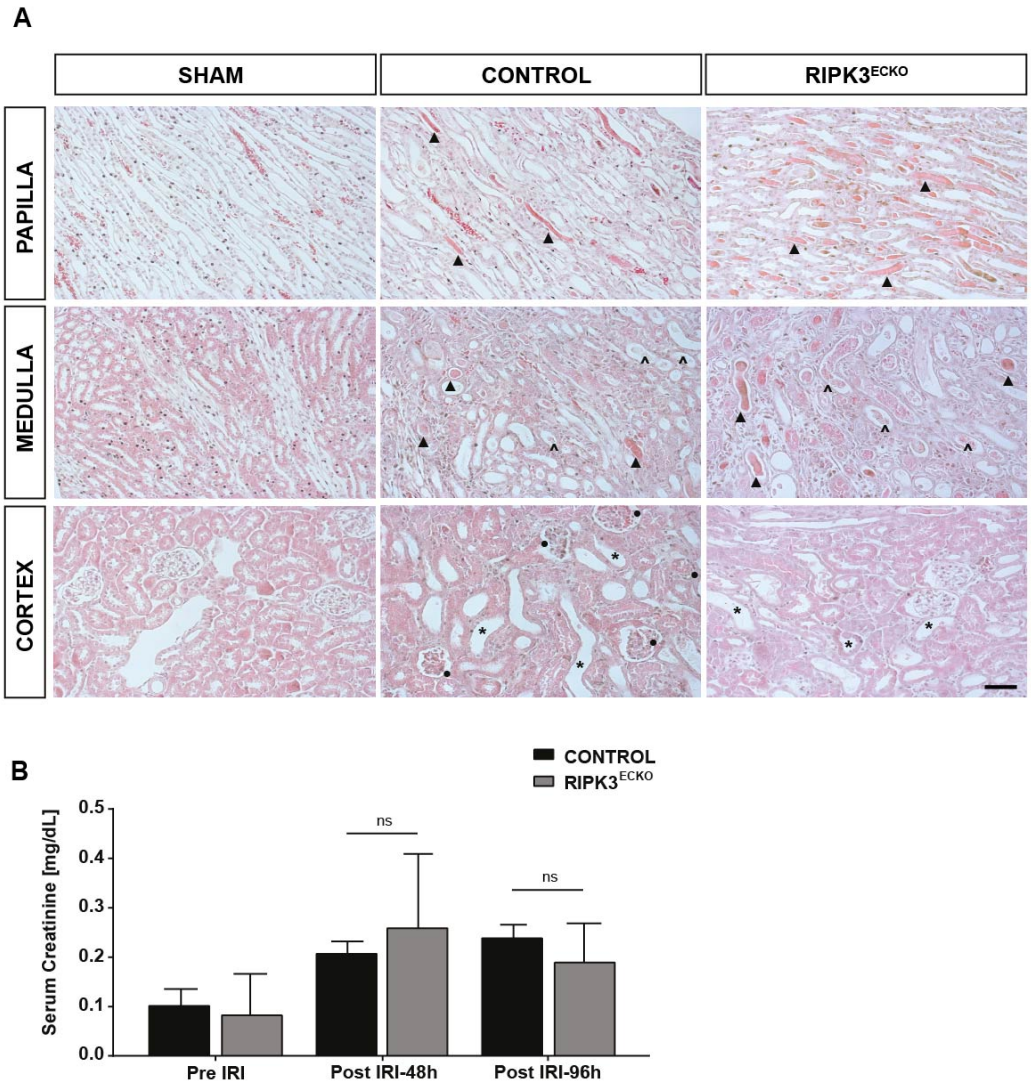

Figure 20: Inhibition of endothelial necroptosis in ECs before bilateral kidney IR does not alter kidney function post injury

(A) Representative images of H and E staining of different regions (papilla, medulla and cortex) in the kidney in the sham group and control and RIPK3^{ECKO} mice are undergoing ischemia for 37 min and then reperfused. Shown are 20x images acquired 96 hours after reperfusion. (▲- indicates papillary and tubular casts; **Λ** - indicates tubular necrosis; ***** - indicates flattened renal tubular cells and tubular dilation; ● - indicates damaged glomerulus with vessel wall thickening and retracted glomerular tuft). (B) Measurement of serum creatinine levels in control and RIPK3^{ECKO} mice at the indicated time points. Shown are representative data with mean values ± s.d. (n=3-4 mice per condition). ns=not significant. (B) Statistical analysis was performed using two-way ANOVA and Bonferroni's post hoc test.

6.2.3 Endothelial cell death in cardiac ischemia-reperfusion injury and its role in cardiac function post-ischemia injury

To analyze the extent of cell death in the heart post cardiac ischemia-reperfusion, we performed left coronary artery ligation for 45 min and reperfusion for 45 min in C57BL/6J mice. By confocal microscopy based imaging, we quantified cells undergoing necrosis in the infarct area extending from the apex to the site of ligation (Figure 21A and B). Based on these sections, we choose the area of maximum necrotic cell death for further analysis. In regions with a larger infarct area, we observed cardiomyocytes as well as endothelial cells undergoing necrosis compared to apoptosis (Figure 22A and B). Furthermore, an increased number of cells undergoing necrosis were IB4 positive, indicating endothelial cells undergoing necrosis (Figure 22C). Quantification of cardiomyocytes undergoing necrosis (Figure 23A and B) within the infarct area was also determined.

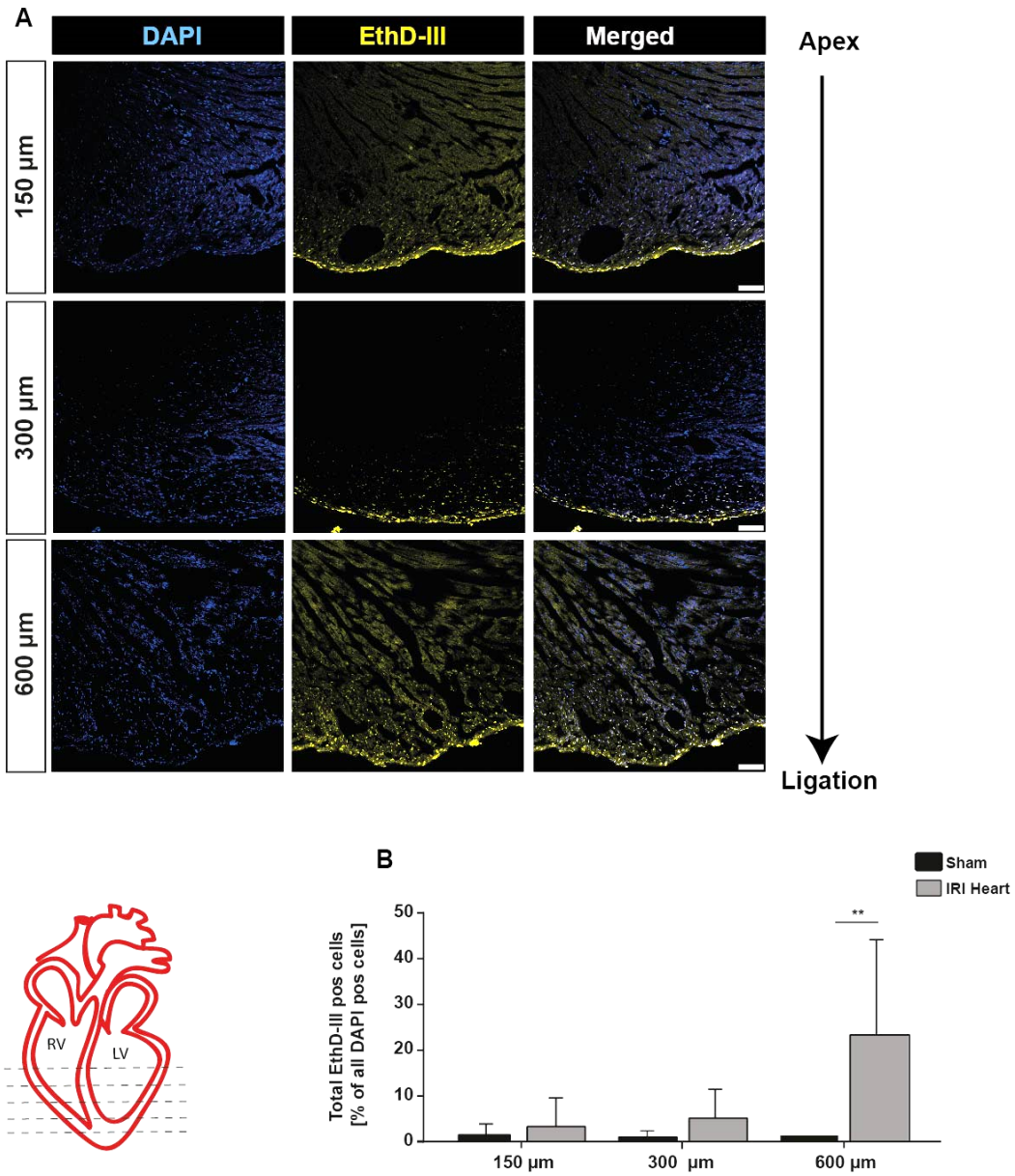

Figure 21: Cardiac ischemia-reperfusion leads to necrosis within the infarct area

(A) Representative confocal images of the heart after ischemia for 45 min and reperfusion for 45 min. Necrosis in areas at an indicated distance from the apex is shown. Bar length: 50µm. (B) Quantification of total cells undergoing necrosis in different regions, predominantly in the epicardium of hearts undergoing IRI. Shown are representative data with mean values ± s.d. (n=3-4 mice per condition). ns=not significant; $^{**}P < 0.01$. (B) Statistical analysis was performed using two-way ANOVA and Bonferroni's post hoc test.

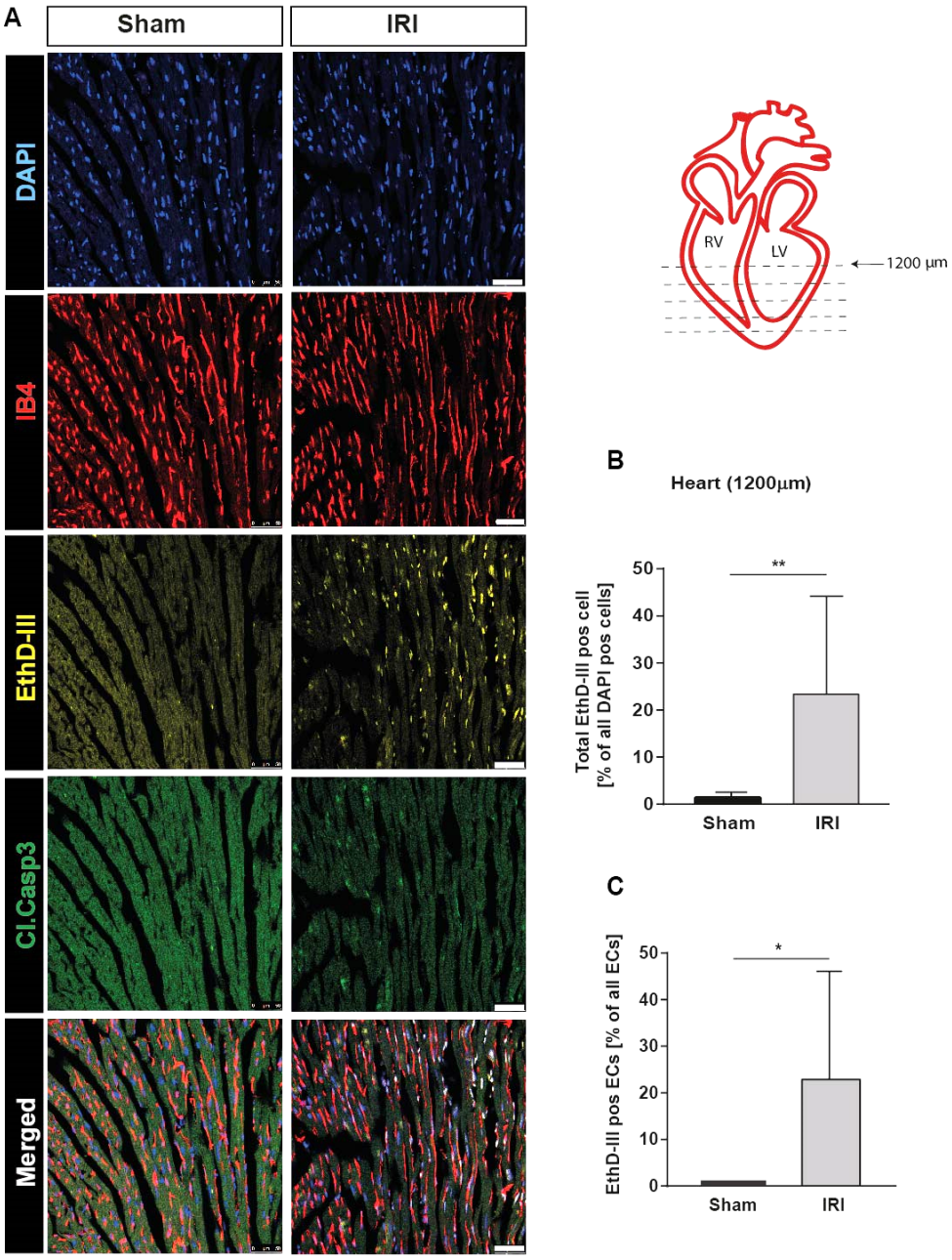

Figure 22: Cardiac ischemia-reperfusion leads to necrosis as opposed to apoptosis

(A) Representative confocal images of the heart of C57BL/6J mice undergoing ischemia for 45 min and reperfusion for 45 min. Necrosis in the area at an indicated distance from the apex is shown. Bar length: 50µm. (B) Quantification of total cells undergoing necrosis in this region. (C) Quantification of total cells undergoing necrosis in this region. Shown are representative data with mean values ± s.d. (n=3-4 mice per condition). ns=not significant; $^{**}P < 0.01$. (B-C) Statistical analysis was performed using unpaired two-tailed student's t-test.

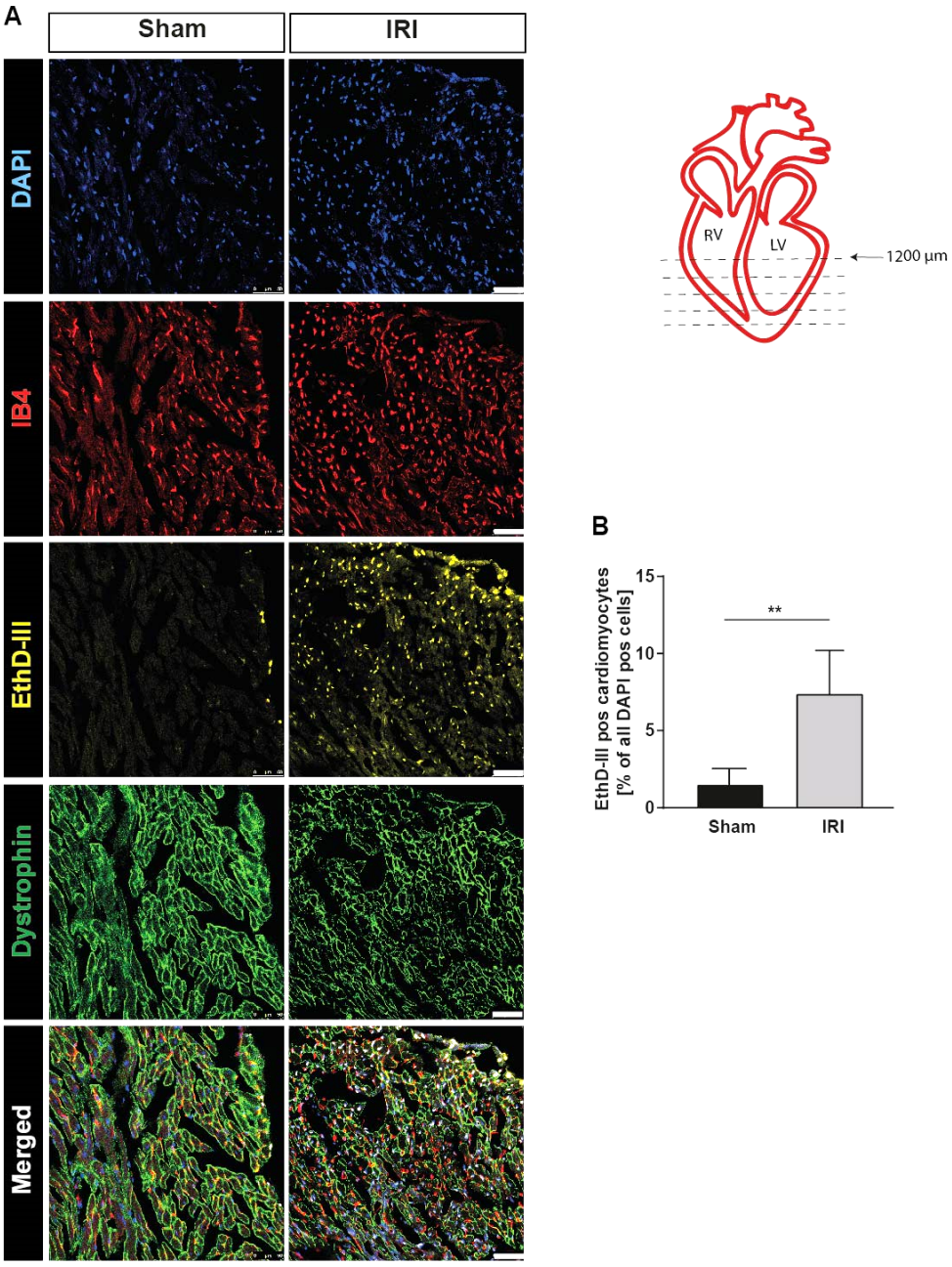

Figure 23: Cardiac ischemia-reperfusion leads to cardiomyocyte necrosis

(A) Representative confocal images of the heart of C57BL/6J mice undergoing ischemia for 45 min and reperfusion for 45 min. Necrosis in the area at indicated distance from the apex is shown. Bar length: 50µm. (B) Quantification of cardiomyocyte undergoing necrosis in this region. Shown are representative data with mean values ± s.d. (n=3-4 mice per condition). ns=not significant; $^{**}P < 0.01$. Statistical analysis was performed using unpaired two-tailed student's t-test (B-C).

Cell death post cardiac ischemia-reperfusion injury, as well as myocardial infarction, is reported to be regulated by RIPK3-mediated necrosis (155-157). However, these studies do not highlight the role of vascular endothelial cell

death observed during cardiac injury. To evaluate the role of endothelial cell death in cardiac ischemia-reperfusion injury, we performed LAD ligation for 45min followed by reperfusion. However, with this model, we faced some technical difficulties wherein the cardiac ischemia-reperfusion did not correspond to a decrease in LVEF (Left ventricular ejection fraction) nor led to infarct formation. Hence, we switched to permanent LAD ligation model. Myocardial infarction, thus induced by permanent LAD was used to evaluate whether inhibition of EC death can influence heart function post-ischemia injury.

To evaluate whether necrotic injury was altered in RIPK3^{ECKO} mice after MI, we measured necrosis in both groups before and after MI. To estimate the relative injury in the control and RIPK3^{ECKO} mice, we measured serum LDH as a necrosis marker. LDH values were highly increased 24 hours post-MI, but the LDH levels were comparable in both control and RIPK3^{ECKO} mice (Figure 24B). This indicates the level of initial injury due to LAD ligation was similar in both control and RIPK3^{ECKO} group. For measuring left ventricular function, magnetic resonance imaging (MRI) technique was used. The LVEF was comparable in control and RIPK3^{ECKO} after 2 weeks and 4 weeks post-MI (Figure 24C).

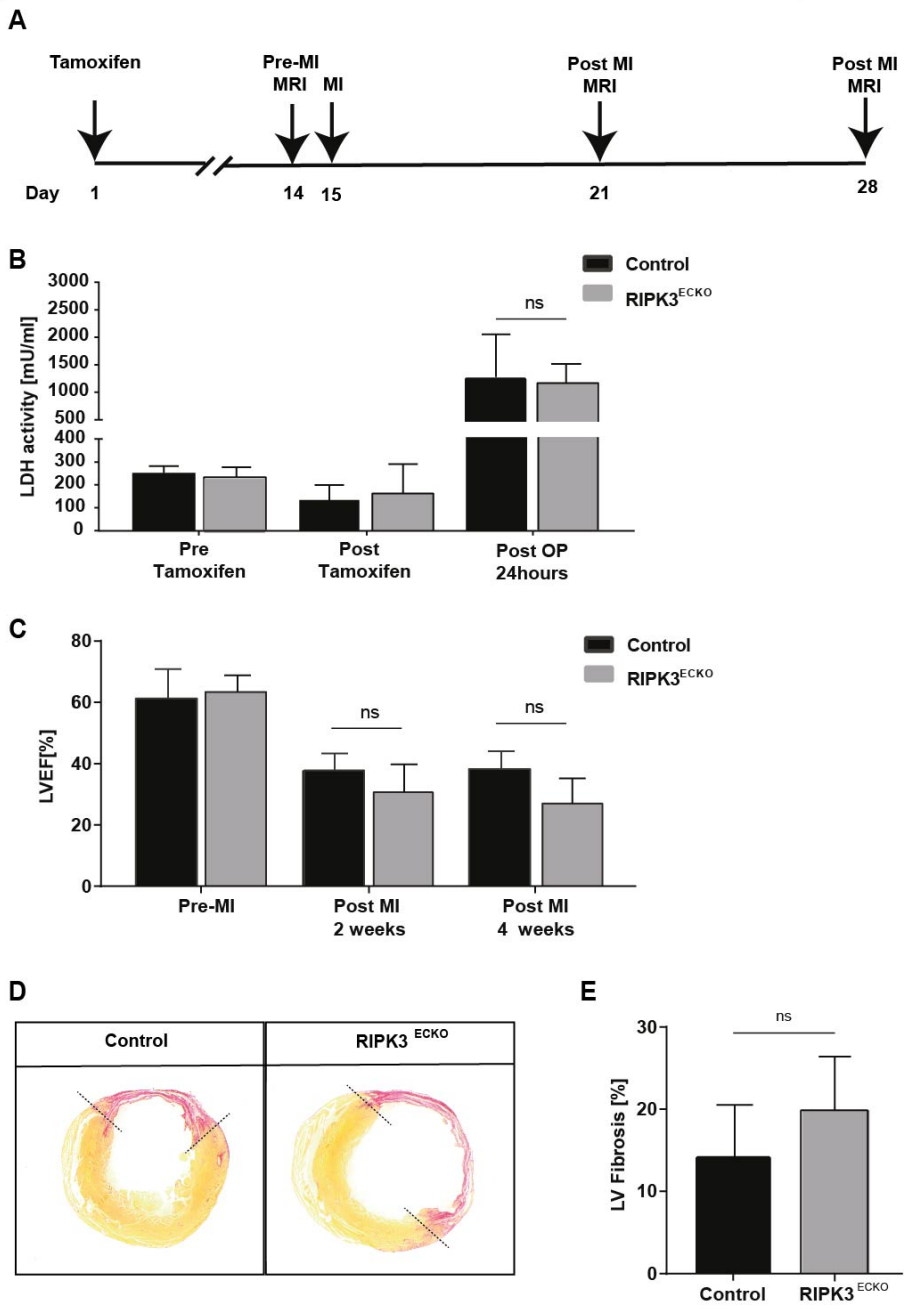

Figure 24: Deletion of RIPK3 in ECs does not alter cardiac function post-MI

(A) Experimental layout (B) Measurement of serum LDH activity before and after knockout induction post tamoxifen injections and final measurement after MI at 24 hours. (C) Quantification of LVEF in control and RIPK3^{ECKO} mice before permanent LAD ligation and 2 weeks and 4 weeks post-ligation. (D) Representative images of the heart from control and RIPK3^{ECKO} mice after MI stained with sirius red depicting infarct area at 4 weeks post LAD ligation. (E) Quantification of LV fibrosis in the heart after 4 weeks of LAD ligation. Shown are representative data with mean values ± s.d. (n=3-4 mice per condition). ns=not significant. Statistical analysis was performed using (B, C) two-way ANOVA and Bonferroni's test and (E) unpaired two-tailed student's t-test.

Inflammatory mediators play an important role in cardiac remodeling post-MI. The endothelial layer regulates several aspects of the inflammatory response post-MI, ranging from recruitment of immune cells and transmigration of immune cells past the endothelial barrier, to the release of inflammatory cytokines. These acute changes post-MI mediate wound healing and regulate scar formation over a subsequent period. We hypothesized whether inhibition of EC necrosis could affect the process of wound healing and thus affect infarct expansion. Hence, we evaluated whether there was a change in fibrosis and infarct formation between control and RIPK3^{ECKO} mice. However, no significant difference was observed in the infarct size in the control and RIPK3^{ECKO} group (Figure 24D and E). Thus, inhibition of RIPK3-mediated necroptosis in ECs during MI did not have a significant influence upon left ventricular function, nor did it affect infarct and scar development.

In summary, inhibition of necroptosis by RIPK3 deletion in ECs during either renal IRI or MI did not influence renal or cardiac dysfunction post-injury. Inhibition of endothelial necroptosis also did not influence the chronic phase of healing in the heart after MI and hence left ventricular fibrosis is also unaffected. Further, our hypothesis that inhibition of endothelial necroptosis can influence arteriogenesis or angiogenesis after hindlimb ischemia was disproved.

7. DISCUSSION

7.1 Lung endothelial necroptosis in LPS-induced sepsis

In our study of cell death during sepsis, we observed necroptosis primarily in the ECs of the lungs, 6 hours after LPS treatment and no cell death was observed in other organs at this time point. However, other studies have reported cell death in organs other than the lungs of septic mice (158, 159). This discrepancy may occur due to the type of septic model used (120, 160) such as LPS-induced sepsis model which mimics the 'cytokine storm' and has a hyper-inflammatory state compared to bacteremia model induced by cecal ligation puncture (CLP) model (160). Owing to the different infectious nature of these models, there is a difference concerning the time course for the development of SIRS to sepsis and further progression to severe sepsis. The LPS-induced septic mice have a higher serum concentration of cytokines like TNF-alpha, IL-6, and IFN-gamma in the serum compared to the other models of sepsis at early time points (160). For these reasons, the overall effect in different organs varies. Nonetheless, cell death in different organs may exist at later stages the LPS-induced sepsis model. However, histological analysis of other organs at later stages of sepsis progression was not performed. The observation that primarily lung ECs in septic mice undergo cell death at an early stage and the fact that this cell death increased with the severity of sepsis was intriguing and hence was followed up in our study.

In vivo and *in vitro* analysis of cell death markers upon LPS stimulation has demonstrated that ECs undergo necroptosis in time as well as concentration-dependent manner. It is interesting to note that in the lungs of septic mice, not all ECs undergo necroptosis, but some are primed to undergo apoptosis. Such a variable response in lung ECs could be possibly due to multiple cell death signaling molecules at play within a septic lung like TNF-alpha, LPS, IFN-gamma etc., or the absence of cues that lead to caspase 8 inactivation within these cells. However, the possibility of multiple signaling molecules exists that affect EC survival by inducing different programmed cell death pathways must

be taken into consideration for medical application targeting cell death regulators.

7.2 Lung EC necroptosis drives sepsis progression via immunomodulation

Our observation that lung ECs undergo necrosis in a time-dependent manner along with the progression of sepsis led to the question whether EC necroptosis is a cause or a consequence of increased sepsis severity and whether it contributes to immune or endothelial dysfunction.

From our *in vivo* survival study in septic mice with a lethal dose of LPS treated with Nec-1, we could interpret that upon necroptosis inhibition, mice had prolonged survival. The abrogation of RIPK1-mediated necroptosis could hinder SIRS progression to severe sepsis. However, Nec-1 is injected intravenously and hence has a systemic effect. Furthermore, the observed effect of Nec-1 on survival does not exclude the effect of necroptosis inhibition in other cell types that may undergo necroptosis. Another limitation of using Nec-1 is that it has a non-specific target viz. enzyme indoleamine 2,3-dioxygenase (IDO) (161). Use of Nec-1s provides a better alternative since it a more specific inhibitor of RIPK1 as well as has a prolonged half-life compared to Nec-1. However, the use of pharmacological inhibitors still does not give cell-specific cell death abrogation. Hence, we use endothelial-specific knockout of key cell death regulators for more specific control of EC death.

Previously, we have reported TAK1 as an important mediator controlling EC survival, which upon deletion causes endothelial cell death via necroptosis (33). From our, *in vitro* studies, we have observed that LPS increased the degree of necroptosis in ECs in the absence of TAK1. Thus, TAK1 plays a critical role in EC survival when challenged with LPS. Consequently, we used $TAK1^{ECKO}$ mice, which have ECs with a higher propensity to LPS-induced necroptosis, to study sepsis progression in these mice. An increase in endothelial necroptosis in $TAK1^{ECKO}$ mice could accelerate sepsis progression as observed by accelerated hypothermia. This accelerated sepsis progression could be due to

necroptosis induced immunomodulation as severity in TAK1^{ECKO} mice correlated with altered IFN-gamma and MIP-2 levels. The physiological influence of IFN-gamma and MIP-2 in lungs is well documented. Studies have reported the role of IFN-gamma in ARDS (162, 163). IFN-gamma has been reported to induce necroptosis in cells with compromised NF-kB signaling (164). Furthermore, it was shown that IFN-gamma primes alveolar macrophages to increase MIP2 expression (165) The TAK1^{ECKO} mice have an increased number of macrophages under physiological conditions, which could be primed further by LPS. MIP-2 (CXCL2) is reported to be highly expressed chemokine in septic mice (166, 167) and MIP-2 is known to be produced by alveolar macrophages upon priming with LPS. It is a functional homolog of human IL-8, and its role in ARDS (168) is well documented, causing lung injury due to increased neutrophil infiltration. The rise in plasma MIP-2 level is also reported to be an early predictor of mortality in CLP-induced sepsis (168), and blockade of MIP-2 receptor has been shown to reduce polymorphonuclear neutrophils (PMN) infiltration in ARDS (169).

Thus, endothelial necroptosis-mediated immunomodulation resulted in a highly pro-inflammatory environment that could lead to accelerated sepsis progression via the development of ARDS.

Interestingly, this accelerated progression of sepsis in TAK1^{ECKO} mice could be rescued by added deletion of RIPK3 in ECs (i.e. by abrogation of endothelial necroptosis). Thus we could interpret that lung endothelial necroptosis is rather an important contributor to the progression of sepsis via immunomodulation and development of ARDS. Hence, abrogation of EC necroptosis in mice lacking TAK1 could reduce sepsis severity as well.

7.3 Critical role of endothelial TAK1 in endothelial cell activation and inflammatory state in response to LPS.

Deletion of TAK1 in ECs, however, has secondary effects other than induction of EC necroptosis in response to LPS. In our study, endothelial TAK1 is found to regulate certain pro-inflammatory as well as anti-inflammatory signaling

molecules. Evidence for this in the lungs of septic TAK1^{ECKO} mice was demonstrated by the fact that lung ECs have further reduced expression of membrane-bound thrombomodulin, thus dampening the anti-inflammatory and anti-coagulant response regulated by thrombomodulin (170, 171). Another key anti-inflammatory transcription factor ERG (172) is also found to be downregulated in ECs lacking TAK1 expression upon LPS stimulation. The importance of ERG in maintaining vascular integrity and identity is well studied (173, 174).

However, the absence of TAK1 promoting EC activation and inflammation may seem counterintuitive, considering that the role of TAK1 in positive regulation of the NF-kB pathway is well known (175). However, the function of TAK1 is different in different cell types (32). In MEFs, T cells and some cancer cell types TAK1 acts as a positive regulator of pro-inflammatory signaling. However, TAK1 acts as a negative regulator of inflammatory signaling in neutrophils (176) and, in our case, endothelial cells. The study which highlights the role of TAK1 as a negative regulator of inflammatory signaling (176), also reports a similar finding in line with our study, that mice with TAK1 deficient neutrophils have a higher susceptibility to LPS-induced inflammation.

Recently, a study reported the key role of TAK1 in preventing EC apoptosis and maintaining vascular integrity (177). However, a key difference in our studies is the endothelial-specific Cre-line in use. They report massive loss of endothelial cells due to apoptosis in the liver and the intestine. Loss of endothelial cells and the resultant hemorrhage increased mortality after induction of knockout. Neither do we observe such an aggressive loss of endothelial cells and drastic lethality due to TAK1 deletion in ECs. However, our studies are rather aligned by the fact that TAK1 deletion indeed increases endothelial cell death in the lungs and have more susceptibility to LPS-induced lung injury due to increased TNF-alpha secretion.

Thus, our findings highlight the importance of endothelial TAK1 in, not only regulating endothelial survival but also in regulating EC activation and inflammatory state.

7.4 Implication of EC necroptosis and endothelial TAK1 regulation in sepsis progression and mortality

From our observations, we could interpret that lung EC necroptosis plays an important role in sepsis progression to severe sepsis. EC necroptosis adds on to ARDS by inducing a hyper-inflammatory environment in the lungs. Several studies have reported that mice with global RIPK3 deletion are protected from SIRS and severe sepsis with a decrease in pro-inflammatory cytokines and chemokines as well as reduced organ injury (158, 178). Another study by Zelic et al. (179) also reported an observation, in line with our study, that cells from a non-hematopoietic lineage with kinase-inactive RIPK1, are more resistant to TNF+zVAD induced SIRS due to reduced necroptosis in kinase-inactive RIPK1 mice.

Thus, biomarkers of endothelial necroptosis have prognostic potential in sepsis. Observational studies have already reported the prognostic potential of plasma RIPK3 in septic patients (180); however, more specific biomarkers of endothelial necroptosis can serve as an early predictor of severe sepsis.

Another important finding from our study is the role of TAK1 in controlling not only necroptosis in ECs but also keeping a check on the pro-inflammatory signals upon exposure to death signals like TNF-alpha or LPS. Deficiency of TAK1 not only sensitizes ECs to increased necroptosis by sustained phospho-ERK1/2 signaling. However, we have not yet addressed how TAK1 regulates either of these pro- or anti-inflammatory signaling pathways.

TAK1 expression in ECs during cytokine or stress condition thus can play an important role in regulating EC pro-inflammatory state. There are yet no direct evidences of reduced TAK1 expression in ECs during sepsis. Considering the cell-type specific nature of TAK1 mediated inflammatory signaling, using TAK1 as a therapeutic target seems unlikely. However, reduced TAK1 expression in ECs can indicate susceptibility to severe sepsis.

Another interesting aspect of $TAK1^{ECKO}$ mice is its physiological state. Mice with TAK1 deficiency in ECs showed increased macrophages in the lungs, even without LPS injection. This could possibly be because $TAK1^{ECKO}$ mice have

increased EC necroptosis that can lead to the recruitment of macrophages within the lung. Thus, patients with such condition, i.e. patients who have more macrophages within lungs (due to underlying conditions like COPD and pulmonary hypertension) or display EC activation, and low-grade local inflammation could have a higher susceptibility to endotoxemia induced ARDS in severe sepsis.

7.5 Inhibition of endothelial necroptosis does not affect organ function post injury

Inhibition of endothelial necroptosis in hindlimb ischemia injury: The role of pre-existing endothelial cells is important in neovascularization of hindlimb post-ischemic injury. Neovascularization post-ischemic injury is mediated either by arteriogenesis or angiogenesis. Our observation that endothelial cells undergo necrosis led to the question of whether the abolition of RIPK3-mediated necroptosis has an impact on either of these re-vascularization processes.

There are limited studies exploring the programmed cell death pathways involved in hindlimb ischemia. Some studies highlight the role of hypoxia-induced ROS species and its role in DNA damage and cell death (181, 182). Especially muscle cell necrosis following hindlimb ligation is discussed, but limited emphasis is given to endothelial cell death or pathways regulating it. A study by Lopez-Pastrana reported induction of Caspase 1 mediated pyroptosis in endothelial cells in a dyslipidemic and inflammatory environment upon hindlimb ischemia. In global caspase 1 knockout mice, they saw an improved hindlimb blood perfusion and angiogenesis (183), thus highlighting the importance of endothelial cell death in hindlimb ischemia injury.

Even though the endothelium plays an important role in hindlimb perfusion, inhibition of RIPK3-mediated endothelial necroptosis could not alter the process of arteriogenesis nor angiogenesis. It could be possible that the surviving cells that do not undergo necrosis are equally potent in mediating arteriogenesis by enhancing eNOS levels (87) or recruitment of immune cells like monocytes or macrophages that augment collateral artery growth (184). Additionally, since

RIPK3-mediated necroptosis in myocytes is not abolished in our RIPK3^{ECKO} mice, DAMP induced inflammatory response is probably unaffected even if endothelial necroptosis is inhibited, thus maintaining inflammatory and healing responses required for neovascularization processes.

Inhibition of endothelial necroptosis in kidney ischemia-reperfusion injury: Several studies have described the role of RIPK1-RIPK3-MLKL signaling in causing necroptosis in kidney IRI and that their inhibition or deletion has reduced kidney injury and increased survival (149, 185, 186). A study has reported that other than the RIPK3-mediated pathway responsible for regulated necrosis, Cyclophilin D, a component of mitochondrial permeability transition pore (MPT) is also responsible in part to regulated necrosis in the kidney (187). Mice with Cyclophilin D and RIPK3 deficiency are more resistant to Kidney IRI injury compared to mice with RIPK3 deficiency alone. However, all these studies have highlighted the role of these cell death regulators in the tubular epithelium.

From our study, we observed that mild IRI induced by 30 min ischemia and after 30 min reperfusion majorly causes endothelial necrosis and hence seems to be the first cells undergoing necrosis followed by the tubular epithelium during a longer duration of reperfusion. This led to our hypothesis that abolishing endothelial cell death in kidney IRI could improve renal function. However, we observed that even though the endothelial necrosis in the glomeruli is in part rescued by RIPK3 deletion, we could not observe improved serum creatinine compared to control mice. Despite having reduced necrosis in the glomeruli, the mice suffer from comparable tubular injury and thus could not be rescued from deleterious IR injury.

Inhibition of endothelial necroptosis in cardiac ischemia injury: The role of RIPK3 has been reported in cardiac IR (157, 188) as well as in myocardial infarction (189, 190). Even though studies focus on cardiomyocyte necroptosis, the role of other cells undergoing necroptosis is not discussed. We have in our study addressed this question whether endothelial cells undergo necroptosis and whether inhibition of endothelial necroptosis can contribute to different

healing stages of post-cardiac injury, including immune infiltration, angiogenesis, scar formation and fibrosis.

A study by Zhang et al. reported reduced LDH levels in RIPK3 global knockout mice after myocardial IR. This shows that mice with global RIPK3 deletion have reduced injury post-MI. However, we did not observe such a difference in our study, wherein LDH levels in RIPK3^{ECKO} and control mice were comparable after LAD ligation. The extent of the injury after MI, in our case, was similar in case of both the control and RIPK3^{ECKO} mice. Hence, RIPK3 deficiency in ECs did not limit the amount of injury caused after LAD ligation.

The role of pre-existing endothelial cells in mediating angiogenesis after cardiac IRI is well studied (109). Furthermore, the endothelium regulates immune cell recruitment and modulates adverse remodeling post-MI (191, 192). From our data, we did not observe a significant difference between the infarct size post-MI of control and RIPK3^{ECKO} mice. The processes that lead up to scar formation and cardiac remodeling (including immune cell recruitment for wound healing, angiogenesis and fibrosis) are unaltered even after inhibition of RIPK3-mediated necroptosis. Thus, overall endothelial protection by RIPK3 deletion did not alter LV function, nor did it affect the process of scar formation.

In summary, inhibiting RIPK3-induced endothelial necroptosis in models of organ dysfunction after ischemia or ischemia-reperfusion injury did not alter organ function. This suggests that endothelial necroptosis alone does not significantly contribute to organ injury and dysfunction. Furthermore, abrogation of endothelial necroptosis does not seem to modulate wound healing or functional recovery in the hindlimb, kidney or the heart after injury. However, the possibility that other member of the necroptotic pathway further downstream of RIPK3 such as MLKL playing crucial role at least in endothelial necroptosis is yet to be investigated.

8. REFERENCES

1. Sandoo A, van Zanten JJCSV, Metsios GS, Carroll D, Kitas GD. The endothelium and its role in regulating vascular tone. Open Cardiovasc Med J. 2010;4:302-12.
2. Yau JW, Teoh H, Verma S. Endothelial cell control of thrombosis. BMC Cardiovasc Disord. 2015;15:130-.
3. Rahimi N. Defenders and Challengers of Endothelial Barrier Function. Front Immunol. 2017;8:1847-.
4. Pober JS, Sessa WC. Evolving functions of endothelial cells in inflammation. Nature Reviews Immunology. 2007;7:803.
5. Shyy John YJ, Chien S. Role of Integrins in Endothelial Mechanosensing of Shear Stress. Circulation Research. 2002;91(9):769-75.
6. Pegu A, Qin S, Fallert Junecko BA, Nisato RE, Pepper MS, Reinhart TA. Human Lymphatic Endothelial Cells Express Multiple Functional TLRs. The Journal of Immunology. 2008;180(5):3399.
7. Reglin B, Pries AR. Metabolic Control of Microvascular Networks: Oxygen Sensing and Beyond. Journal of Vascular Research. 2014;51(5):376-92.
8. Chatterjee S. Endothelial Mechanotransduction, Redox Signaling and the Regulation of Vascular Inflammatory Pathways. Frontiers in Physiology. 2018;9(524).
9. Wagner Denisa D, Burger Peter C. Platelets in Inflammation and Thrombosis. Arteriosclerosis, Thrombosis, and Vascular Biology. 2003;23(12):2131-7.
10. Ruggeri ZM. Von Willebrand factor, platelets and endothelial cell interactions. Journal of Thrombosis and Haemostasis. 2003;1(7):1335-42.
11. Lijnen HR. Pleiotropic functions of plasminogen activator inhibitor-1. Journal of Thrombosis and Haemostasis. 2005;3(1):35-45.
12. Esmon CT. Regulation of blood coagulation. Biochimica et Biophysica Acta (BBA) - Protein Structure and Molecular Enzymology. 2000;1477(1):349-60.
13. Hartsock A, Nelson WJ. Adherens and tight junctions: structure, function and connections to the actin cytoskeleton. Biochim Biophys Acta. 2008;1778(3):660-9.
14. Sukriti S, Tauseef M, Yazbeck P, Mehta D. Mechanisms regulating endothelial permeability. Pulmonary circulation. 2014;4(4):535-51.
15. Rondaij Mariska G, Bierings R, Kragt A, van Mourik Jan A, Voorberg J. Dynamics and Plasticity of Weibel-Palade Bodies in Endothelial Cells. Arteriosclerosis, Thrombosis, and Vascular Biology. 2006;26(5):1002-7.
16. Wallace JL. Nitric oxide as a regulator of inflammatory processes. Memórias do Instituto Oswaldo Cruz. 2005;100:5-9.
17. Karsan A, Yee E, Harlan JM. Endothelial Cell Death Induced by Tumor Necrosis Factor-α Is Inhibited by the Bcl-2 Family Member, A1. Journal of Biological Chemistry. 1996;271(44):27201-4.
18. Javanmard SH, Dana N. The effect of interferon γ on endothelial cell nitric oxide production and apoptosis. Adv Biomed Res. 2012;1:69-.
19. Galluzzi L, Vitale I, Abrams JM, Alnemri ES, Baehrecke EH, Blagosklonny MV, et al. Molecular definitions of cell death subroutines: recommendations of the Nomenclature Committee on Cell Death 2012. Cell Death And Differentiation. 2011;19:107.
20. Newmeyer DD, Farschon DM, Reed JC. Cell-free apoptosis in Xenopus egg extracts: Inhibition by Bcl-2 and requirement for an organelle fraction enriched in mitochondria. Cell. 1994;79(2):353-64.

21. Martin SJ, Green DR. Protease activation during apoptosis: Death by a thousand cuts? Cell. 1995;82(3):349-52.
22. Walczak H. Death receptor-ligand systems in cancer, cell death, and inflammation. Cold Spring Harb Perspect Biol.5(5):a008698-a.
23. Sprick MR, Weigand MA, Rieser E, Rauch CT, Juo P, Blenis J, et al. FADD/MORT1 and Caspase-8 Are Recruited to TRAIL Receptors 1 and 2 and Are Essential for Apoptosis Mediated by TRAIL Receptor 2. Immunity. 2000;12(6):599-609.
24. Walczak H. TNF and ubiquitin at the crossroads of gene activation, cell death, inflammation, and cancer. Immunological Reviews. 2011;244(1):9-28.
25. Tenev T, Bianchi K, Darding M, Broemer M, Langlais C, Wallberg F, et al. The Ripoptosome, a Signaling Platform that Assembles in Response to Genotoxic Stress and Loss of IAPs. Molecular Cell. 2011;43(3):432-48.
26. Wang L, Du F, Wang X. TNF-α Induces Two Distinct Caspase-8 Activation Pathways. Cell. 2008;133(4):693-703.
27. Gonzalvez F, Lawrence D, Yang B, Yee S, Pitti R, Marsters S, et al. TRAF2 Sets a Threshold for Extrinsic Apoptosis by Tagging Caspase-8 with a Ubiquitin Shutoff Timer. Molecular Cell. 2012;48(6):888-99.
28. Li J, McQuade T, Siemer AB, Napetschnig J, Moriwaki K, Hsiao Y-S, et al. The RIP1/RIP3 necrosome forms a functional amyloid signaling complex required for programmed necrosis. Cell. 2012;150(2):339-50.
29. Wang H, Sun L, Su L, Rizo J, Liu L, Wang L-F, et al. Mixed Lineage Kinase Domain-like Protein MLKL Causes Necrotic Membrane Disruption upon Phosphorylation by RIP3. Molecular Cell. 2014;54(1):133-46.
30. Morioka S, Inagaki M, Komatsu Y, Mishina Y, Matsumoto K, Ninomiya-Tsuji J. TAK1 kinase signaling regulates embryonic angiogenesis by modulating endothelial cell survival and migration. Blood. 2012;120(18):3846.
31. Morioka S, Broglie P, Omori E, Ikeda Y, Takaesu G, Matsumoto K, et al. TAK1 kinase switches cell fate from apoptosis to necrosis following TNF stimulation. The Journal of Cell Biology. 2014;204(4):607.
32. Ajibade AA, Wang HY, Wang R-F. Cell type-specific function of TAK1 in innate immune signaling. Trends in Immunology. 2013;34(7):307-16.
33. Yang L, Joseph S, Sun T, Hoffmann J, Thevissen S, Offermanns S, et al. TAK1 regulates endothelial cell necroptosis and tumor metastasis. Cell Death & Differentiation. 2019.
34. Oberst A, Dillon CP, Weinlich R, McCormick LL, Fitzgerald P, Pop C, et al. Catalytic activity of the caspase-8–FLIPL complex inhibits RIPK3-dependent necrosis. Nature. 2011;471:363.
35. Green DR, Ferguson T, Zitvogel L, Kroemer G. Immunogenic and tolerogenic cell death. Nature Reviews Immunology. 2009;9:353.
36. Fadok VA, Voelker DR, Campbell PA, Cohen JJ, Bratton DL, Henson PM. Exposure of phosphatidylserine on the surface of apoptotic lymphocytes triggers specific recognition and removal by macrophages. The Journal of Immunology. 1992;148(7):2207.
37. deCathelineau AM, Henson PM. The final step in programmed cell death: phagocytes carry apoptotic cells to the grave. Essays In Biochemistry. 2003;39:105.
38. Juncadella IJ, Kadl A, Sharma AK, Shim YM, Hochreiter-Hufford A, Borish L, et al. Apoptotic cell clearance by bronchial epithelial cells critically influences airway inflammation. Nature. 2012;493:547.
39. Zelenay S, Reis e Sousa C. Adaptive immunity after cell death. Trends in Immunology. 2013;34(7):329-35.
40. Joussen AM, Poulaki V, Mitsiades N, Cai W-Y, Suzuma I, Pak J, et al. Suppression of Fas-FasL-induced endothelial cell apoptosis prevents diabetic blood–retinal barrier breakdown in a model of streptozotocin-induced diabetes. The FASEB Journal. 2002;17(1):76-8.

41. Mizutani M, Kern TS, Lorenzi M. Accelerated death of retinal microvascular cells in human and experimental diabetic retinopathy. The Journal of clinical investigation. 1996;97(12):2883-90.
42. Wu X, Zhang H, Qi W, Zhang Y, Li J, Li Z, et al. Nicotine promotes atherosclerosis via ROS-NLRP3-mediated endothelial cell pyroptosis. Cell Death & Disease. 2018;9(2):171.
43. Reinhart K, Daniels R, Kissoon N, Machado FR, Schachter RD, Finfer S. Recognizing Sepsis as a Global Health Priority — A WHO Resolution. New England Journal of Medicine. 2017;377(5):414-7.
44. Sonneville R, Verdonk F, Rauturier C, Klein IF, Wolff M, Annane D, et al. Understanding brain dysfunction in sepsis. Ann Intensive Care. 2013;3(1):15-.
45. Levy MM, Evans LE, Rhodes A. The Surviving Sepsis Campaign Bundle: 2018 update. Intensive Care Medicine. 2018;44(6):925-8.
46. Zarbock A, Gomez H, Kellum JA. Sepsis-induced acute kidney injury revisited: pathophysiology, prevention and future therapies. Curr Opin Crit Care. 2014;20(6):588-95.
47. Castro CY. ARDS and Diffuse Alveolar Damage: A Pathologist's Perspective. Seminars in Thoracic and Cardiovascular Surgery. 2006;18(1):13-9.
48. Han S, Mallampalli RK. The acute respiratory distress syndrome: from mechanism to translation. J Immunol. 2015;194(3):855-60.
49. Moore FA, Moore EE. Evolving Concepts in the Pathogenesis of Postinjury Multiple Organ Failure. Surgical Clinics of North America. 1995;75(2):257-77.
50. Singer M, Deutschman CS, Seymour CW, Shankar-Hari M, Annane D, Bauer M, et al. The Third International Consensus Definitions for Sepsis and Septic Shock (Sepsis-3)Consensus Definitions for Sepsis and Septic ShockConsensus Definitions for Sepsis and Septic Shock. JAMA. 2016;315(8):801-10.
51. Mogensen TH. Pathogen recognition and inflammatory signaling in innate immune defenses. Clin Microbiol Rev. 2009;22(2):240-73.
52. Akira S, Uematsu S, Takeuchi O. Pathogen Recognition and Innate Immunity. Cell. 2006;124(4):783-801.
53. Surbatovic M, Popovic N, Vojvodic D, Milosevic I, Acimovic G, Stojicic M, et al. Cytokine profile in severe gram-positive and gram-negative abdominal sepsis. Scientific Reports. 2015;5:11355.
54. van der Poll T. Pro-Inflammatory Cytokines: Double-Edged Swords in the Pathogenesis of Bacterial Infection. In: Evans TW, Fink MP, editors. Mechanisms of Organ Dysfunction in Critical Illness. Berlin, Heidelberg: Springer Berlin Heidelberg; 2002. p. 146-58.
55. Chaudhry H, Zhou J, Zhong Y, Ali MM, McGuire F, Nagarkatti PS, et al. Role of cytokines as a double-edged sword in sepsis. In Vivo. 2013;27(6):669-84.
56. Wu H-P, Chen C-K, Chung K, Tseng J-C, Hua C-C, Liu Y-C, et al. Serial cytokine levels in patients with severe sepsis. Inflammation Research. 2009;58(7):385-93.
57. Kim JH, Oh SJ, Ahn S, Chung DH. IFN-γ-producing NKT cells exacerbate sepsis by enhancing C5a generation via IL-10-mediated inhibition of CD55 expression on neutrophils. European Journal of Immunology. 2014;44(7):2025-35.
58. Mera S, Tatulescu D, Cismaru C, Bondor C, Slavcovici A, Zanc V, et al. Multiplex cytokine profiling in patients with sepsis. APMIS. 2011;119(2):155-63.
59. Wang Y, Kong B-b, Yang W-p, Zhao X, Zhang R. Immunomodulatory intervention with Gamma interferon in mice with sepsis. Life Sciences. 2017;185:85-94.
60. Clark PR, Kim RK, Pober JS, Kluger MS. Tumor Necrosis Factor Disrupts Claudin-5 Endothelial Tight Junction Barriers in Two Distinct NF-κB-Dependent Phases. PLoS One. 2015;10(3):e0120075.
61. Schmidt EP, Yang Y, Janssen WJ, Gandjeva A, Perez MJ, Barthel L, et al. The pulmonary endothelial glycocalyx regulates neutrophil adhesion and lung injury during experimental sepsis. Nature Medicine. 2012;18:1217.

62. Steinberg KP, Milberg JA, Martin TR, Maunder RJ, Cockrill BA, Hudson LD. Evolution of bronchoalveolar cell populations in the adult respiratory distress syndrome. American Journal of Respiratory and Critical Care Medicine. 1994;150(1):113-22.
63. Grommes J, Soehnlein O. Contribution of neutrophils to acute lung injury. Mol Med. 2011;17(3-4):293-307.
64. Craciun FL, Schuller ER, Remick DG. Early enhanced local neutrophil recruitment in peritonitis-induced sepsis improves bacterial clearance and survival. J Immunol. 2010;185(11):6930-8.
65. Sohn RH, Deming CB, Johns DC, Champion HC, Bian C, Gardner K, et al. Regulation of endothelial thrombomodulin expression by inflammatory cytokines is mediated by activation of nuclear factor-kappa B. Blood. 2005;105(10):3910.
66. Gando S, Levi M, Toh C-H. Disseminated intravascular coagulation. Nature Reviews Disease Primers. 2016;2:16037.
67. Levi M, van der Poll T. Coagulation and sepsis. Thrombosis Research. 2017;149:38-44.
68. Takatani Y, Ono K, Suzuki H, Inaba M, Sawada M, Matsuda N. Inducible nitric oxide synthase during the late phase of sepsis is associated with hypothermia and immune cell migration. Laboratory Investigation. 2018;98(5):629-39.
69. Iba T, Hashiguchi N, Nagaoka I, Tabe Y, Murai M. Neutrophil cell death in response to infection and its relation to coagulation. J Intensive Care. 2013;1(1):13.
70. Iba T, Hashiguchi N, Nagaoka I, Tabe Y, Murai M. Neutrophil cell death in response to infection and its relation to coagulation. J Intensive Care. 2013;1(1):13-.
71. Yipp BG, Petri B, Salina D, Jenne CN, Scott BNV, Zbytnuik LD, et al. Infection-induced NETosis is a dynamic process involving neutrophil multitasking in vivo. Nature Medicine. 2012;18:1386.
72. Chen L, Zhao Y, Lai D, Zhang P, Yang Y, Li Y, et al. Neutrophil extracellular traps promote macrophage pyroptosis in sepsis. Cell Death & Disease. 2018;9(6):597.
73. Kang R, Zeng L, Zhu S, Xie Y, Liu J, Wen Q, et al. Lipid Peroxidation Drives Gasdermin D-Mediated Pyroptosis in Lethal Polymicrobial Sepsis. Cell Host & Microbe. 2018;24(1):97-108.e4.
74. Exline MC, Justiniano S, Hollyfield JL, Berhe F, Besecker BY, Das S, et al. Microvesicular Caspase-1 Mediates Lymphocyte Apoptosis in Sepsis. PLoS One. 2014;9(3):e90968.
75. Hotchkiss RS, Tinsley KW, Swanson PE, Karl IE. Endothelial cell apoptosis in sepsis. Critical Care Medicine. 2002;30(5):S225-S8.
76. Kawasaki M, Kuwano K, Hagimoto N, Matsuba T, Kunitake R, Tanaka T, et al. Protection from lethal apoptosis in lipopolysaccharide-induced acute lung injury in mice by a caspase inhibitor. Am J Pathol. 2000;157(2):597-603.
77. Matsuda N, Takano Y, Kageyama S-i, Hatakeyama N, Shakunaga K, Kitajima I, et al. Silencing of caspase-8 and caspase-3 by RNA interference prevents vascular endothelial cell injury in mice with endotoxic shock. Cardiovascular Research. 2007;76(1):132-40.
78. Yellon DM, Hausenloy DJ. Myocardial Reperfusion Injury. New England Journal of Medicine. 2007;357(11):1121-35.
79. Ogawa S, Koga S, Kuwabara K, Brett J, Morrow B, Morris SA, et al. Hypoxia-induced increased permeability of endothelial monolayers occurs through lowering of cellular cAMP levels. American Journal of Physiology-Cell Physiology. 1992;262(3):C546-C54.
80. Eltzschig HK, Carmeliet P. Hypoxia and Inflammation. New England Journal of Medicine. 2011;364(7):656-65.
81. Hidalgo A, Chang J, Jang J-E, Peired AJ, Chiang EY, Frenette PS. Heterotypic interactions enabled by polarized neutrophil microdomains mediate thromboinflammatory injury. Nature Medicine. 2009;15:384.
82. Lang JD, Jr., Teng X, Chumley P, Crawford JH, Isbell TS, Chacko BK, et al. Inhaled NO accelerates restoration of liver function in adults following orthotopic liver transplantation. The Journal of Clinical Investigation. 2007;117(9):2583-91.

83. Eltzschig HK, Collard CD. Vascular ischaemia and reperfusion injury. British Medical Bulletin. 2004;70(1):71-86.
84. Zhou T, Prather ER, Garrison DE, Zuo L. Interplay between ROS and Antioxidants during Ischemia-Reperfusion Injuries in Cardiac and Skeletal Muscle. Int J Mol Sci. 2018;19(2):417.
85. Shireman PK. The chemokine system in arteriogenesis and hind limb ischemia. Journal of Vascular Surgery. 2007;45(6, Supplement):A48-A56.
86. Bernardini G, Ribatti D, Spinetti G, Morbidelli L, Ziche M, Santoni A, et al. Analysis of the role of chemokines in angiogenesis. Journal of Immunological Methods. 2003;273(1):83-101.
87. Yu J, deMuinck ED, Zhuang Z, Drinane M, Kauser K, Rubanyi GM, et al. Endothelial nitric oxide synthase is critical for ischemic remodeling, mural cell recruitment, and blood flow reserve. Proc Natl Acad Sci U S A. 2005;102(31):10999.
88. Krishnasamy K, Limbourg A, Kapanadze T, Gamrekelashvili J, Beger C, Häger C, et al. Blood vessel control of macrophage maturation promotes arteriogenesis in ischemia. Nature Communications. 2017;8(1):952.
89. Sasaki K, Murohara T, Ikeda H, Sugaya T, Shimada T, Shintani S, et al. Evidence for the importance of angiotensin II type 1 receptor in ischemia-induced angiogenesis. The Journal of clinical investigation. 2002;109(5):603-11.
90. Urao N, Sudhahar V, Kim S-J, Chen G-F, McKinney RD, Kojda G, et al. Critical Role of Endothelial Hydrogen Peroxide in Post-Ischemic Neovascularization. PLoS One. 2013;8(3):e57618.
91. Abu Jawdeh BG, Govil A. Acute Kidney Injury in Transplant Setting: Differential Diagnosis and Impact on Health and Health Care. Advances in Chronic Kidney Disease. 2017;24(4):228-32.
92. Basile DP. Rarefaction of peritubular capillaries following ischemic acute renal failure: a potential factor predisposing to progressive nephropathy. Current Opinion in Nephrology and Hypertension. 2004;13(1).
93. David PB, Mervin CY. Renal Endothelial Dysfunction in Acute Kidney Ischemia Reperfusion Injury. Cardiovascular & Hematological Disorders-Drug Targets. 2014;14(1):3-14.
94. Sutton TA, Fisher CJ, Molitoris BA. Microvascular endothelial injury and dysfunction during ischemic acute renal failure. Kidney International. 2002;62(5):1539-49.
95. Matsuyama M, Yoshimura R, Akioka K, Okamoto M, Ushigome H, Kadotani Y, et al. Tissue factor antisense oligonucleotides prevent renal ischemia-reperfusion injury. Transplantation. 2003;76(5):786-91.
96. Kinsey GR, Li L, Okusa MD. Inflammation in acute kidney injury. Nephron Exp Nephrol. 2008;109(4):e102-e7.
97. Wang W, Mitra A, Poole B, Falk S, Lucia MS, Tayal S, et al. Endothelial nitric oxide synthase-deficient mice exhibit increased susceptibility to endotoxin-induced acute renal failure. American Journal of Physiology-Renal Physiology. 2004;287(5):F1044-F8.
98. Basile DP, Donohoe D, Roethe K, Osborn JL. Renal ischemic injury results in permanent damage to peritubular capillaries and influences long-term function. American Journal of Physiology-Renal Physiology. 2001;281(5):F887-F99.
99. Sun In O, Santelli A, Abumoawad A, Eirin A, Ferguson Christopher M, Woollard John R, et al. Loss of Renal Peritubular Capillaries in Hypertensive Patients Is Detectable by Urinary Endothelial Microparticle Levels. Hypertension. 2018;72(5):1180-8.
100. Patschan D, Schwarze K, Henze E, Patschan S, Müller GA. Endothelial autophagy and Endothelial-to-Mesenchymal Transition (EndoMT) in eEPC treatment of ischemic AKI. J Nephrol. 2016;29(5):637-44.
101. Pepine Carl J. Multiple Causes for Ischemia Without Obstructive Coronary Artery Disease. Circulation. 2015;131(12):1044-6.
102. Vanhoutte PM. Endothelial Dysfunction The First Step Toward Coronary Arteriosclerosis. Circulation Journal. 2009;73(4):595-601.

103. Vinten-Johansen J, Buckberg GD. Chapter 41 - Role of Nitric Oxide in Myocardial Ischemia-Reperfusion Injury. In: Ignarro LJ, editor. Nitric Oxide. San Diego: Academic Press; 2000. p. 661-85.
104. Kaul S, Ito H. Microvasculature in Acute Myocardial Ischemia: Part II. Circulation. 2004;109(3):310-5.
105. Brutsaert DL. Cardiac Endothelial-Myocardial Signaling: Its Role in Cardiac Growth, Contractile Performance, and Rhythmicity. Physiological Reviews. 2003;83(1):59-115.
106. Lee S-J, Lee C-K, Kang S, Park I, Kim YH, Kim SK, et al. Angiopoietin-2 exacerbates cardiac hypoxia and inflammation after myocardial infarction. The Journal of clinical investigation. 2018;128(11):5018-33.
107. Zhao X, Zhang W, Xing D, Li P, Fu J, Gong K, et al. Endothelial cells overexpressing IL-8 receptor reduce cardiac remodeling and dysfunction following myocardial infarction. American Journal of Physiology-Heart and Circulatory Physiology. 2013;305(4):H590-H8.
108. Li Y, Lui KO, Zhou B. Reassessing endothelial-to-mesenchymal transition in cardiovascular diseases. Nature Reviews Cardiology. 2018;15(8):445-56.
109. He L, Huang X, Kanisicak O, Li Y, Wang Y, Li Y, et al. Preexisting endothelial cells mediate cardiac neovascularization after injury. The Journal of Clinical Investigation. 2017;127(8):2968-81.
110. Gottlieb RA. Cell Death Pathways in Acute Ischemia/Reperfusion Injury. Journal of Cardiovascular Pharmacology and Therapeutics. 2011;16(3-4):233-8.
111. Singhal AK, Symons JD, Boudina S, Jaishy B, Shiu Y-T. Role of Endothelial Cells in Myocardial Ischemia-Reperfusion Injury. Vasc Dis Prev. 2010;7:1-14.
112. Sato S, Sanjo H, Takeda K, Ninomiya-Tsuji J, Yamamoto M, Kawai T, et al. Essential function for the kinase TAK1 in innate and adaptive immune responses. Nature Immunology. 2005;6:1087.
113. Strilic B, Yang L, Albarrán-Juárez J, Wachsmuth L, Han K, Müller UC, et al. Tumour-cell-induced endothelial cell necroptosis via death receptor 6 promotes metastasis. Nature. 2016;536:215.
114. Lalazar G, Ilyas G, Malik SA, Liu K, Zhao E, Amir M, et al. Autophagy confers resistance to lipopolysaccharide-induced mouse hepatocyte injury. American journal of physiology Gastrointestinal and liver physiology. 2016;311(3):G377-G86.
115. Yang J, Zhao Y, Zhang P, Li Y, Yang Y, Yang Y, et al. Hemorrhagic shock primes for lung vascular endothelial cell pyroptosis: role in pulmonary inflammation following LPS. Cell Death &Amp; Disease. 2016;7:e2363.
116. Xu X, Gou L, Zhou M, Yang F, Zhao Y, Feng T, et al. Progranulin protects against endotoxin-induced acute kidney injury by downregulating renal cell death and inflammatory responses in mice. International Immunopharmacology. 2016;38:409-19.
117. Zhang Y, Chen X, Gueydan C, Han J. Plasma membrane changes during programmed cell deaths. Cell Research. 2017;28:9.
118. Shrum B, Anantha RV, Xu SX, Donnelly M, Haeryfar SMM, McCormick JK, et al. A robust scoring system to evaluate sepsis severity in an animal model. BMC Research Notes. 2014;7(1):233.
119. Hotchkiss RS, Swanson PE, Freeman BD, Tinsley KW, Cobb JP, Matuschak GM, et al. Apoptotic cell death in patients with sepsis, shock, and multiple organ dysfunction. Critical Care Medicine. 1999;27(7).
120. Doi K, Leelahavanichkul A, Yuen PST, Star RA. Animal models of sepsis and sepsis-induced kidney injury. The Journal of clinical investigation. 2009;119(10):2868-78.
121. Luan Y-y, Yao Y-m, Xiao X-z, Sheng Z-y. Insights into the Apoptotic Death of Immune Cells in Sepsis. Journal of Interferon & Cytokine Research. 2014;35(1):17-22.
122. Wesche DE, Lomas-Neira JL, Perl M, Chung C-S, Ayala A. Leukocyte apoptosis and its significance in sepsis and shock. Journal of Leukocyte Biology. 2005;78(2):325-37.

123. Hotchkiss RS, Tinsley KW, Swanson PE, Karl IE. Endothelial cell apoptosis in sepsis. Critical Care Medicine. 2002;30(5).
124. Jersmann HP, Hii CS, Hodge GL, Ferrante A. Synthesis and surface expression of CD14 by human endothelial cells. Infection and immunity. 2001;69(1):479-85.
125. Zhang X, Dowling JP, Zhang J. RIPK1 can mediate apoptosis in addition to necroptosis during embryonic development. Cell Death & Disease. 2019;10(3):245.
126. Chauhan A, Hudobenko J, Al Mamun A, Koellhoffer EC, Patrizz A, Ritzel RM, et al. Myeloid-specific TAK1 deletion results in reduced brain monocyte infiltration and improved outcomes after stroke. Journal of neuroinflammation. 2018;15(1):148-.
127. Bast DJ, Yue M, Chen X, Bell D, Dresser L, Saskin R, et al. Novel Murine Model of Pneumococcal Pneumonia: Use of Temperature as a Measure of Disease Severity To Compare the Efficacies of Moxifloxacin and Levofloxacin. Antimicrobial Agents and Chemotherapy. 2004;48(9):3343.
128. Vlach KD, Boles JW, Stiles BG. Telemetric Evaluation of Body Temperature and Physical Activity as Predictors of Mortality in a Murine Model of Staphylococcal Enterotoxic Shock. Comparative Medicine. 2000;50(2):160-6.
129. Abraham E. Coagulation Abnormalities in Acute Lung Injury and Sepsis. American Journal of Respiratory Cell and Molecular Biology. 2000;22(4):401-4.
130. Rezoagli E, Fumagalli R, Bellani G. Definition and epidemiology of acute respiratory distress syndrome. Annals of translational medicine. 2017;5(14):282-.
131. Kim W-Y, Hong S-B. Sepsis and Acute Respiratory Distress Syndrome: Recent Update. Tuberculosis and respiratory diseases. 2016;79(2):53-7.
132. Palud A, Parmentier-Decrucq E, Pastre J, De Freitas Caires N, Lassalle P, Mathieu D. Evaluation of endothelial biomarkers as predictors of organ failures in septic shock patients. Cytokine. 2015;73(2):213-8.
133. Hendrickson CM, Matthay MA. Endothelial biomarkers in human sepsis: pathogenesis and prognosis for ARDS. Pulmonary circulation. 2018;8(2):2045894018769876-.
134. Zinter MS, Spicer A, Orwoll BO, Alkhouli M, Dvorak CC, Calfee CS, et al. Plasma angiopoietin-2 outperforms other markers of endothelial injury in prognosticating pediatric ARDS mortality. American journal of physiology Lung cellular and molecular physiology. 2016;310(3):L224-L31.
135. Okamoto T, Tanigami H, Suzuki K, Shimaoka M. Thrombomodulin: a bifunctional modulator of inflammation and coagulation in sepsis. Critical care research and practice. 2012;2012:614545-.
136. Ikezoe T. Thrombomodulin/activated protein C system in septic disseminated intravascular coagulation. J Intensive Care. 2015;3(1):1-.
137. Dragoni S, Hudson N, Kenny B-A, Burgoyne T, McKenzie JA, Gill Y, et al. Endothelial MAPKs Direct ICAM-1 Signaling to Divergent Inflammatory Functions. The Journal of Immunology. 2017;198(10):4074.
138. Nikolova-Krstevski V, Yuan L, Le Bras A, Vijayaraj P, Kondo M, Gebauer I, et al. ERG is required for the differentiation of embryonic stem cells along the endothelial lineage. BMC developmental biology. 2009;9:72-.
139. McLaughlin F, Ludbrook VJ, Kola I, Campbell CJ, Randi AM. Characterisation of the tumour necrosis factor (TNF)-(alpha) response elements in the human ICAM-2 promoter. Journal of Cell Science. 1999;112(24):4695.
140. Dryden NH, Sperone A, Martin-Almedina S, Hannah RL, Birdsey GM, Khan ST, et al. The transcription factor Erg controls endothelial cell quiescence by repressing activity of nuclear factor (NF)-κB p65. The Journal of biological chemistry. 2012;287(15):12331-42.
141. Sperone A, Dryden Nicola H, Birdsey Graeme M, Madden L, Johns M, Evans Paul C, et al. The Transcription Factor Erg Inhibits Vascular Inflammation by Repressing NF-κB Activation and Proinflammatory Gene Expression in Endothelial Cells. Arteriosclerosis, Thrombosis, and Vascular Biology. 2011;31(1):142-50.

142. Yuan L, Nikolova-Krstevski V, Zhan Y, Kondo M, Bhasin M, Varghese L, et al. Antiinflammatory Effects of the ETS Factor ERG in Endothelial Cells Are Mediated Through Transcriptional Repression of the Interleukin-8 Gene. Circulation Research. 2009;104(9):1049-57.
143. Walley KR, Lukacs NW, Standiford TJ, Strieter RM, Kunkel SL. Elevated levels of macrophage inflammatory protein 2 in severe murine peritonitis increase neutrophil recruitment and mortality. Infection and immunity. 1997;65(9):3847-51.
144. Doherty GM, Lange JR, Langstein HN, Alexander HR, Buresh CM, Norton JA. Evidence for IFN-gamma as a mediator of the lethality of endotoxin and tumor necrosis factor-alpha. The Journal of Immunology. 1992;149(5):1666.
145. Takeyama N, Tanaka T, Yabuki T, Nakatani K, Nakatani T. Effect of interferon gamma on sepsis-related death in patients with immunoparalysis. Crit Care. 2004;8(Suppl 1):P207-P.
146. Zhao H, Jaffer T, Eguchi S, Wang Z, Linkermann A, Ma D. Role of necroptosis in the pathogenesis of solid organ injury. Cell Death &Amp; Disease. 2015;6:e1975.
147. Chavez-Valdez R, Martin LJ, Northington FJ. Programmed Necrosis: A Prominent Mechanism of Cell Death following Neonatal Brain Injury. Neurol Res Int. 2012;2012:257563-.
148. Lau A, Wang S, Jiang J, Haig A, Pavlosky A, Linkermann A, et al. RIPK3-Mediated Necroptosis Promotes Donor Kidney Inflammatory Injury and Reduces Allograft Survival. American Journal of Transplantation. 2013;13(11):2805-18.
149. Linkermann A, Bräsen JH, Himmerkus N, Liu S, Huber TB, Kunzendorf U, et al. Rip1 (Receptor-interacting protein kinase 1) mediates necroptosis and contributes to renal ischemia/reperfusion injury. Kidney International. 2012;81(8):751-61.
150. Yang Q, He G-W, Underwood MJ, Yu C-M. Cellular and molecular mechanisms of endothelial ischemia/reperfusion injury: perspectives and implications for postischemic myocardial protection. Am J Transl Res. 2016;8(2):765-77.
151. Leaf-nosed bat. Encyclopædia Britannica: Encyclopædia Britannica Online; 2009.
152. Heil M, Eitenmüller I, Schmitz-Rixen T, Schaper W. Arteriogenesis versus angiogenesis: similarities and differences. Journal of cellular and molecular medicine. 2006;10(1):45-55.
153. Yang J-R, Yao F-H, Zhang J-G, Ji Z-Y, Li K-L, Zhan J, et al. Ischemia-reperfusion induces renal tubule pyroptosis via the CHOP-caspase-11 pathway. American Journal of Physiology-Renal Physiology. 2013;306(1):F75-F84.
154. Linkermann A, Bräsen JH, Darding M, Jin MK, Sanz AB, Heller J-O, et al. Two independent pathways of regulated necrosis mediate ischemia–reperfusion injury. Proceedings of the National Academy of Sciences. 2013;110(29):12024-9.
155. Li J, Wang X, Teng Y, Li Z, Chen J, Huang N, et al. The role of RIP3 in cardiomyocyte necrosis induced by mitochondrial damage of myocardial ischemia–reperfusion. Acta Biochimica et Biophysica Sinica. 2018;50(11):1131-40.
156. Newton K, Dugger DL, Maltzman A, Greve JM, Hedehus M, Martin-McNulty B, et al. RIPK3 deficiency or catalytically inactive RIPK1 provides greater benefit than MLKL deficiency in mouse models of inflammation and tissue injury. Cell Death And Differentiation. 2016;23:1565.
157. Zhu P, Hu S, Jin Q, Li D, Tian F, Toan S, et al. Ripk3 promotes ER stress-induced necroptosis in cardiac IR injury: A mechanism involving calcium overload/XO/ROS/mPTP pathway. Redox biology. 2018;16:157-68.
158. Sureshbabu A, Patino E, Ma KC, Laursen K, Finkelsztein EJ, Akchurin O, et al. RIPK3 promotes sepsis-induced acute kidney injury via mitochondrial dysfunction. JCI Insight. 2018;3(11).
159. Qin S, Wang H, Yuan R, Li H, Ochani M, Ochani K, et al. Role of HMGB1 in apoptosis-mediated sepsis lethality. The Journal of Experimental Medicine. 2006;203(7):1637.
160. Seemann S, Zohles F, Lupp A. Comprehensive comparison of three different animal models for systemic inflammation. Journal of Biomedical Science. 2017;24(1):60.

161. Takahashi N, Duprez L, Grootjans S, Cauwels A, Nerinckx W, DuHadaway JB, et al. Necrostatin-1 analogues: critical issues on the specificity, activity and in vivo use in experimental disease models. Cell Death &Amp; Disease. 2012;3:e437.
162. Ramana CV, DeBerge MP, Kumar A, Alia CS, Durbin JE, Enelow RI. Inflammatory impact of IFN-γ in CD8+ T cell-mediated lung injury is mediated by both Stat1-dependent and -independent pathways. American journal of physiology Lung cellular and molecular physiology. 2015;308(7):L650-L7.
163. Lang S, Li L, Wang X, Sun J, Xue X, Xiao Y, et al. CXCL10/IP-10 Neutralization Can Ameliorate Lipopolysaccharide-Induced Acute Respiratory Distress Syndrome in Rats. PLoS One. 2017;12(1):e0169100.
164. Thapa RJ, Basagoudanavar SH, Nogusa S, Irrinki K, Mallilankaraman K, Slifker MJ, et al. NF-κB Protects Cells from Gamma Interferon-Induced RIP1-Dependent Necroptosis. Molecular and Cellular Biology. 2011;31(14):2934.
165. Wang MJ, Jeng KCG, Shih PC. Differential Expression and Regulation of Macrophage Inflammatory Protein (MIP)-1α and MIP-2 Genes by Alveolar and Peritoneal Macrophages in LPS-Hyporesponsive C3H/HeJ Mice. Cellular Immunology. 2000;204(2):88-95.
166. Guo R-F, Riedemann NC, Sun L, Gao H, Shi KX, Reuben JS, et al. Divergent Signaling Pathways in Phagocytic Cells during Sepsis. The Journal of Immunology. 2006;177(2):1306.
167. Reutershan J, Morris MA, Burcin TL, Smith DF, Chang D, Saprito MS, et al. Critical role of endothelial CXCR2 in LPS-induced neutrophil migration into the lung. The Journal of clinical investigation. 2006;116(3):695-702.
168. Tsujimoto H, Ono S, Mochizuki H, Aosasa S, Majima T, Ueno C, et al. Role of Macrophage Inflammatory Protein 2 in Acute Lung Injury in Murine Peritonitis. Journal of Surgical Research. 2002;103(1):61-7.
169. Lomas-Neira JL, Chung C-S, Grutkoski PS, Miller EJ, Ayala A. CXCR2 inhibition suppresses hemorrhage-induced priming for acute lung injury in mice. Journal of Leukocyte Biology. 2004;76(1):58-64.
170. Okamoto T, Tanigami H, Suzuki K, Shimaoka M. Thrombomodulin: A Bifunctional Modulator of Inflammation and Coagulation in Sepsis. Critical Care Research and Practice. 2012;2012:10.
171. Li Y-H, Kuo C-H, Shi G-Y, Wu H-L. The role of thrombomodulin lectin-like domain in inflammation. Journal of Biomedical Science. 2012;19(1):34.
172. Yuan L, Nikolova-Krstevski V, Zhan Y, Kondo M, Bhasin M, Varghese L, et al. Antiinflammatory effects of the ETS factor ERG in endothelial cells are mediated through transcriptional repression of the interleukin-8 gene. Circulation research. 2009;104(9):1049-57.
173. Shah AV, Birdsey GM, Peghaire C, Pitulescu ME, Dufton NP, Yang Y, et al. The endothelial transcription factor ERG mediates Angiopoietin-1-dependent control of Notch signalling and vascular stability. Nature communications. 2017;8:16002-.
174. Nagai N, Ohguchi H, Nakaki R, Matsumura Y, Kanki Y, Sakai J, et al. Downregulation of ERG and FLI1 expression in endothelial cells triggers endothelial-to-mesenchymal transition. PLOS Genetics. 2018;14(11):e1007826.
175. Takaesu G, Surabhi RM, Park K-J, Ninomiya-Tsuji J, Matsumoto K, Gaynor RB. TAK1 is Critical for IκB Kinase-mediated Activation of the NF-κB Pathway. Journal of Molecular Biology. 2003;326(1):105-15.
176. Alagbala Ajibade A, Wang Q, Cui J, Zou J, Xia X, Wang M, et al. TAK1 Negatively Regulates NF-κB and p38 MAP Kinase Activation in Gr-1+CD11b+ Neutrophils. Immunity. 2012;36(1):43-54.
177. Naito H, Iba T, Wakabayashi T, Tai-Nagara I, Suehiro J-i, Jia W, et al. TAK1 Prevents Endothelial Apoptosis and Maintains Vascular Integrity. Developmental Cell. 2019;48(2):151-66.e7.

178. Hansen LW, Jacob A, Yang WL, Bolognese AC, Prince J, Nicastro JM, et al. Deficiency of receptor-interacting protein kinase 3 (RIPK3) attenuates inflammation and organ injury in neonatal sepsis. Journal of Pediatric Surgery. 2018;53(9):1699-705.
179. Zelic M, Roderick JE, O'Donnell JA, Lehman J, Lim SE, Janardhan HP, et al. RIP kinase 1–dependent endothelial necroptosis underlies systemic inflammatory response syndrome. The Journal of Clinical Investigation. 2018;128(5):2064-75.
180. Wang B, Li J, Gao H-M, Xing Y-H, Lin Z, Li H-J, et al. Necroptosis regulated proteins expression is an early prognostic biomarker in patient with sepsis: a prospective observational study. Oncotarget. 2017;8(48):84066-73.
181. Zaccagnini G, Martelli F, Fasanaro P, Magenta A, Gaetano C, Di Carlo A, et al. p66ShcA Modulates Tissue Response to Hindlimb Ischemia. Circulation. 2004;109(23):2917-23.
182. Han Y-S, Lee JH, Yoon YM, Yun CW, Noh H, Lee SH. Hypoxia-induced expression of cellular prion protein improves the therapeutic potential of mesenchymal stem cells. Cell Death &Amp; Disease. 2016;7:e2395.
183. Lopez-Pastrana J, Ferrer LM, Li Y-F, Xiong X, Xi H, Cueto R, et al. Inhibition of Caspase-1 Activation in Endothelial Cells Improves Angiogenesis: A NOVEL THERAPEUTIC POTENTIAL FOR ISCHEMIA. Journal of Biological Chemistry. 2015;290(28):17485-94.
184. Fung E, Helisch A. Macrophages in collateral arteriogenesis. Frontiers in physiology. 2012;3:353-.
185. Liu W, Chen B, Wang Y, Meng C, Huang H, Huang X-R, et al. RGMb protects against acute kidney injury by inhibiting tubular cell necroptosis via an MLKL-dependent mechanism. Proceedings of the National Academy of Sciences. 2018;115(7):E1475.
186. Linkermann A, Heller J-O, Prókai Á, Weinberg JM, De Zen F, Himmerkus N, et al. The RIP1-Kinase Inhibitor Necrostatin-1 Prevents Osmotic Nephrosis and Contrast-Induced AKI in Mice. Journal of the American Society of Nephrology. 2013;24(10):1545.
187. Linkermann A, Bräsen JH, Darding M, Jin MK, Sanz AB, Heller J-O, et al. Two independent pathways of regulated necrosis mediate ischemia–reperfusion injury. Proceedings of the National Academy of Sciences. 2013;110(29):12024.
188. Zhang T, Zhang Y, Cui M, Jin L, Wang Y, Lv F, et al. CaMKII is a RIP3 substrate mediating ischemia- and oxidative stress–induced myocardial necroptosis. Nature Medicine. 2016;22:175.
189. Hippe H-J, Luedde M, Lutz M, Carter N, Frey N, Adam D, et al. RIP3, a kinase promoting necroptotic cell death, mediates adverse remodelling after myocardial infarction. Cardiovascular Research. 2014;103(2):206-16.
190. K Kashlov J, Donev I, G Doneva J, Valkov V, D Kirkorova A, Ghenev P, et al. Serum levels of RIPK3 and troponin I as potential biomarkers for predicting impaired left ventricular function in patients with myocardial infarction with ST segment elevation and normal troponin I levels prior percutaneous coronary intervention2016.
191. Zhu M, Goetsch Sean C, Wang Z, Luo R, Hill Joseph A, Schneider J, et al. FoxO4 Promotes Early Inflammatory Response Upon Myocardial Infarction via Endothelial Arg1. Circulation Research. 2015;117(11):967-77.
192. Kong Q, Dai L, Wang Y, Zhang X, Li C, Jiang S, et al. HSPA12B Attenuated Acute Myocardial Ischemia/reperfusion Injury via Maintaining Endothelial Integrity in a PI3K/Akt/mTOR-dependent Mechanism. Scientific Reports. 2016;6:33636.

SUMMARY

Endothelial dysfunction plays an important role in different pathological conditions, but whether endothelial cell death contributes to the development and progression of certain pathological conditions is rather unclear. Here we found that endothelial cells undergo cell death during pathologies such as LPS-induced sepsis and in models of hindlimb, renal and cardiac ischemia-reperfusion injury. Analyses of mice lacking endothelial key cell death regulators such as TAK1, RIPK3 and Caspase 8 gave us insight in the role of endothelial cell death in these pathological models. For example, increased endothelial necroptosis along with basal inflammation in lungs of $TAK1^{ECKO}$ mice affects susceptibility to LPS-induced sepsis and mortality, which correlated with elevated IFN-gamma and MIP-2 serum levels. Furthermore, we found that inhibition of RIPK3-mediated endothelial necroptosis could reduce the susceptibility of $TAK1^{ECKO}$ mice to LPS-induced sepsis and mortality. In ischemia or ischemia-reperfusion models, inhibition of RIPK3-mediated endothelial necroptosis did not reduce injury in the heart after ischemia, nor did it have any effect on organ function post-injury in the kidney or the heart. Inhibition of necroptosis also did not alter vascularization processes in hindlimb post-ischemia. Taken together, endothelial necroptosis contributes to increased sepsis severity and progression whereas inhibition of endothelial necroptosis can ameliorate susceptibility to sepsis in the absence of endothelial TAK1. Inhibition of endothelial necroptosis however does not play an important role during ischemia or ischemia-reperfusion induced organ injury.

ZUSAMMENFASSUNG

Die Dysfunktion von Endothelzellen spielt eine wichtige Rolle bei verschiedenen Krankheiten, wobei unklar ist, ob Endothelzelltod an deren Entwicklung und/oder Fortschreiten beteiligt ist. Wir fanden heraus, dass Endothelzellen bei Pathologien wie der LPS-induzierten Sepsis und in Modellen von Verletzungen durch Ischämie und Reperfusion der Hinterbeine, der Nieren und des Herzens Zelltod erleiden. Weitere Analysen an Mäusen, denen wichtige Regulatoren für den Zelltod im Endothel fehlen, wie TAK1, RIPK3 und Caspase 8, ergaben weitere Aufschlüsse über die Rolle des Zelltods in diesen pathologischen Modellen. Beispielsweise beeinflusst eine erhöhte endotheliale Nekroptose zusammen mit einer basalen Entzündung in der Lunge von $TAK1^{ECKO}$-Mäusen die Anfälligkeit für LPS-induzierte Sepsis und Mortalität, was mit erhöhten IFN-gamma- und MIP-2 Serumwerten korreliert. Darüber hinaus fanden wir heraus, dass die Hemmung der RIPK3-vermittelten endothelialen Nekroptose die Anfälligkeit von $TAK1^{ECKO}$-Mäusen für LPS-induzierte Sepsis und die Mortalitätsrate verringern kann. In Ischämie- oder Ischämie-Reperfusionsmodellen reduzierte die Hemmung der RIPK3-vermittelten endothelialen Nekroptose weder die Verletzung des Herzens nach der Ischämie noch hatte sie irgendeine Auswirkung auf die Organfunktion nach der Verletzung der Niere und des Herzens. Die Hemmung der Nekroptose veränderte auch nicht die Vaskularisationsprozesse nach Ischämie der hinteren Extremitäten. Zusammenfassen kann man sagen, dass endotheliale Nekroptose bei Sepsis vorkommt und diese durch Ausschalten von TAK1 erhöht werden kann, was zu einer erhöhten Schwere und Progression der Sepsis führt. Die Hemmung der endothelialen Nekroptose hat jedoch keinen Einfluss auf den Verlauf einer durch Ischämie oder Ischämie-Reperfusion verursachten Organverletzung.

PUBLICATIONS

Lida Yang, **Sayali Joseph**, Tian Sun, Julia Hoffmann, Sophia Thevissen, Stefan Offermanns and Boris Strilic: TAK1 regulates endothelial cell necroptosis and tumor metastasis. Cell death and differentiation 2019. doi: 10.1038/s41418-018-0271-8

Julián Albarrán-Juárez, Andras Iring, ShengPeng Wang, **Sayali Joseph**, Myriam Grimm, Boris Strilic, Nina Wettschureck, Till F. Althoff, Stefan Offermanns: Piezo1 and Gq/G11 promote endothelial inflammation depending on flow pattern and integrin activation. Journal of Experimental Medicine 2018. doi.org/10.1084/jem.20180483

Schriftliche Erklärung

Ich erkläre ehrenwörtlich, dass ich die dem Fachbereich Medizin der Johann Wolfgang Goethe-Universität Frankfurt am Main zur Promotionsprüfung eingereichte Dissertation mit dem Titel

The role of endothelial cell death in different pathologies

am Max-Planck-Institut für Herz- und Lungenforschung, Bad Nauheim und Zentrum für Molekulare Medizin, Universität Frankfurt unter Betreuung und Anleitung von Prof. Dr. Stefan Offermanns ohne sonstige Hilfe selbst durchgeführt und bei der Abfassung der Arbeit keine anderen als die in der Dissertation angeführten Hilfsmittel benutzt habe. Darüber hinaus versichere ich, nicht die Hilfe einer kommerziellen Promotionsvermittlung in Anspruch genommen zu haben.

Ich habe bisher an keiner in- oder ausländischen Universität ein Gesuch um Zulassung zur Promotion eingereicht. Die vorliegende Arbeit wurde bisher nicht als Dissertation eingereicht.

_____ _____

(Ort, Datum) (Unterschrift)